

LA-UR-

*Approved for public release;
distribution is unlimited.*

Title:

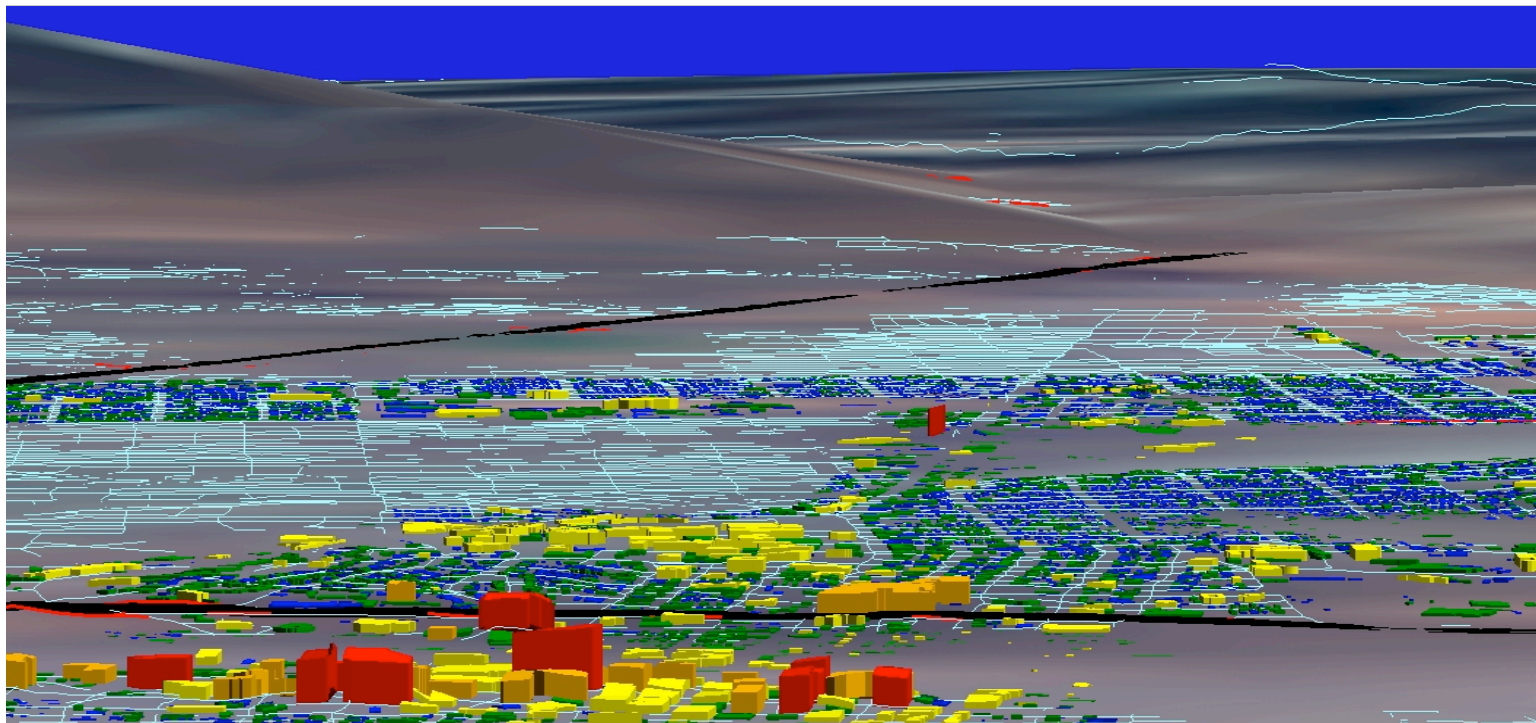
Author(s):

Submitted to:

Los Alamos

NATIONAL LABORATORY

Los Alamos National Laboratory, an affirmative action/equal opportunity employer, is operated by the University of California for the U.S. Department of Energy under contract W-7405-ENG-36. By acceptance of this article, the publisher recognizes that the U.S. Government retains a nonexclusive, royalty-free license to publish or reproduce the published form of this contribution, or to allow others to do so, for U.S. Government purposes. Los Alamos National Laboratory requests that the publisher identify this article as work performed under the auspices of the U.S. Department of Energy. Los Alamos National Laboratory strongly supports academic freedom and a researcher's right to publish; as an institution, however, the Laboratory does not endorse the viewpoint of a publication or guarantee its technical correctness.



Morphological Analyses using 3D Building Databases: Albuquerque, New Mexico

**Steven J. Burian, Sri Ram Kumar Maddula,
and Srinivas Pradeep Velugubantla**

Department of Civil Engineering
University of Arkansas
Email: sburian@engr.uark.edu

Michael J. Brown

Energy and Environmental Analysis Group
Los Alamos National Laboratory
Email: mbrown@lanl.gov

LA-UR-
Los Alamos National Laboratory
November 2002

Abstract

This report summarizes our calculations of building morphological characteristics for a 48.5-km² area centered around the downtown of Albuquerque, New Mexico. A three-dimensional building dataset, digital orthophotos, detailed land use/cover information, bare-earth topography, and roads were integrated and analyzed using a geographic information system (GIS). Building height characteristics (e.g., mean height, variance of height, height histograms) were determined for the entire study area and broken down by land use type using a dataset that contained 22,662 buildings. Other parameters describing the urban morphology that were calculated include the building plan area fraction (\bar{f}_p), building area density ($a_p(z)$), rooftop area density ($a_r(z)$), frontal area index (\bar{f}_f), frontal area density ($a_f(z)$), complete aspect ratio (\bar{c}), building surface area to plan area ratio (\bar{f}_s), and the height-to-width ratio (\bar{h}_w). Aerodynamic roughness length (z_o) and zero-plane displacement height (z_d) were calculated for the entire study area and for each land use type using standard morphometric equations and the computed urban morphological parameters.

The urban morphological parameters were computed as a function of land use type, on spatial grids, and in some cases as a function of height above ground elevation. Building statistics were correlated to underlying land use using two different land use classification schemes: the seven USGS Anderson Level 2 urban land use types and a second scheme containing more detailed residential, industrial, and commercial categories. Most of the morphometric parameters that we calculated were found to be similar to values computed for other cities by other researchers. The results indicate that the calculated urban morphological parameters are significantly different between different land use types. Significant differences were also noted between subcategories of residential land use. Moreover, commercial areas were found to have very different morphological characteristics as compared to other urban land use types, primarily because commercial areas have pockets of densely packed tall buildings. The findings presented herein are intended to be utilized in urban canopy parameterizations found in mesoscale meteorological and urban dispersions models.

1.0 Introduction

Describing the urban terrain and land use/land cover (LULC) characteristics accurately is vital for urban planning, environmental management, environmental modeling, and many other applications. Urban terrain elements can be broadly classified as natural landscape, ornamental vegetation, bare soil or rock, buildings, impervious surfaces, driveways, sidewalks, or other infrastructure. Comprehensive urban databases containing urban terrain and LULC information are essential inputs for numerous meteorological modeling applications, e.g., simulating the atmospheric flow over cities, quantifying energy fluxes radiated to and from urban surfaces, determining the fate and transport of atmospheric contaminants in built-up areas. The minimum datasets required to describe the urban terrain in three dimensions include bare-earth digital elevation model (DEM), tree canopy and vegetative cover, land use/land cover, infrastructure, and building footprint outlines with height attribute.

The motivation for this research is the need to efficiently compute building morphological parameters for mesoscale meteorological modeling and air quality applications (see Ratti et al. 2001 and Brown 1999). The research objectives are to collect detailed urban datasets in a geographic information system (GIS) environment, develop automated procedures to calculate building morphological parameters, and integrate these urban canopy parameter values with detailed LULC datasets to derive relationships between the parameters and urban land use type. This report describes our efforts for a 48.5-km² section centered on the downtown of Albuquerque, New Mexico. In the next section of this report a brief accounting of prior efforts in this area is given, followed by a description of the accumulated datasets in the Albuquerque GIS database in Section 3.0. In Section 4.0, we include an overview of how the building morphological parameters are used in the models, a short description of the calculation procedures for deriving the morphological parameters, and then present the calculation results. The report ends with a summary in Section 5.0.

2.0 Background

A handful of researchers over the years have pioneered the work on obtaining building morphological statistics for cities (e.g., Ellefsen 1990, Voogt and Oke 1997, Cionco and Ellefsen 1998, Grimmond and Oke 1999). These studies have provided much useful information on building parameters, focusing mostly on residential areas and, for a few cities, industrial and commercial areas as well. There are not enough analyses, however, to make generalizations about building statistics for all U.S. cities. In addition, many of the analyses did not include the full complement of building statistics required by the CBNP suite of atmospheric transport and dispersion models. Past work involved detailed *in situ* studies, using visual surveys of buildings in an area encompassing a few city blocks and extrapolating the results to the entire city. With the recent availability of digital 3D building datasets, calculation of building statistics has become automated using image analysis and geographical information system (GIS) software allowing larger areas to be analyzed (e.g., Ratti et al., 2001; Burian et al., 2002a). We have recently completed data reports on building morphological statistics for downtown Los Angeles (Burian et al., 2002b), Phoenix (Burian et al. 2002c), Portland (Burian et al. 2002d), and Salt Lake City (Burian et al. 2002e), and have been working on analyses for Oklahoma City, Seattle, and Houston. Eastern U.S. cities will be addressed in future studies.

3.0 Albuquerque Urban Database

3.1 Urban Morphology

Urban building, tree canopy, and DEM datasets can be purchased from commercial vendors or derived in-house. The resolution, accuracy, cost, and level of detail are important dataset characteristics to consider during the acquisition phase. The basic level of information supplied with purchased building datasets is typically the building footprint and the elevation of the rooftop. More sophisticated (and likely more expensive) datasets will have greater detail of the building (e.g., representation of rooftop structures) and include additional pieces of information (e.g., rooftop color and pitch, materials). Table 1 lists several commercial vendors that provide building, tree canopy, and DEM datasets and other digital urban data products. Digital building datasets can currently be obtained for numerous U.S. and international cities and more are rapidly becoming available. In most cases the vendor can provide the dataset in a variety of generic vector or raster data formats or data formats specific to the commercial software packages (e.g., ESRI shapefiles).

Table 1. Commercial vendors of building datasets

Vendor	Web Site
i-cubed, LLC	www.i3.com
Istar USA	www.istar.com
The Gemi Store	www.gemistore.com
Urban Data Solutions, Inc.	www.u-data.com
Vexcel Corporation	www.vexcel.com
Terrapoint (lidar)	www.transamerica.com/business_services/real_estate/terrapoint/default.asp

We contracted i-cubed to prepare the high-resolution building dataset of the Albuquerque downtown area in ESRI ArcView shapefile format. The GIS shapefile-format building data are in the form of 2D polygons for the building topprint and footprint. The dataset is based on vintage photography obtained 3/11/1998 at 1:20,000 scale. The absolute planimetric (x,y) accuracy is 5~8 meters and vertical (z) accuracy is approximately 2 meters. The relative accuracy is between 1~3 meter RMSE (Root Mean Square Error) in XY and 1 meter RMSE for 3D object height measurements. Having a topprint and footprint is advantageous compared to single-polygon datasets because buildings that change dimensions significantly in the vertical direction can be accurately represented. Unfortunately, the analysis procedures established during this research effort operate on single polygons. Therefore, in non-residential areas the footprint height and topprint height were summed to represent the total building height when the area of the topprint was greater than 20% of the area of the footprint. In cases where the topprint area was less than 20% of the footprint area and the topprint height was less than 3 meters, the topprint polygon was deleted. In Residential areas a different rule was needed because the topprint in nearly all cases represented the maximum height of a pitched roof. Therefore, to represent the pitched rooftops in the analysis we chose to add the height of the topprint to the footprint and use the footprint as the building polygon. We feel it is more accurate to include the pitched rooftop as a rectangular polygon rather than delete it. Tree canopy data were not obtained for the study area because analysis of an aerial photograph indicated that the trees and bushes present in the downtown area have negligible height and surface area compared to the buildings. The Albuquerque dataset we obtained includes 22,662 buildings in the downtown

region and adjacent areas of predominantly residential, commercial, institutional, and industrial land uses (see Figures 1 and 2).

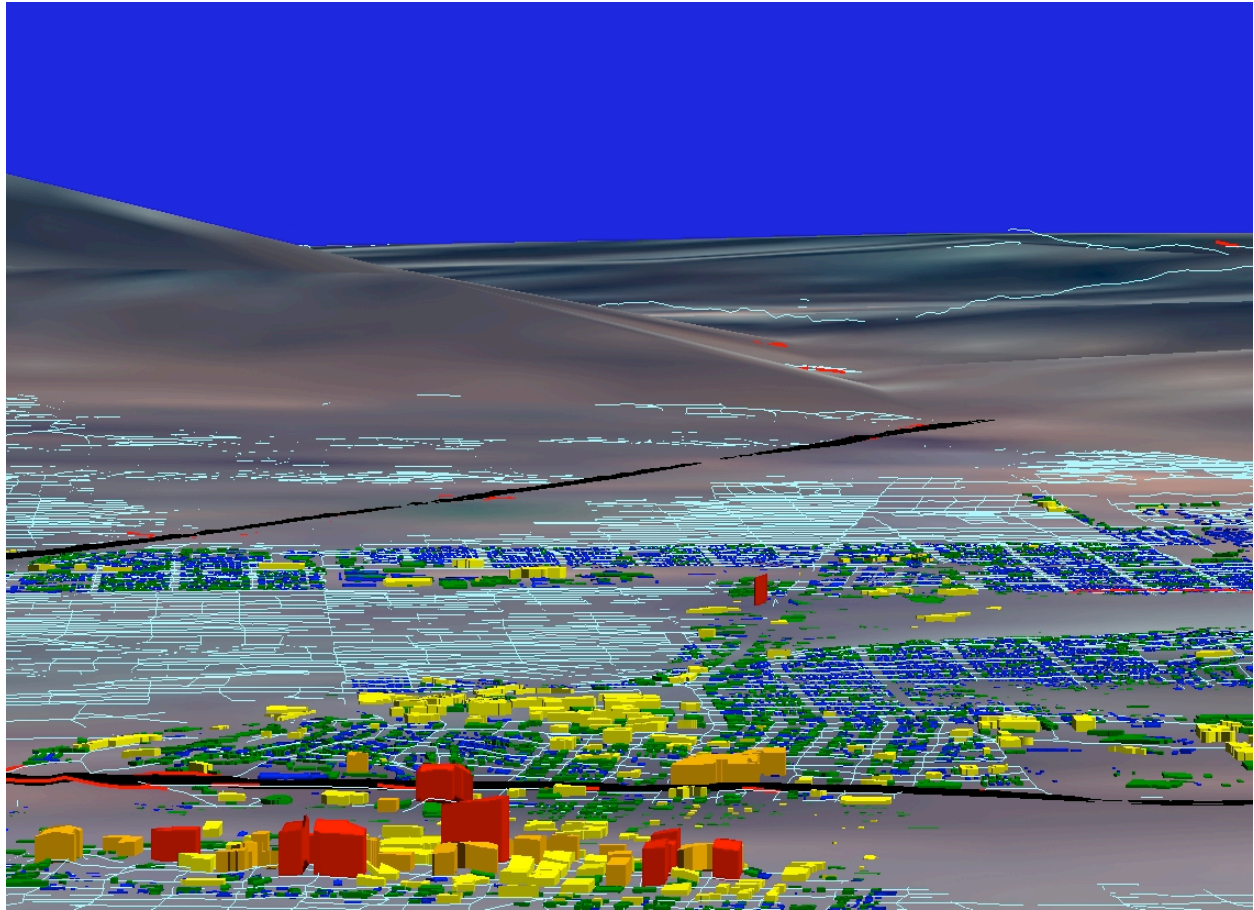


Figure 1. 3-D view from the west of the modified Albuquerque building database. The domain covers a polygonal area 7-km by 12-km at its largest dimensions. Buildings are color coded by height (see Figure 2) and are overlaid onto a street map and digital orthophoto. The downtown core area is located at the bottom, center part of the figure.

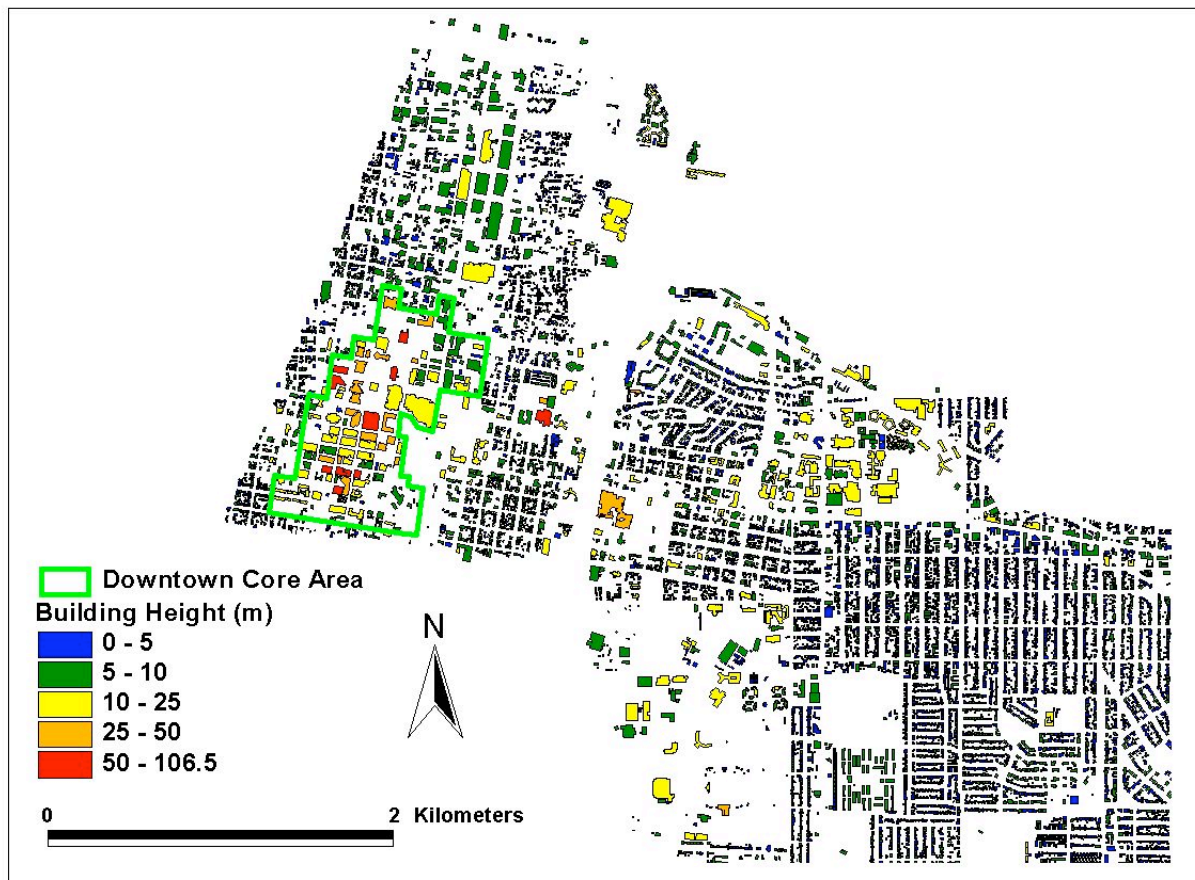


Figure 2. Plan view of the Albuquerque building database. The domain covers 48.5 km² (~10 km² is shown). Buildings are color-coded by height.

3.2 Urban Land Use/Land Cover (LULC)

A major objective of this research project is to derive relationships between building morphological parameters and urban land use type. To meet this objective we need to spatially relate building morphological parameters with a manageable number of urban land use types. LULC data for areas in the United States can be obtained from several sources including federal agencies (e.g., U.S. Geological Survey (USGS), U.S. Environmental Protection Agency (USEPA)), state agencies, local/regional planning agencies, universities, researchers, commercial vendors, and others. In general, datasets obtained from the federal, state, local/regional planning agencies, universities, or other researchers are free or cost a nominal fee. Commercial vendors on the other hand will provide a specific product with additional quality control for a greater price.

The land use dataset selected for the Albuquerque study area was obtained from the City of Albuquerque Geographic Information Systems (AGIS) web site (<http://www.cabq.gov/gis/>). The Albuquerque land use dataset is based on updates using permits, aerial photos, and occasional field trips and has a resolution of 1:2400. The dataset contains 13 urban land use categories, as

shown in Appendix 1. The 13 land use types were aggregated into the two land use classification schemes consistent with the two used in previous urban morphological studies (Burian et al. 2002b). The first land use classification scheme corresponds to the USGS Anderson Level 2 categories (Anderson et al. 1976) and the second includes more detailed classification of the Residential, Industrial, Commercial & Services, and Other Urban or Built-up land use categories. The seven categories for the first scheme are (1) Residential, (2) Commercial & Services, (3) Industrial, (4) Transportation/Communications/Utilities, (5) Mixed Industrial & Commercial, (6) Mixed Urban or Built-up, and (7) Other Urban or Built-up. This is the same scheme used to classify urban land use in the USGS/EPA GIRAS national LULC dataset. Mixed Industrial & Commercial and Mixed Urban or Built-up land uses were not found within the study area. The second classification scheme contains subcategories for Residential, Industrial, Commercial & Services, and Other Urban or Built-up land use types. The Residential category is divided into four subcategories: (1) Low-density Single-family, (2) High-density Single-family, (3) Multifamily, and (4) Mixed. The study area does not contain Residential land use defined as Mixed, but the three other types of Residential land use are present. The Industrial category is divided into Manufacturing and Wholesale & Warehousing subcategories. The Commercial & Services category is divided into two subcategories: Commercial Service and Commercial Retail. We did not divide Commercial & Services land use into high-rise and non-high-rise categories as has been done in previous studies because the data were not available for the division and we chose to study the morphological differences between the Service and Retail land use types instead. The Other Urban or Built-up category is also divided into three subcategories: Predominantly Vegetated, Predominantly Bare Soil, and Predominantly Built-up based on analysis of a digital orthophoto. Table 2, shown below, summarizes the land use types in each classification scheme and Appendix 2 provides further descriptions of the land use categories. Appendix 1 shows the aggregation of AGIS data to the two land use classification schemes.

In order to analyze and better define the characteristics of high-rise areas throughout the city a new land use category called Urban High-rise was defined. For this study we classified land use polygons containing at least one building with a height greater than or equal to 17.5 m (corresponding to approximately 5 stories) as Urban High-rise land use. In addition, a Downtown Core Area land use category was defined in order to investigate the characteristics of the city center. The Downtown Core Area delineation was based on the digital orthophoto, site visits, and our collective knowledge of the city. The Urban High-rise and Downtown Core Area land uses will overlap with the land uses in our two classification schemes, but they are needed so we can analyze and better define the characteristics of the city center area of Albuquerque.

Our land use data indicates that the 48.5-km² study area is a highly urbanized region of Albuquerque consisting of a part of the downtown region (containing high-rise buildings), as well as significant tracts of High-density Single-family Residential, Multifamily Residential, Public & Institutional, and Industrial areas. The land use distribution listed in Table 2 suggests that most of the land use is Other Urban or Built-up, Residential, Commercial & Services, and Transportation/Communications/Utilities, with a smaller amount of Industrial. Public & Institutional land use accounts for approximately 24% of the study area, and is aggregated into the Other Urban or Built-up level 1 land use category. The presence of the Albuquerque International Airport, county fairgrounds, government offices, Sandia National Laboratory, and other public land uses in the study area account for the high amount of Other Urban and Built-up

land use. An interesting feature of the Albuquerque study area is the intersection of Interstate 25 (north-south) and Interstate 40 (east-west) and the presence of the Albuquerque International Airport at the southern end of the study area. Both of these features elevate the amount of Transportation/Communications/Utilities land use in the study area, and include a significant level of open space which will be reflected in the urban canopy parameters.

Figure 3 shows our derived LULC dataset for the 48.5-km² study area in Albuquerque after aggregation to the 14-category land use scheme. Also shown is the boundary of the Downtown Core Area. The LULC dataset was intersected with the building dataset using the ESRI ArcView GIS software to identify which buildings were associated with which land use type. Fortran codes and Avenue scripts previously written, as well as standard ArcView GIS functions, were used to calculate a suite of urban morphological parameters. The calculation procedures and the results of the analyses are described next in Section 4.

Table 2. Urban land use coverage in the 48.5-km² study area

Land Use Class	Area (ha)*	Percent of Total (%)
Residential	1659	34
Low-density Single-family (< 8 units/hectare)	165	3
High-density Single-family (≥ 8 units/hectare)	1143	24
Multifamily	351	7
Mixed	---	---
Commercial & Services	799	17
Service	586	12
Retail	213	5
Industrial	93	2
Manufacturing	31	<1
Wholesale & Warehousing	62	1
Transportation/Communications/Utilities	517	11
Mixed Industrial & Commercial	---	---
Mixed Urban or Built-up	---	---
Other Urban or Built-up	1781	37
Predominantly Vegetated	300	6
Predominantly Bare Soil	317	7
Predominantly Built-up	1164	24
Urban High-rise	507	11
Downtown Core Area	91	2

* The areas are given in hectares (ha) (100 ha = 1 km²).

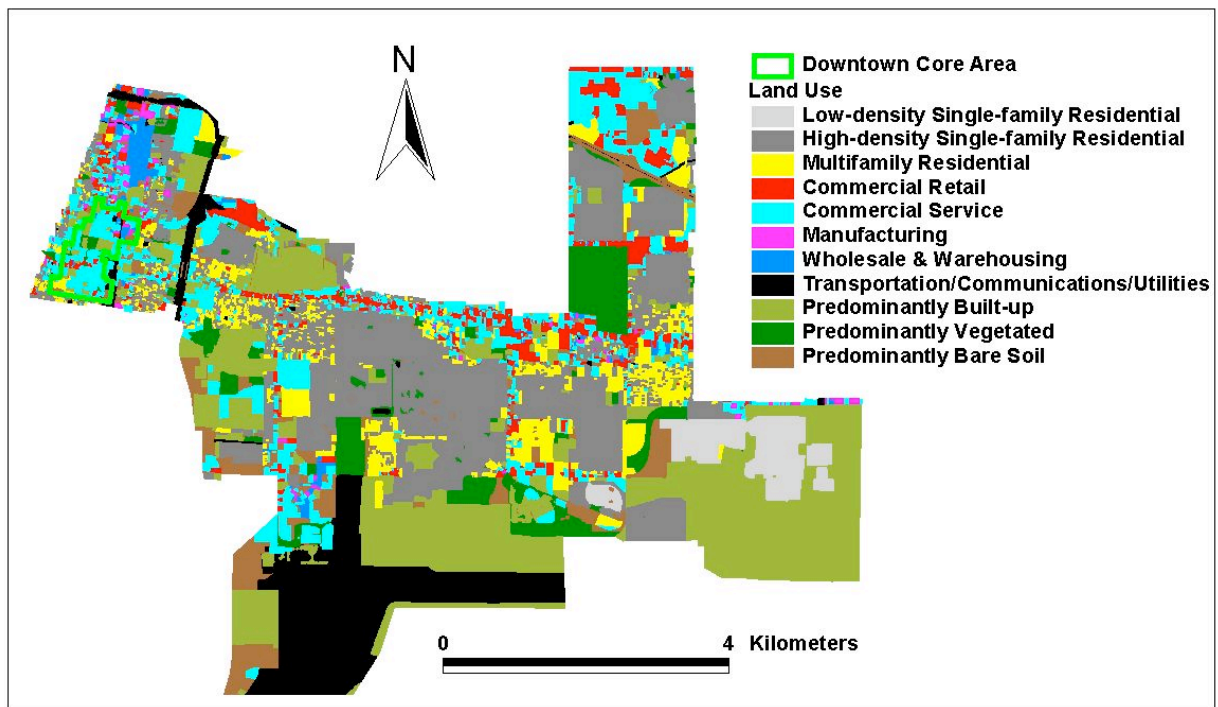


Figure 3. LULC dataset for the 48.5-km² study area aggregated to 14-category building analysis land use classification scheme.

4.0 Derivation of Urban Morphological Parameters

In the next ten sub-sections, we calculate building morphological parameters that are used in atmospheric models and dispersion models to account for urban effects. These calculations include building height statistics, the building plan area fraction (\bar{f}_p), building area density ($a_p(z)$), rooftop area density ($a_r(z)$), frontal area index (\bar{f}_F), frontal area density ($a_F(z)$), complete aspect ratio (\bar{f}_C), building surface area to plan area ratio (\bar{f}_B), height-to-width ratio (\bar{f}_S), the roughness length (z_o), and the displacement height (z_d). The calculation procedures and results are summarized in each sub-section.

4.1 Building Height Characteristics

Background. In this sub-section we summarize the height characteristics of buildings in the 48.5-km² study area. Average building height yields information on the depth through which the urban canopy directly impacts the atmosphere. Average building height (multiplied by a proportionality constant) can be used as a first-order approximation of the surface roughness z_o (see Section 4.10). Surface roughness is used in air quality and meteorological models to account for enhanced mixing and the drag effects of the underlying surface. Canopy height is often used as the length scale in the canopy layer. Urban field experiment data evaluations have suggested that similarity theory is valid somewhere above the canopy height. Below canopy height, drag parameterizations can be used to account for reduced air flow due to the urban fabric. Variation in canopy height may prove to be important in parameterizations of turbulence production.

Calculation Methods. The mean and standard deviation of building height were calculated using the following equations:

$$\bar{h} = \frac{\sum_{i=1}^N h_i}{N} \quad (1)$$

$$s_h = \sqrt{\frac{\sum_{i=1}^N (h_i - \bar{h})^2}{N - 1}} \quad (2)$$

where \bar{h} is the mean building height, s_h is the standard deviation of building height, h_i is the height of building i , and N is the total number of buildings in the area. The average building height weighted by building plan area was calculated using the following equation:

$$\bar{h}_{AW} = \frac{\sum_{i=1}^N A_i h_i}{\sum_{i=1}^N A_i} \quad (3)$$

where \bar{h}_{AW} is the mean building height weighted by building plan area, and A_i is the plan area at ground level of building i .

Results. For the 48.5-km² study area, the mean building height based on Eqn. (1) was calculated to be 4.7 m and the standard deviation was calculated to be 2.7 m. The mean building height weighted by plan area was computed to be 8.3 m for the study area. The building heights in the study area range from 3 m to 106.5 m.

Figure 4 is a histogram of building heights for the study area. Note that the building height bin widths are not equal and grow in size with height. The distribution is unimodal, with more than 70% of the buildings in the 0-5 m height bin. There is only 1 building with a height greater than 100 meters.

Figures 5, 6, 7, and 8 show the building height histograms for four of the land uses in the 7-category land use scheme: Residential, Commercial & Services, Industrial, and Other Urban or Built-up. The other land uses in the 7-category scheme do not have a sufficient number of buildings to produce meaningful histograms. Figure 5 shows that Residential buildings are predominantly one or two story structures, with a few high-rise buildings (> 15 m) present (likely apartment buildings or condominiums). In the Commercial & Services land use category (Fig. 6) we observe a similar distribution of building heights, but with a higher frequency of buildings with heights greater than 25 meters, which is expected because it includes the downtown area with high rises. The height distribution in the Industrial category has the mode located at the 5-10 meter height bin, indicating the higher frequency of 2-3 story structures compared to the more frequent single story structures in the Residential land use. All four distributions are unimodal with greater than 85% of the buildings with heights less than 10 m.

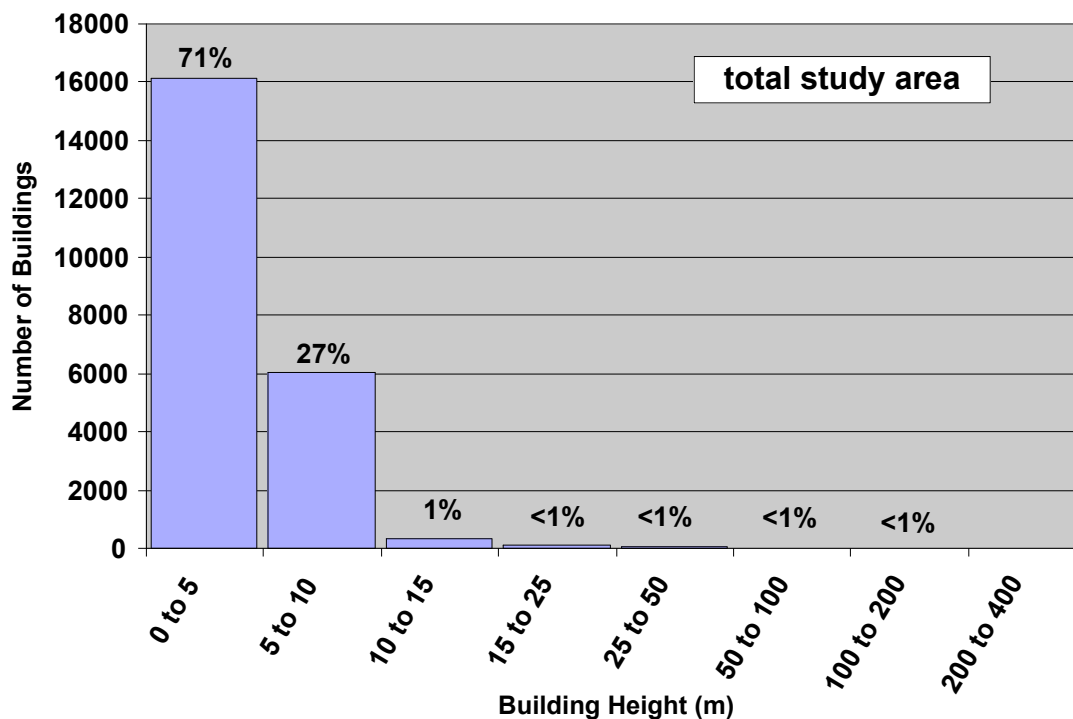


Figure 4. Distribution of building heights in the 48.5-km² Albuquerque study area. The percent of buildings in each height category are shown above each bar in the chart.

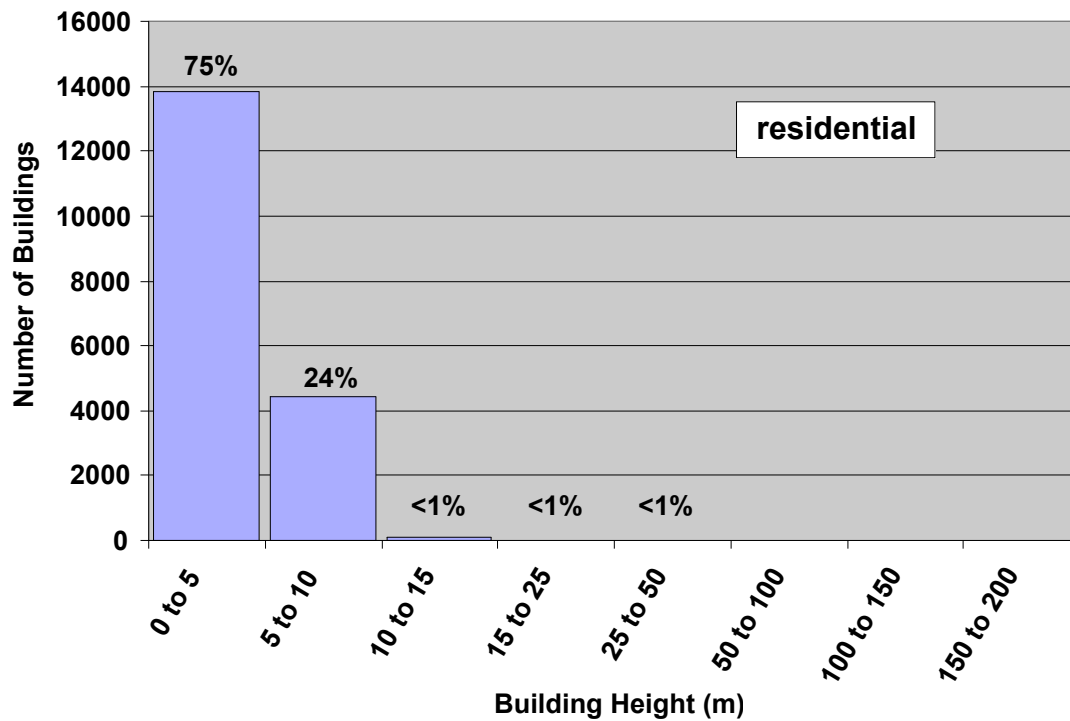


Figure 5. Distribution of building heights in the residential land use category.

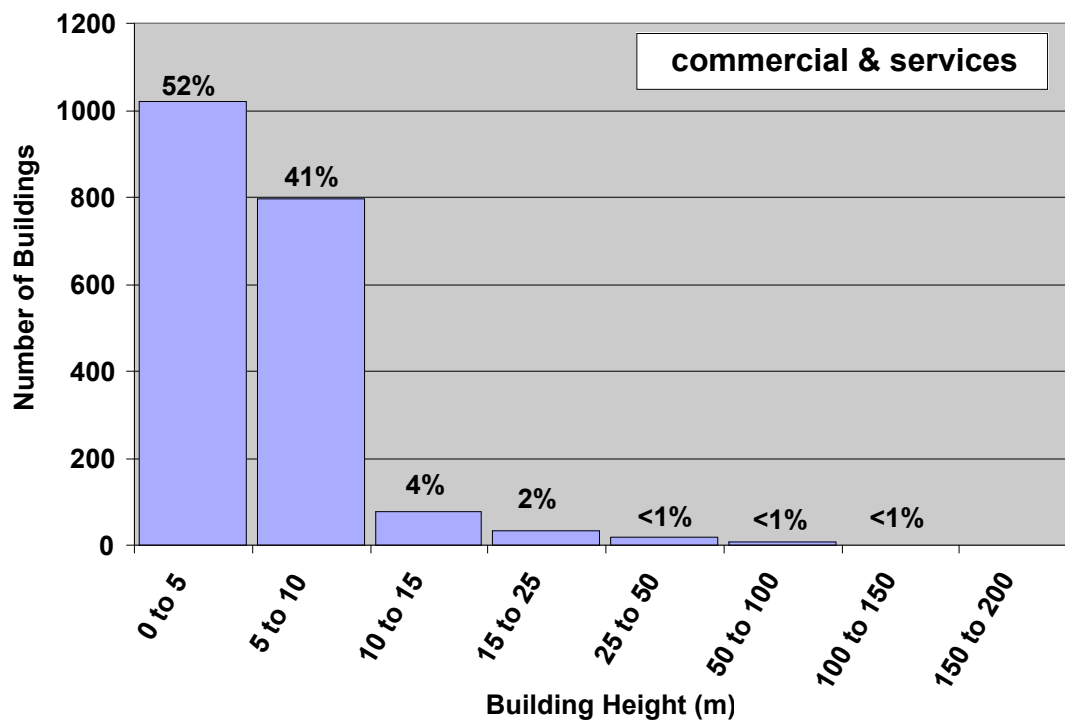


Figure 6. Distribution of building heights in the Commercial & Services land use category.

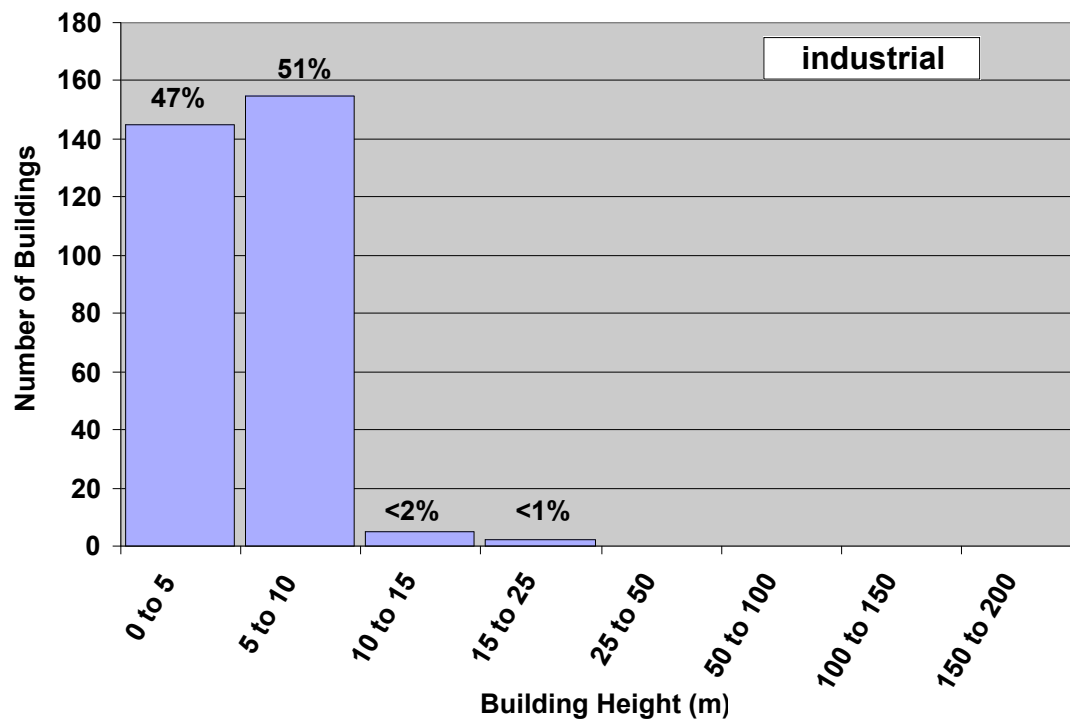


Figure 7. Distribution of building heights in the Industrial land use category.

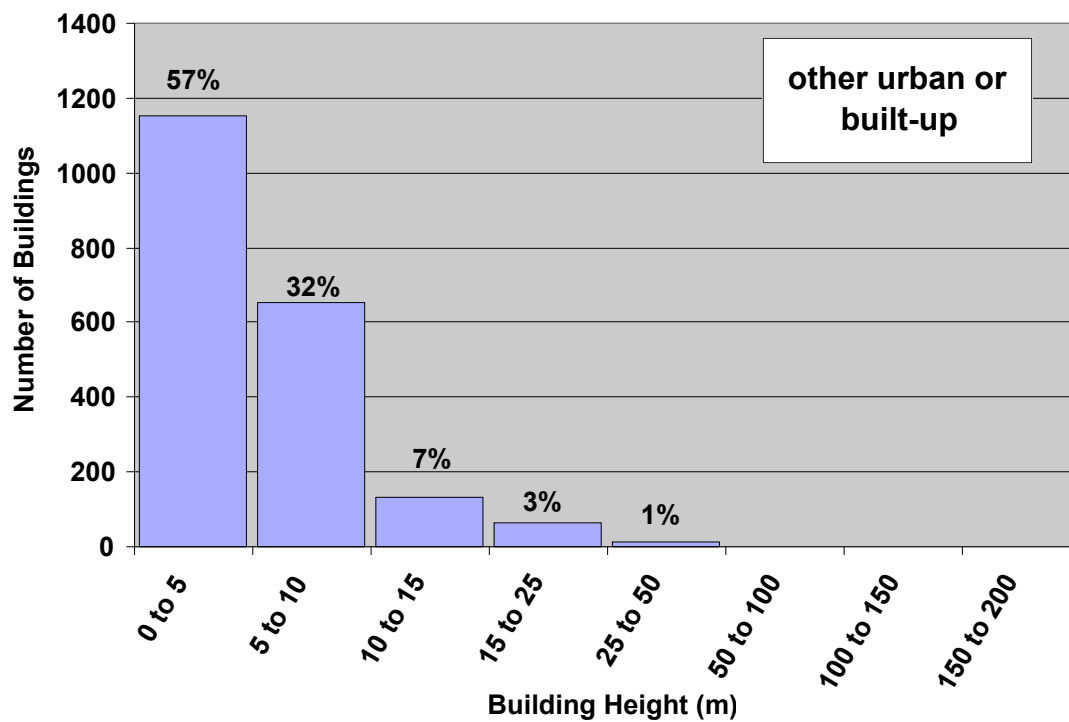


Figure 8. Distribution of building heights in the Other Urban or Built-up land use category.

Figures 9, 10, and 11 show the building height distributions for the Low-density Single-family Residential, High-density Single-family Residential, and the Multifamily Residential land use categories. The Low-density and High-density categories have very similar distributions, while the Multifamily Residential land use category contains a higher frequency of buildings in the 5-10 and 10-15 meter height categories.

Figures 12 and 13 show the building height histograms for the Commercial & Services sub-categories: Service and Retail. The two sub-categories have very similar histograms, except the Commercial Service category contains more high-rise structures (5% of the Commercial Service buildings are taller than 15 meters, compared to less than 1% for the Commercial Retail category).

Figures 14 and 15 show the building height histograms for the Industrial sub-categories: Manufacturing and Wholesale & Warehousing. The two sub-categories have very similar histograms, except the Wholesale & Warehousing has more structures in the 5-10 and 15-25 meter height categories.

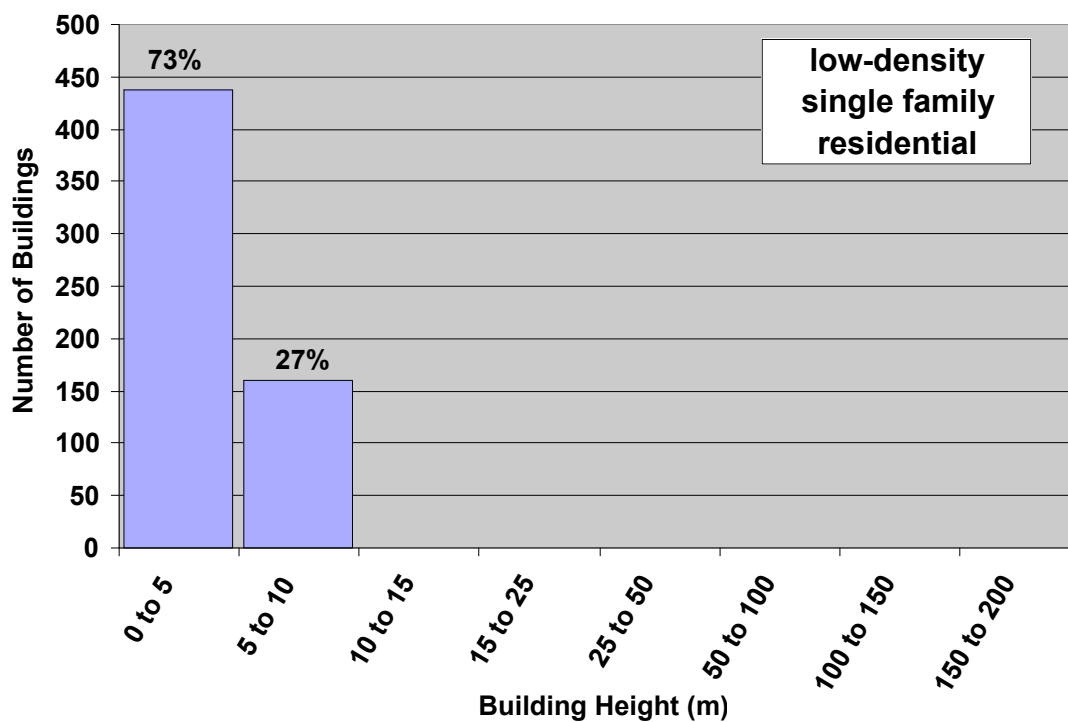


Figure 9. Distribution of building heights in the Low-density Single-family Residential land use category.

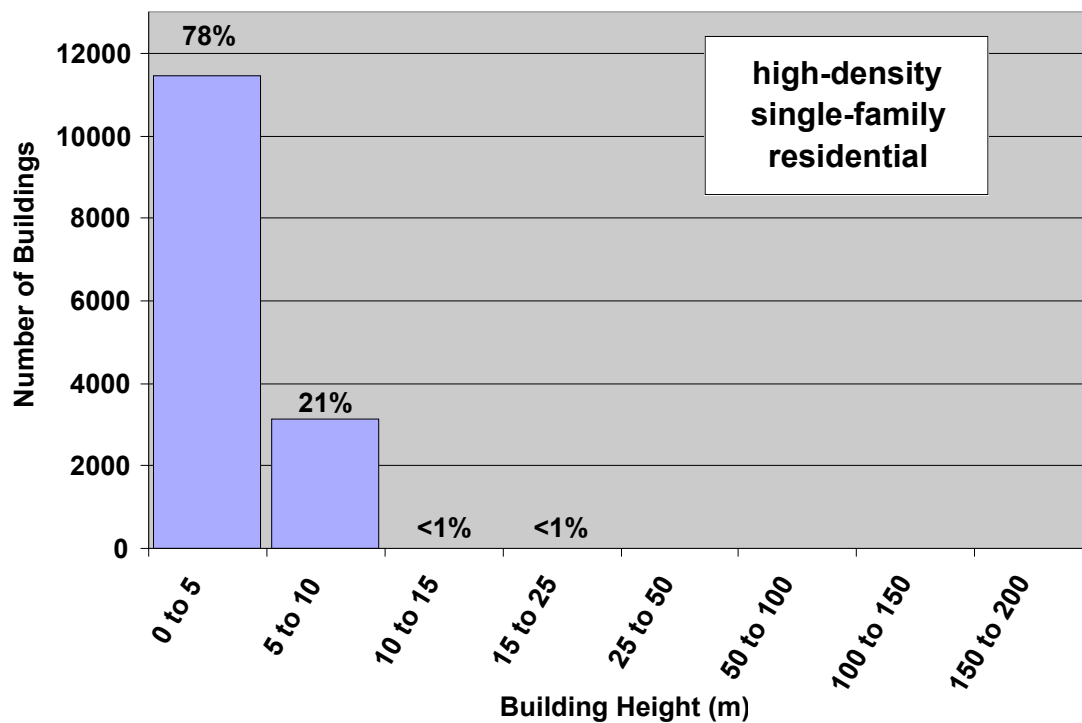


Figure 10. Distribution of building heights in the High-density Single-family Residential land use category.

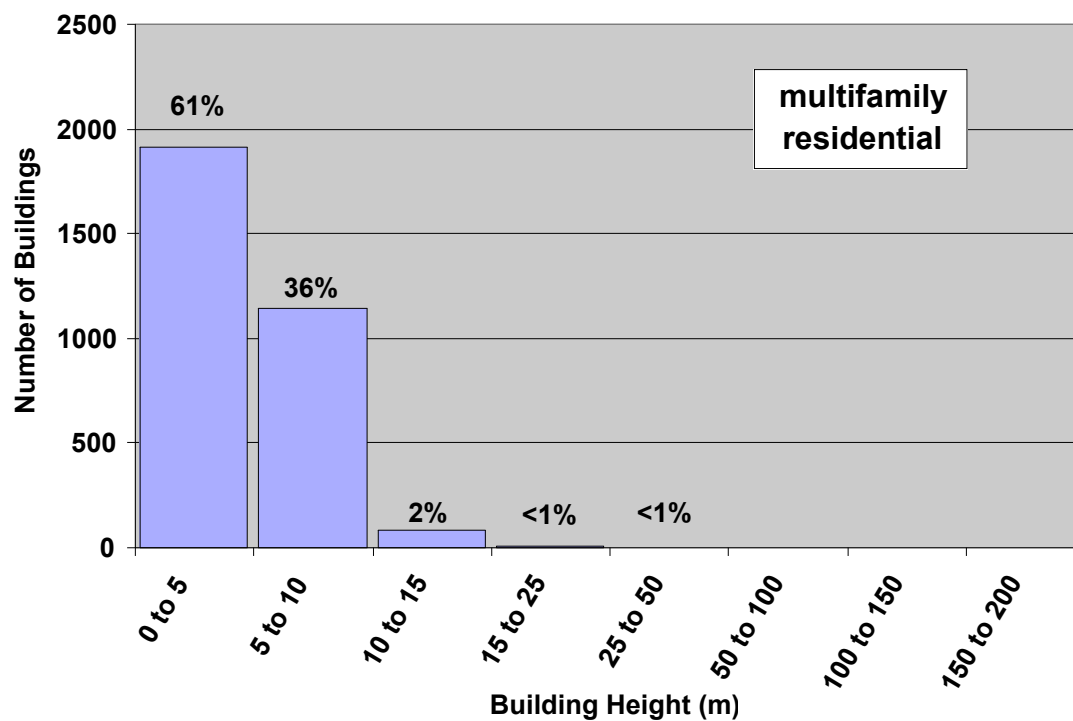


Figure 11. Distribution of building heights in the Multifamily Residential land use category.

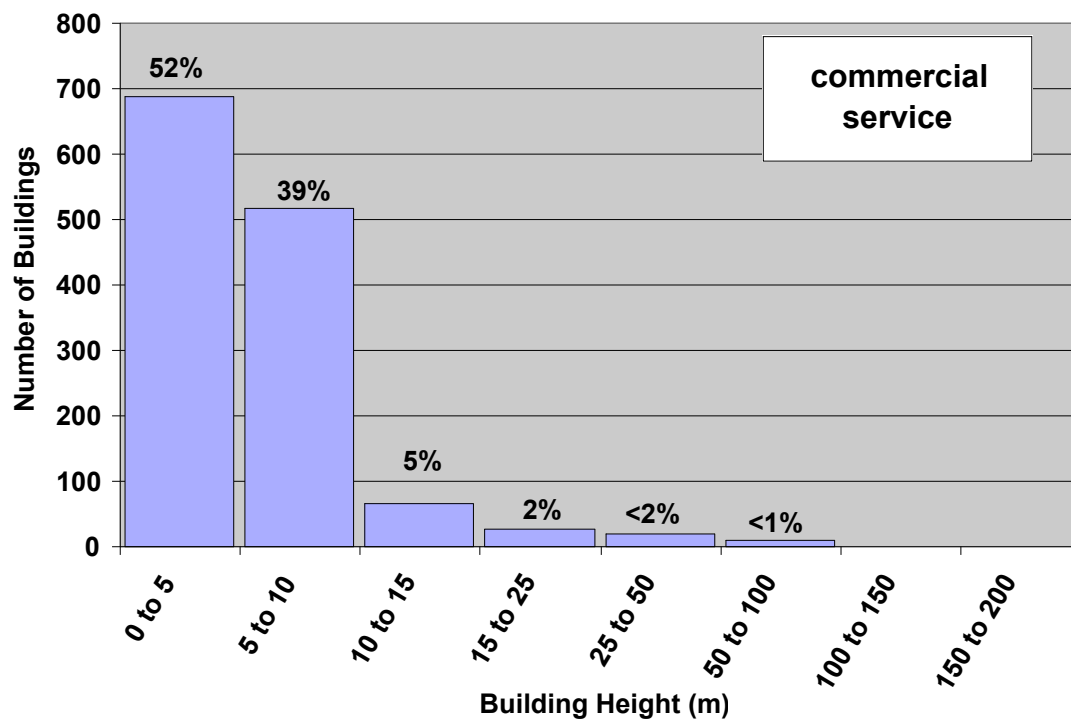


Figure 12. Distribution of building heights in the Commercial Service land use category.

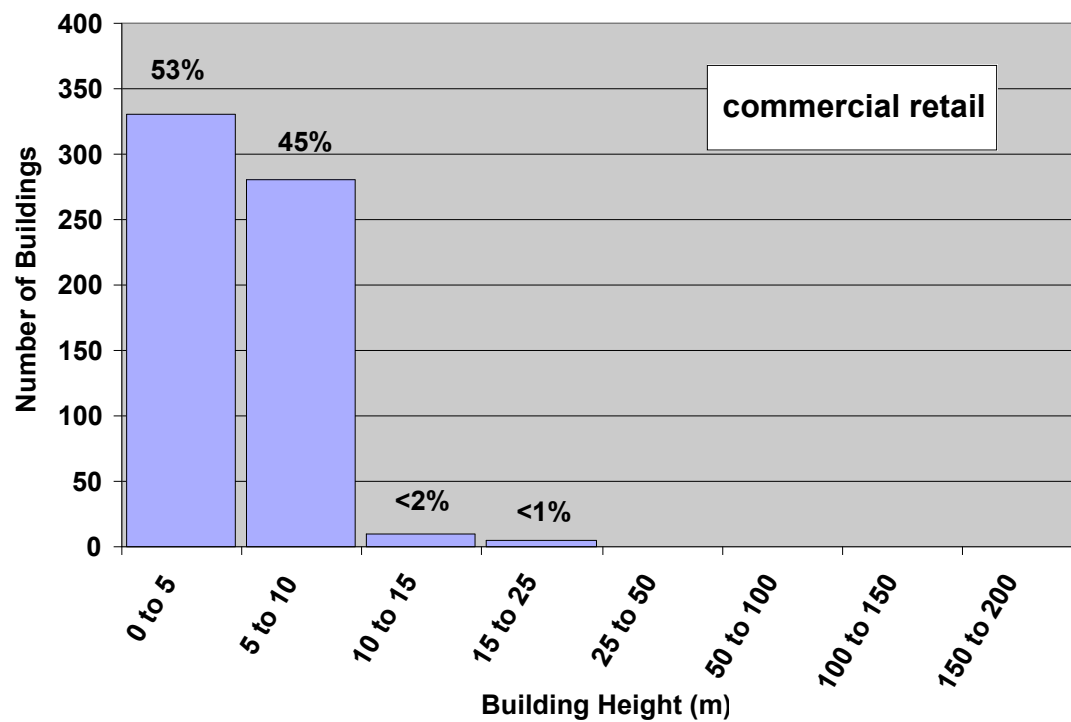


Figure 13. Distribution of building heights in the Commercial Retail land use category.

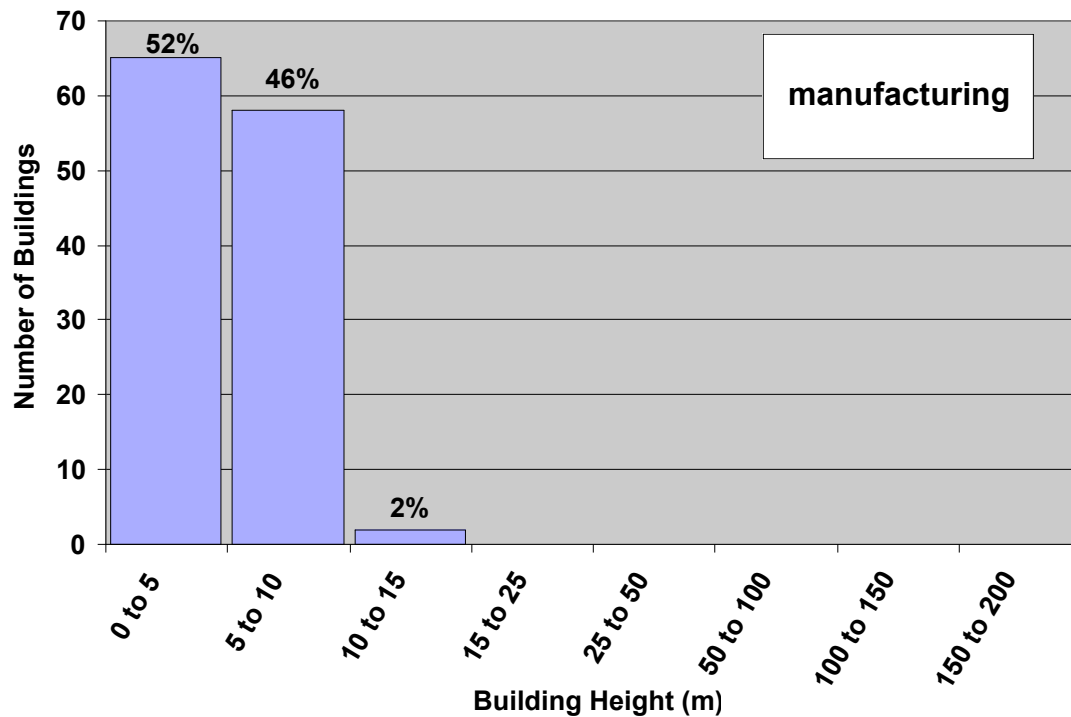


Figure 14. Distribution of building heights in the Manufacturing sub-category of Industrial land use.

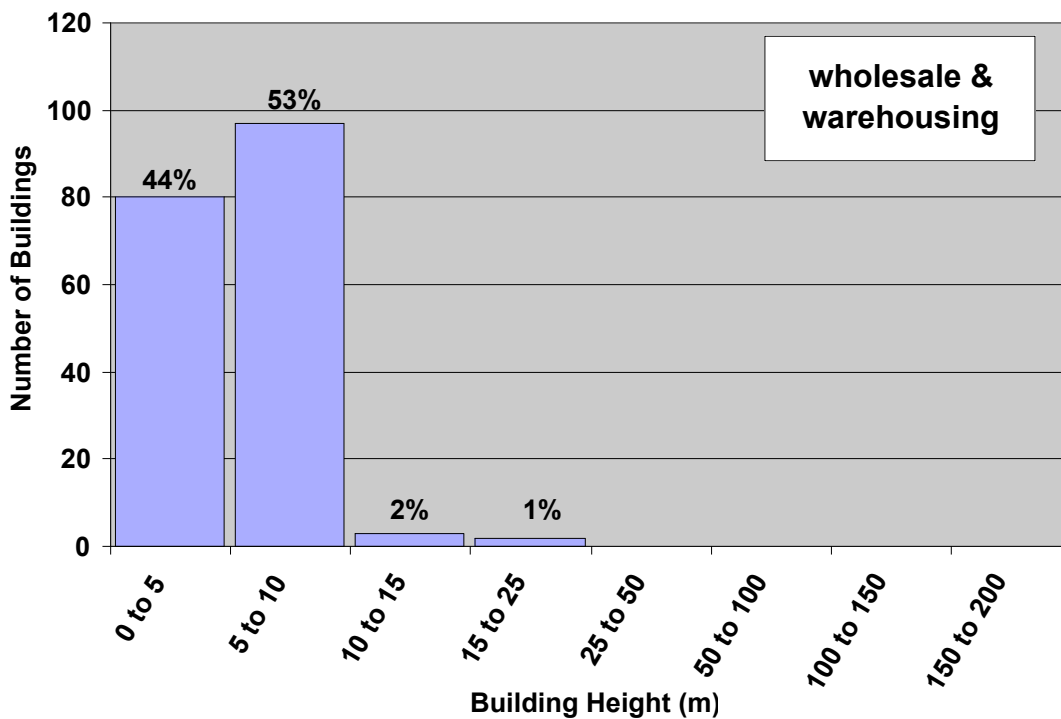


Figure 15. Distribution of building heights in the Wholesale & Warehousing sub-category of Industrial land use.

Figures 16, 17, and 18 show the building height histograms for the Other Urban or Built-up land use sub-categories: Predominantly Vegetated, Predominantly Bare Soil, and Predominantly Built-up. The building height distributions of the Predominantly Vegetated and Predominantly Bare Soil sub-categories are very similar. The Predominantly Built-up sub category contains more than two times the number of buildings with heights greater than 10 meters than the Vegetated and Bare Soil sub-categories.

Figures 19 and 20 show the building height histograms for the Urban High-rise land use and the Downtown Core Area. The Urban High-rise land use is by definition comprised of high-rise buildings (at least one building greater than 17.5 meters in the land use polygon), which explains the bimodal building height distribution. The Downtown Core Area building height distribution contains more than 60% of the buildings between 10 and 100 m.

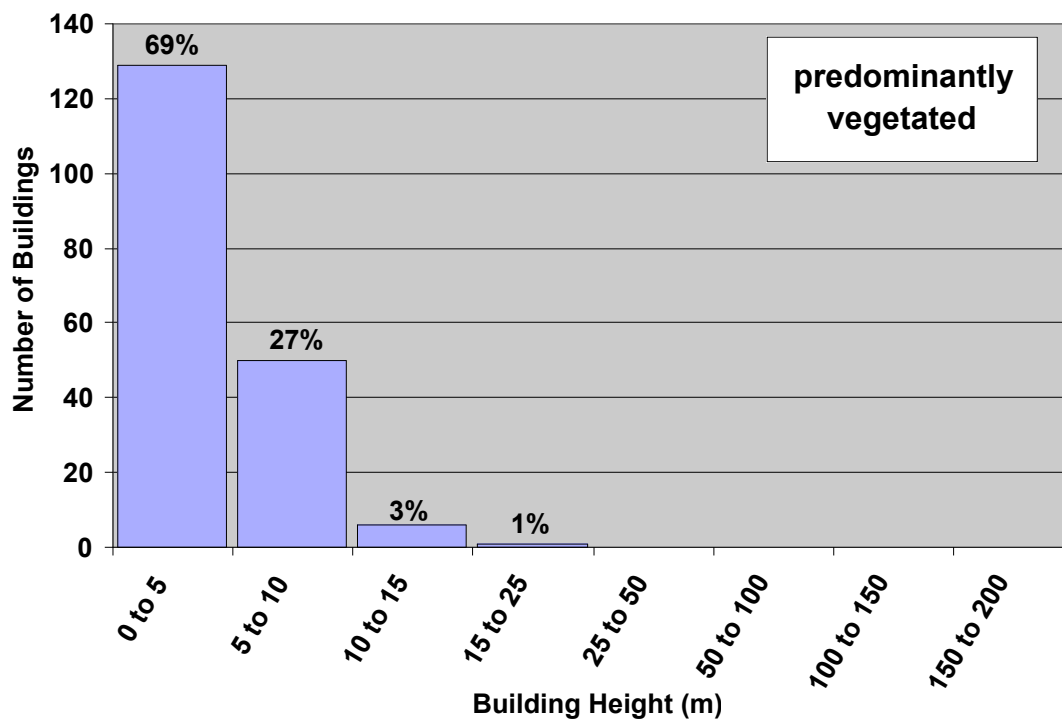


Figure 16. Distribution of building heights in the Predominantly Vegetated sub-category of the Other Urban or Built-up land use category.

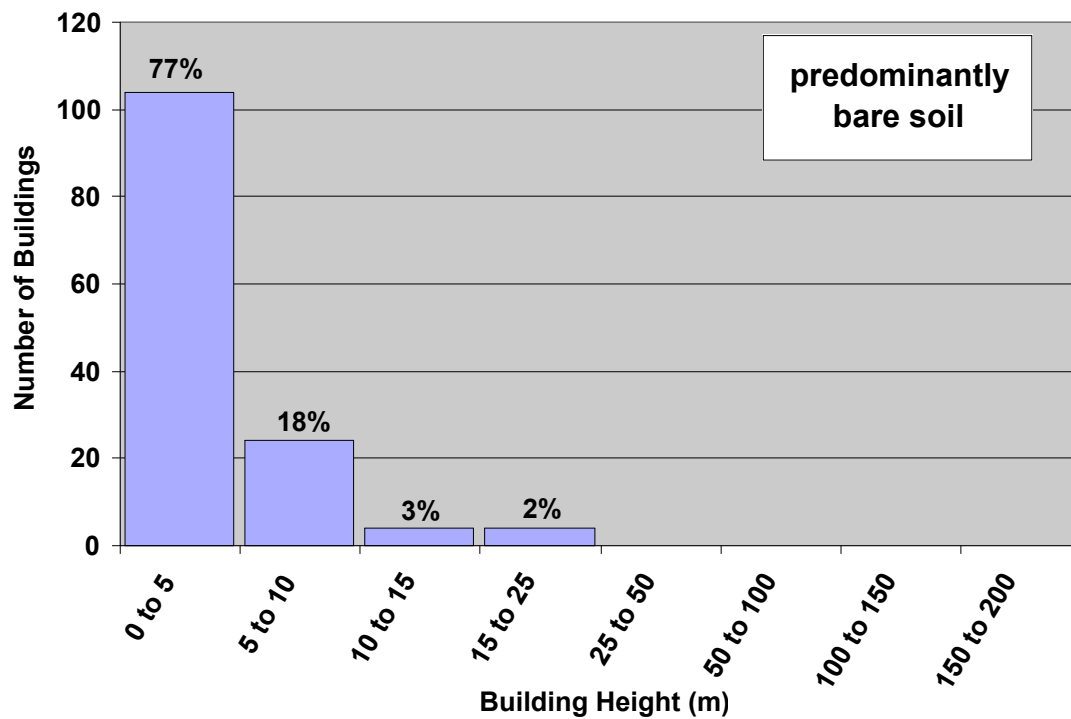


Figure 17. Distribution of building heights in the Predominantly Bare Soil sub-category of the Other Urban or Built-up land use category.

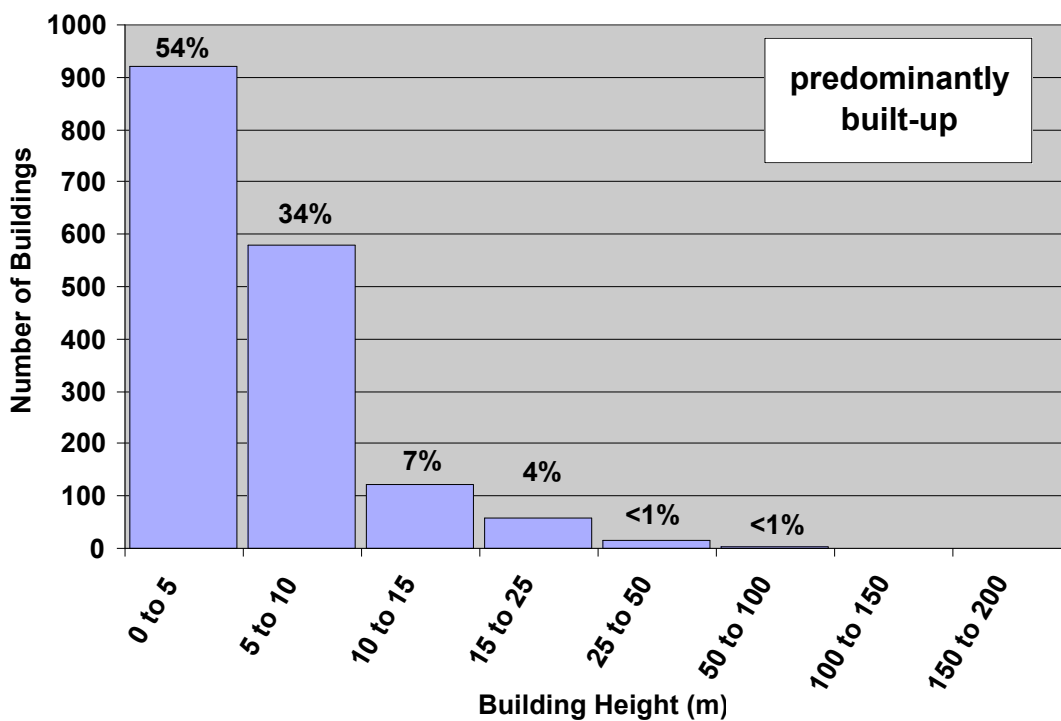


Figure 18. Distribution of building heights in the Predominantly Built-up sub-category of the Other Urban or Built-up land use category.

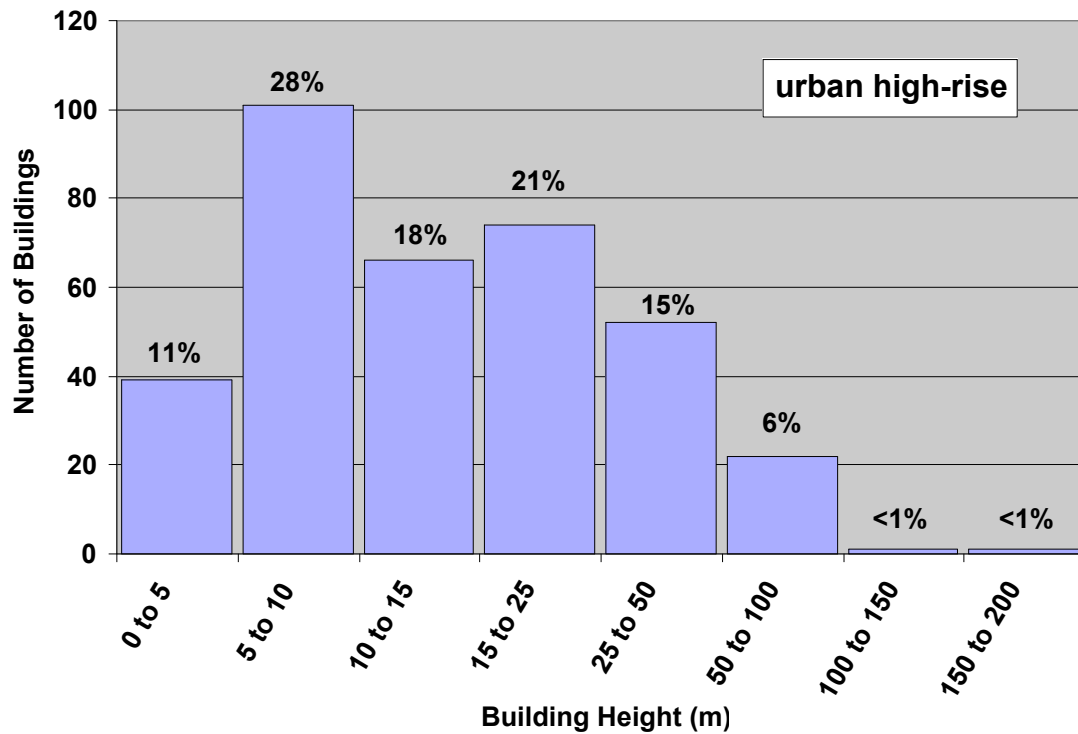


Figure 19. Distribution of building heights in the Urban High-rise land use category.

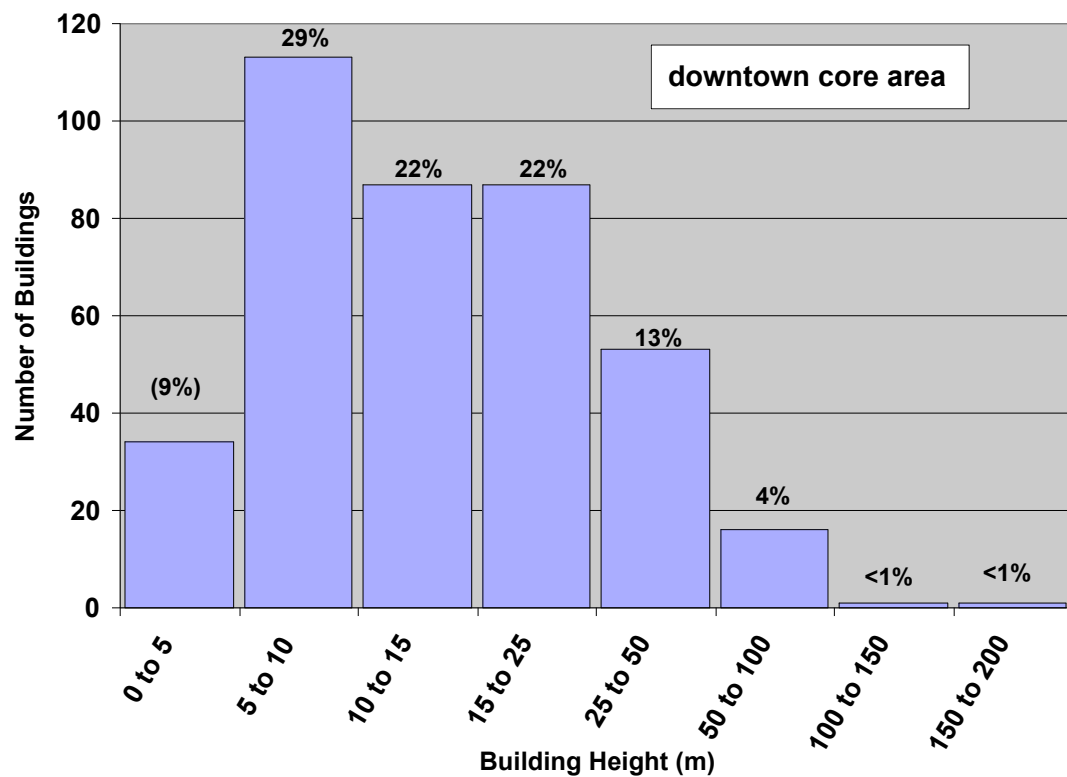


Figure 20. Distribution of building heights in the Downtown Core Area land use category.

Figure 21 displays a comparison of building height histograms in percentage form for all land use types in the 7-category classification scheme all in the same plot. Figure 22 shows the height histogram comparison for the 14-category land use scheme (the plots only include those land uses containing a significant number of buildings) and Urban High-rise land uses and the Downtown Core Area. One can better see in these plots the similarities and differences between different land use categories. For example, in Figure 21 the differences between the Residential and Commercial & Services land use distribution is apparent. In Figure 22, the differences between the Urban High-rise and Downtown Core Area and the other land uses is especially apparent for the height categories above 10 meters. Recall, however, that some of the land uses have significantly more buildings than others.

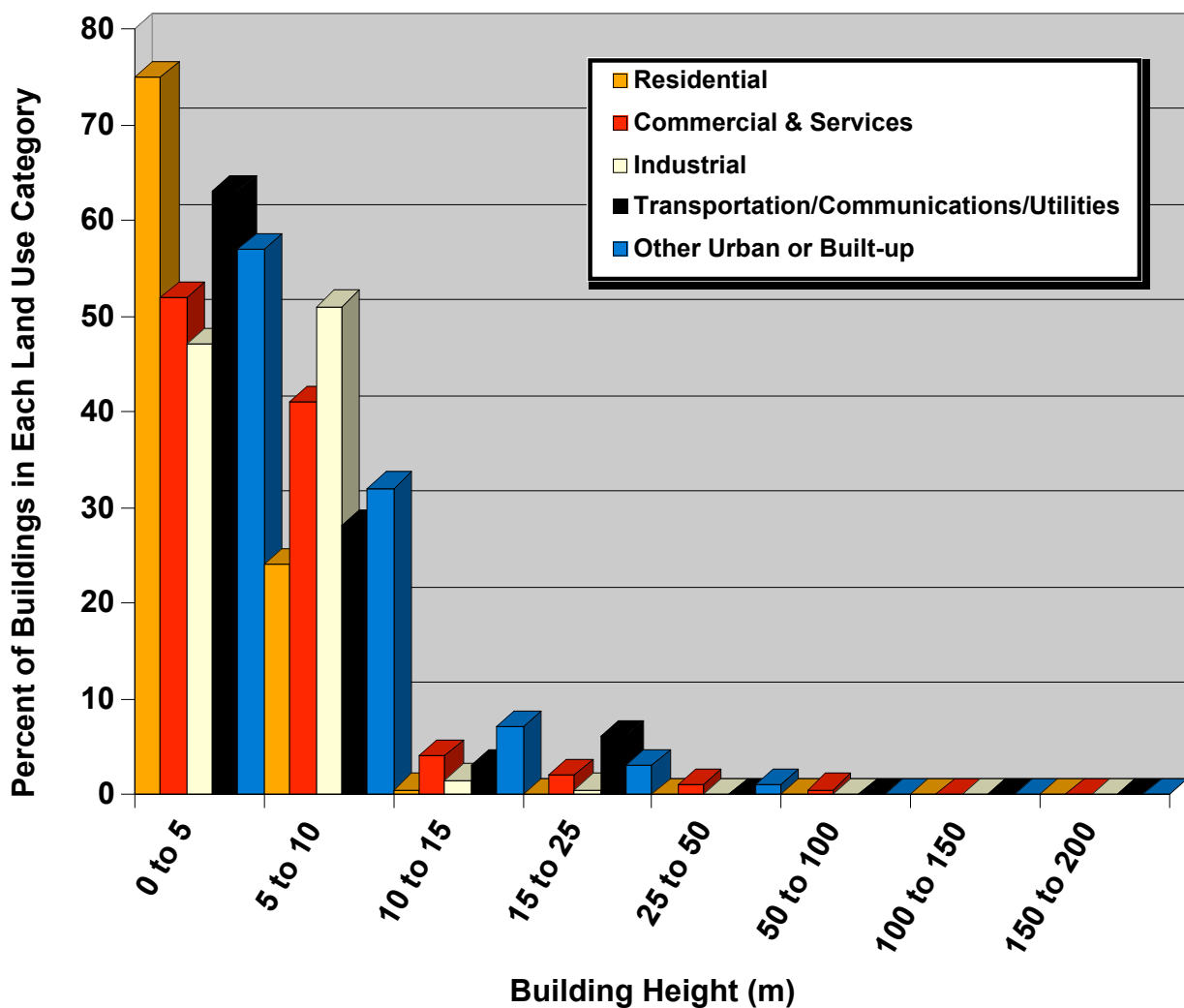


Figure 21. Comparison of the percent of buildings in each height increment for each 7-category land use type.

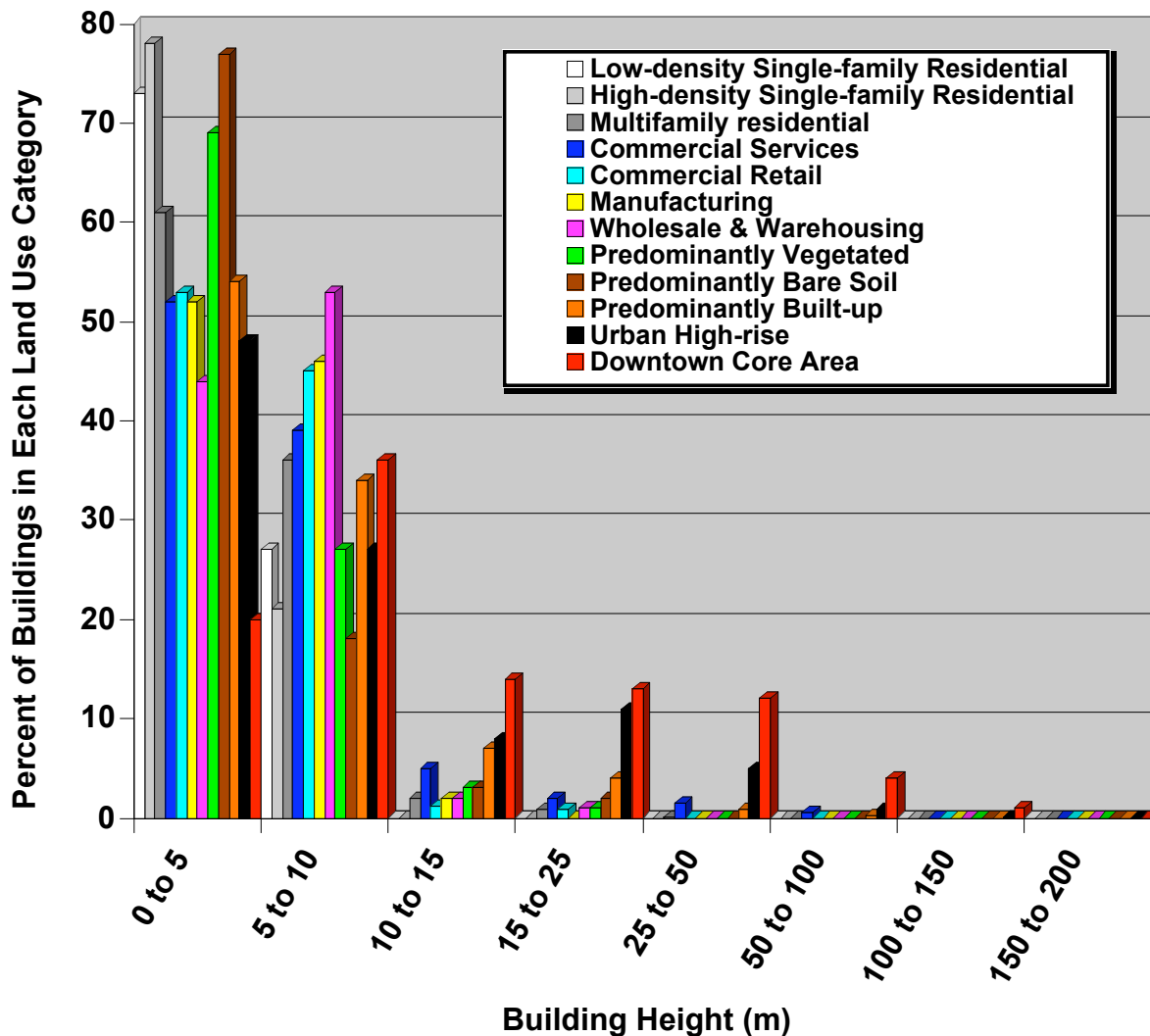


Figure 22. Comparison of the percent of buildings in each height increment for each 14-category land use class and the Urban High-rise and Downtown Core Area land uses.

Table 3 summarizes the building height characteristics as a function of land use. Several interesting features stand out. The building heights in the Residential land use average 1 story, and this does not change when looking at the plan-area weighted average. Table 3 also shows that the Commercial Service land use type has a higher mean building height (6.57 m) compared to the Commercial Retail land use type (5.24 m). Moreover, the Commercial Service land use has a much higher height standard deviation compared to Commercial Retail. Both of these facts indicate that the Commercial Service category contains more high-rise buildings. The relatively high standard deviations in the Urban High-rise and Downtown Core Area categories indicate a wide range of building heights in these categories. The buildings in the Urban High-rise land use have an average height of 9.43, which is much less than the Downtown Core Area average height of 15.15 m. The average height in the Downtown Core Area (15.15m) is similar to the value computed for Phoenix (17.2 m) (Burian et al. 2002c), but less than the value found for Salt Lake City (23.6 m) (Burian et al. 2002e), and much lower than the average height of 45.0 m in the Los Angeles Downtown Core Area (Burian et al. 2002b).

Table 3. Summary of building characteristics for the Albuquerque study area as a function of land use type.

Land Use Class	Number of Buildings	Average Height (m)	Standard Deviation	Plan Area-weighted Average Height (m)
Residential	18,346	4.34	1.43	4.88
Low-density Single-family (< 8 units/hectare)	598	4.20	1.07	4.40
High-density Single-family (≥ 8 units/hectare)	14,602	4.20	1.17	4.45
Multifamily	3,146	5.03	2.17	6.14
Mixed	---	---	---	---
Commercial & Services	1,955	6.14	5.95	12.22
Service	1,328	6.57	7.03	12.98
Retail	627	5.24	2.16	11.09
Industrial	307	5.53	2.24	7.61
Manufacturing	125	5.12	1.78	6.36
Wholesale & Warehousing	182	5.81	2.48	8.05
Transportation/Communications/Utilities	35	5.56	3.62	8.77
Mixed Industrial & Commercial	---	---	---	---
Mixed Urban or Built-up	---	---	---	---
Other Urban or Built-up	2,019	6.14	4.55	11.84
Predominantly Vegetated	186	4.86	2.41	7.53
Predominantly Bare Soil	136	5.04	3.00	9.00
Predominantly Built-up	1,697	6.37	4.79	12.39
Urban High-rise	767	9.43	10.58	19.15
Downtown Core Area	165	15.15	16.00	24.64

4.2 Building Plan Area Fraction (\square_p)

Background. Building plan area fraction has been shown to be related to the surface roughness z_0 (see Section 4.10). Surface roughness is used in air quality and meteorological models to account for enhanced mixing and drag effects of the rough surface. In the urban context, as the density of buildings (plan area fraction) increases so does the roughness of the system, but a threshold is eventually reached where adding new elements effectively reduces the drag of the elements present (Grimmond and Oke 1999). The density of buildings also indicates the potential flow regime. Hussain and Lee (1980) performed wind-tunnel experiments and found that three flow regimes develop in idealized urban street canyons: (1) isolated flow, (2) wake interference flow, and (3) skimming flow. The isolated flow regime occurs when elements are spaced relatively far apart ($0 < \square_p < 0.1$), the wake interference flow occurs when elements are spaced at a medium density level ($0.1 < \square_p < 0.6$), and the skimming flow regime occurs for high-density building arrangements ($\square_p > 0.6$) (Oke 1988).

Calculation Methods. The building plan area fraction (\square_p) is defined as the ratio of the plan area of buildings to the total surface area of the study region:

$$\square_p = \frac{A_p}{A_T} \quad (4)$$

where A_p is the plan area of buildings at ground level, i.e., the footprint area, and A_T is the total plan area of the region of interest, i.e., an arbitrary area that encompasses the buildings (see Figure 23). The computed value of the plan area fraction is dependent on the size of the area or the specific land use types included in the calculation. In most cases the plan area fraction will vary significantly from one city block to the next because of the heterogeneous nature of the urban landscape. The appropriate size of the calculation element should be chosen such that the characteristics of interest in the urban area are homogeneous and discernible.

Results. For the 48.5-km² study area the plan area fraction at ground level was calculated to be 0.13. This value is significantly lower than the plan area fraction of 0.47 found for Mexico City, Mexico (Grimmond and Oke 1999) and the 0.37 found for Vancouver, British Columbia, Canada (Voogt and Oke 1997), but more consistent with the 0.23 found for Salt Lake City (Burian et al. 2002c), another Western U.S. city. The difference between the two Western U.S. cities and Mexico City and Vancouver is partially due to the newer development patterns with relatively wide streets and greater amounts of open space. Another reason is the study area for Albuquerque is much greater in aerial extent than the Mexico City and Vancouver sites and includes a higher amount of residential areas, which usually have lower building plan area fractions than commercial and industrial areas. Another major factor is the presence of two major highways and the Albuquerque International Airport in the study area, which include a significant amount of open space.

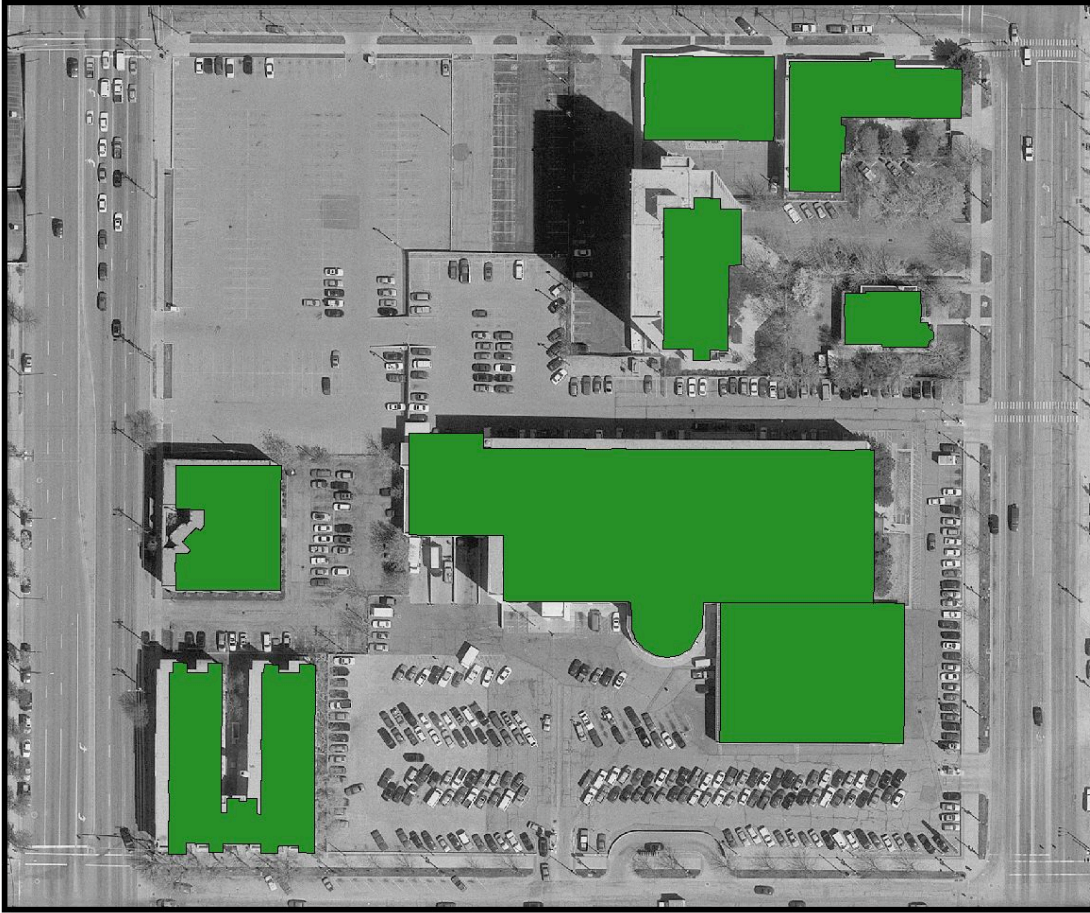


Figure 23. Illustration of building plan area fraction. The building plan area (A_p) in this scene is the sum of the areas of the building footprints shown in green. The total plan area (A_T) is the area enclosed by the outline of the figure. The building plan area fraction ($\bar{\square}_p$) is computed by dividing building plan area (A_p) by total plan area (A_T).

We have calculated the plan area fraction (and subsequent parameters) on two meshes overlaid onto the study area in order to view the spatial heterogeneity. Figure 24 shows the two meshes overlaid onto land use: in the first case, a uniform 100-m X 100-m rectilinear grid cell mesh covering the entire 48.5-km² study area, and in the second case a non-uniform polygonal grid cell mesh based on the land use polygons. Figure 25 shows the plan area fraction according to the two grid cell meshes. The open space associated with the airport is clearly shown. Moreover the relatively high amount of open space in the city is displayed by the distribution of blue throughout both parts of the figure. It is more difficult to see a one-to-one correlation with urban land use type, i.e., there appears to be significant variation in $\bar{\square}_p$ within an urban land use type, except for Residential, which is predominantly in the 0.1-0.25 range (as indicated in part (a) of Fig. 25).

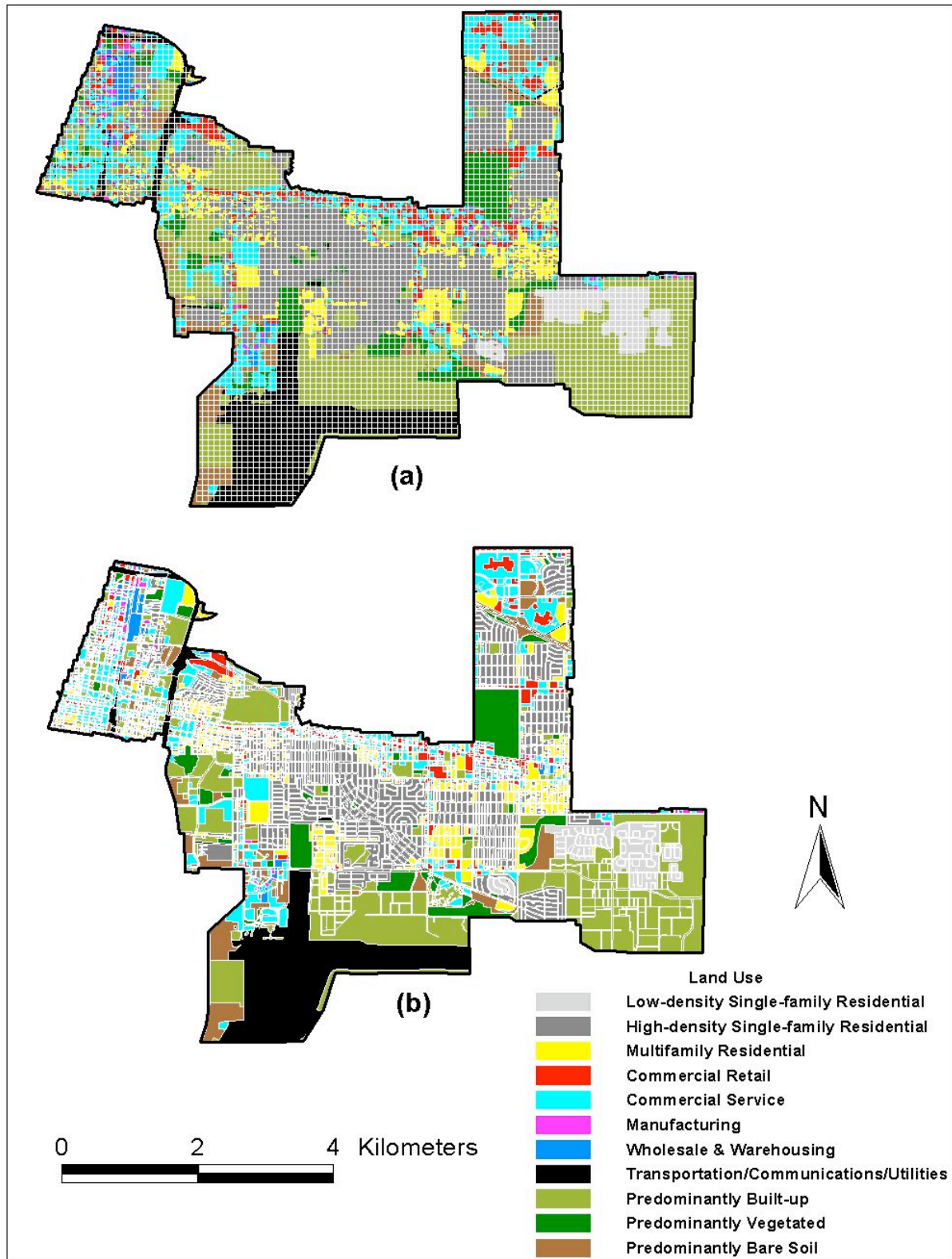


Figure 24. Grid cells used to display and analyze the spatial heterogeneity of the Albuquerque building morphology for the 48.5-km² study area. Urban land use type overlaid with (a) the 100m X 100m uniform grid cell mesh, and (b) the non-uniform grid cells based on land use polygons.

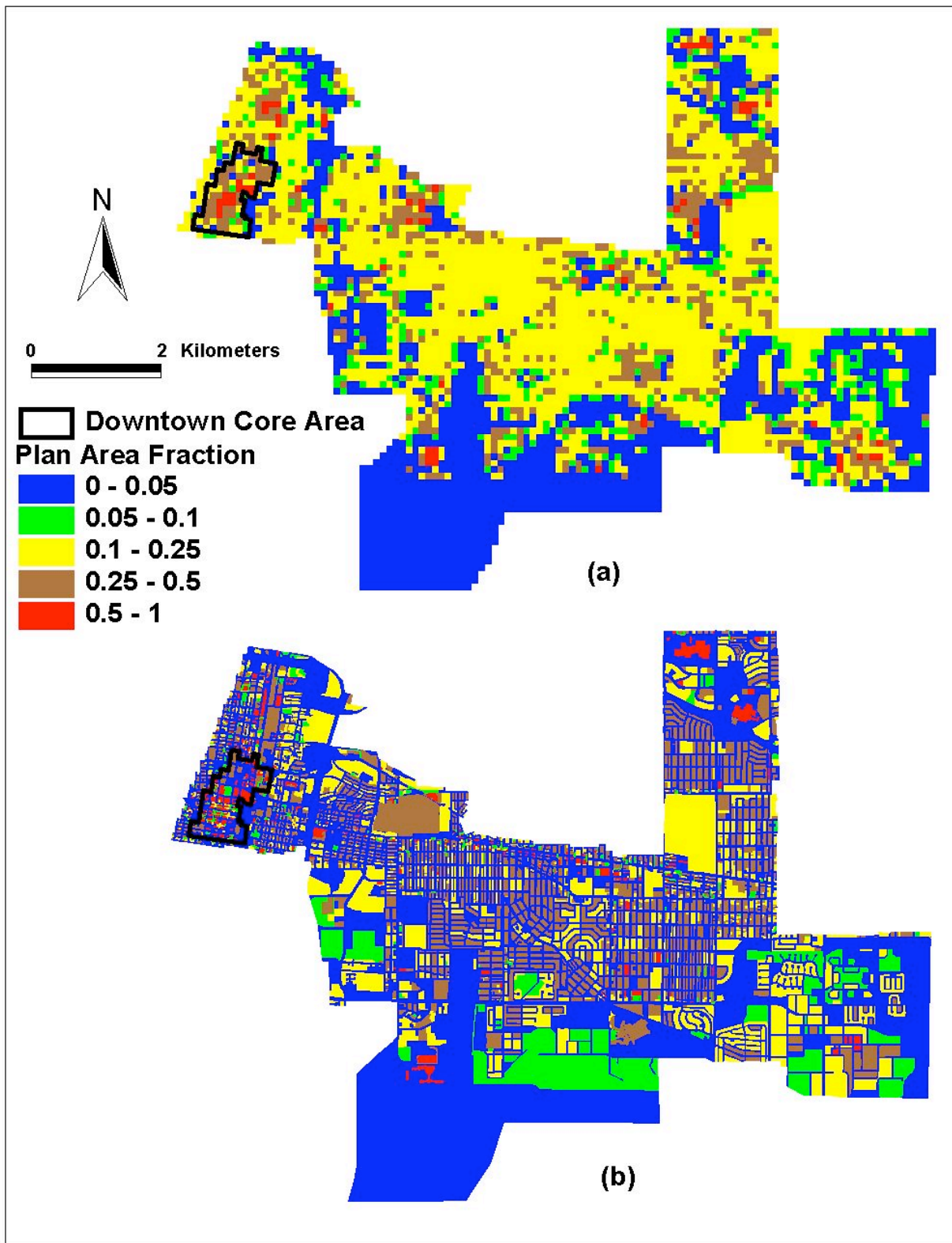


Figure 25. Spatial variability of building plan area fraction (\bar{f}_p) distributed according to a uniform 100-m X 100-m grid mesh and a non-uniform grid mesh based on the land use polygons.

Table 4 contains the computed $\bar{\lambda}_p$ for each land use type in the land use classification schemes described in Section 3.2. Table 4 indicates that the Residential, Commercial & Services, and the Industrial land use categories all have relatively high building plan area fractions (near 0.20 or above). The Other Urban or Built-up land use contains a significant amount of institutional land use that contains large amounts of open space. Most of the average values shown in Table 4 fall within the $\bar{\lambda}_p$ range for wake interference flow ($0.1 < \bar{\lambda}_p < 0.6$) (Hussain and Lee 1980).

Table 4. Plan area fraction as a function of land use type

Land Use Class	$\bar{\lambda}_p$
Residential	0.19
Low-density Single-family (< 8 units/hectare)	0.10
High-density Single-family (≥ 8 units/hectare)	0.19
Multifamily	0.24
Mixed	---
Commercial & Services	0.17
Service	0.14
Retail	0.25
Industrial	0.29
Manufacturing	0.22
Wholesale & Warehousing	0.32
Transportation/Communications/Utilities	0.00
Mixed Industrial & Commercial	---
Mixed Urban or Built-up	---
Other Urban or Built-up	0.09
Predominantly Vegetated	0.05
Predominantly Bare Soil	0.01
Predominantly Built-up	0.13
Urban High-rise	0.22
Downtown Core Area	0.30

In Table 5, we compare the computed building plan area fraction values for several land use types in Albuquerque to those reported in other studies. Our computed values of $\bar{\lambda}_p$ for Residential and Industrial land use types are smaller than those of other cities. The High-density Single-family Residential value of 0.19 in Albuquerque is the same as the plan area fraction of High-density Single-family Residential land use in Salt Lake City. The data indicate that the Downtown Core Area of Albuquerque has a plan area fraction (0.30) similar to the plan area fractions of Downtown Core Areas of other Western U.S. cities (e.g., Los Angeles, Phoenix, Portland, and Salt Lake City). The plan area fraction values computed for some of these other studies have included the plan area of trees in residential areas, which can be a significant fraction of the plan area. Trees are not included in our calculations of $\bar{\lambda}_p$ and explain some of the differences. Visual inspection of aerial photos suggests that there are relatively few trees and shrubs in the downtown areas of our study region.

Table 5. Comparison of plan area fraction (\bar{f}_p) for Albuquerque to other cities. Locations grouped by land use type and then listed in order of decreasing \bar{f}_p .

Location	Land Use Class	\bar{f}_p	Source
Vancouver, BC, Canada	Suburban residential	0.62	Voogt and Oke (1997)
Sacramento, CA	Suburban residential	0.58	Grimmond and Oke (1999)
Arcadia, CA	Suburban residential	0.53	Grimmond and Oke (1999)
Chicago, IL	Suburban residential #1	0.47	Grimmond and Oke (1999)
Chicago, IL	Suburban residential #2	0.38	Grimmond and Oke (1999)
San Gabriel, CA	Suburban residential	0.36	Grimmond and Oke (1999)
Miami, FL	Suburban residential	0.35	Grimmond and Oke (1999)
Tucson, AZ	Suburban residential	0.33	Grimmond and Oke (1999)
Los Angeles, CA	Mixed residential	0.29	Burian et al. (2002b)
Los Angeles, CA	High-density single-family residential	0.27	Burian et al. (2002b)
Portland, OR	Multifamily residential	0.26	Burian et al. (2002d)
Albuquerque, NM	High-density single-family residential	0.19	This Report
Salt Lake City, UT	High-density single-family residential	0.19	Burian et al. (2002e)
Phoenix, AZ	Multifamily residential	0.18	Burian et al. (2002c)
Los Angeles, CA	Industrial	0.38	Burian et al. (2002b)
Vancouver, BC, Canada	Light industrial	0.38	Voogt and Oke (1997)
Portland, OR	Industrial	0.31	Burian et al. (2002d)
Albuquerque, NM	Industrial	0.29	This Report
Salt Lake City, UT	Industrial	0.27	Burian et al. (2002e)
Phoenix, AZ	Industrial	0.19	Burian et al. (2002c)
Mexico City, Mexico	Downtown	0.47	Grimmond and Oke (1999)
Vancouver, BC, Canada	Downtown	0.37	Voogt and Oke (1997)
Portland, OR	Downtown core area	0.34	Burian et al. (2002d)
Salt Lake City, UT	Downtown core area	0.33	Burian et al. (2002e)
Los Angeles, CA	Urban high-rise	0.32	Burian et al. (2002b)
Phoenix, AZ	Downtown core area	0.32	Burian et al. (2002c)
Albuquerque, NM	Downtown core area	0.30	This Report
Los Angeles, CA	Downtown core area	0.29	Burian et al. (2002b)

4.3 Building Plan Area Density ($a_p(z)$)

Background. The building plan area density gives information on how much of the air volume is occupied by buildings (when multiplied by the height increment of the volume of interest). The change in building plan area density with height yields the roof fraction (see Section 4.4). The roof fraction is important from a thermodynamic perspective because of the significant solar gain and heat loss at the building roof level. The building plan area density can be used to derive the roof area density, which is analogous to the leaf area density. The leaf area density gives information on how much long- and short-wave radiation travels through the canopy and how much is intercepted. Something similar might be done for urban areas with buildings using the building plan area density. Building plan area density can also be used as a surrogate for frontal area density (see Section 4.5) in evaluating the drag force as a function of height due to buildings in urban areas.

Calculation Methods. The building plan area density ($a_p(z)$) is defined as the average building plan area within a height increment divided by the volume of the height increment:

$$a_p(z) = \frac{\frac{1}{\Delta z} \int_{z - \frac{1}{2}\Delta z}^{z + \frac{1}{2}\Delta z} A_p(z') dz'}{A_T \Delta z} \quad (5)$$

where, $A_p(z')$ is the plan area of buildings at height z' , A_T is the plan area of the site, and Δz is the height increment for the calculation. Since A_T is not a function of height we can bring it into the integral in the numerator and obtain:

$$a_p(z) = \frac{\frac{1}{\Delta z} \int_{z - \frac{1}{2}\Delta z}^{z + \frac{1}{2}\Delta z} \frac{A_p(z')}{A_T} dz'}{\Delta z} \quad (6)$$

Knowing $\overline{A_p}(z') = A_p(z')/A_T$ and assuming that the building plan area does not change appreciably within a height increment Δz , eq. (6) can be approximated by:

$$a_p(z) \approx \frac{\overline{A_p}(z)}{\Delta z} \quad (7)$$

Results. Figure 26 illustrates the building plan area density function ($a_p(z)$) for the Albuquerque study area using a 1-m height increment. As expected, $a_p(z)$ is constant for the first few meters

above ground elevation until the rooftop height of the shortest buildings are reached (approximately four meters). Building plan area density then rapidly declines with height and asymptotically approaches $\bar{a}_p = 0$. Only the first 60 m above ground elevation are shown because $a_p(z)$ is nearly zero above this height.

Figure 27 shows $a_p(z)$ for the 7-category land use scheme. Only the land uses that have sufficient buildings to produce meaningful plots are illustrated. The building plan area density of the Industrial and Residential land uses decreases relatively rapidly with height above four meters, indicating that these land use categories contain mostly one, two, and three story buildings. The Other Urban or Built-up land use decreases less rapidly, while the Commercial & Services category decreases the slowest. The $a_p(z)$ for the Industrial land use is the largest near the ground, indicating that the buildings in this land use type have a relatively large footprint and are densely packed. Figure 28 shows $a_p(z)$ for several land use types in the 14-category scheme, as well as the Downtown Core Area. The plot shows that the $a_p(z)$ associated with the Downtown Core Area decreases much less rapidly than the other land use types.

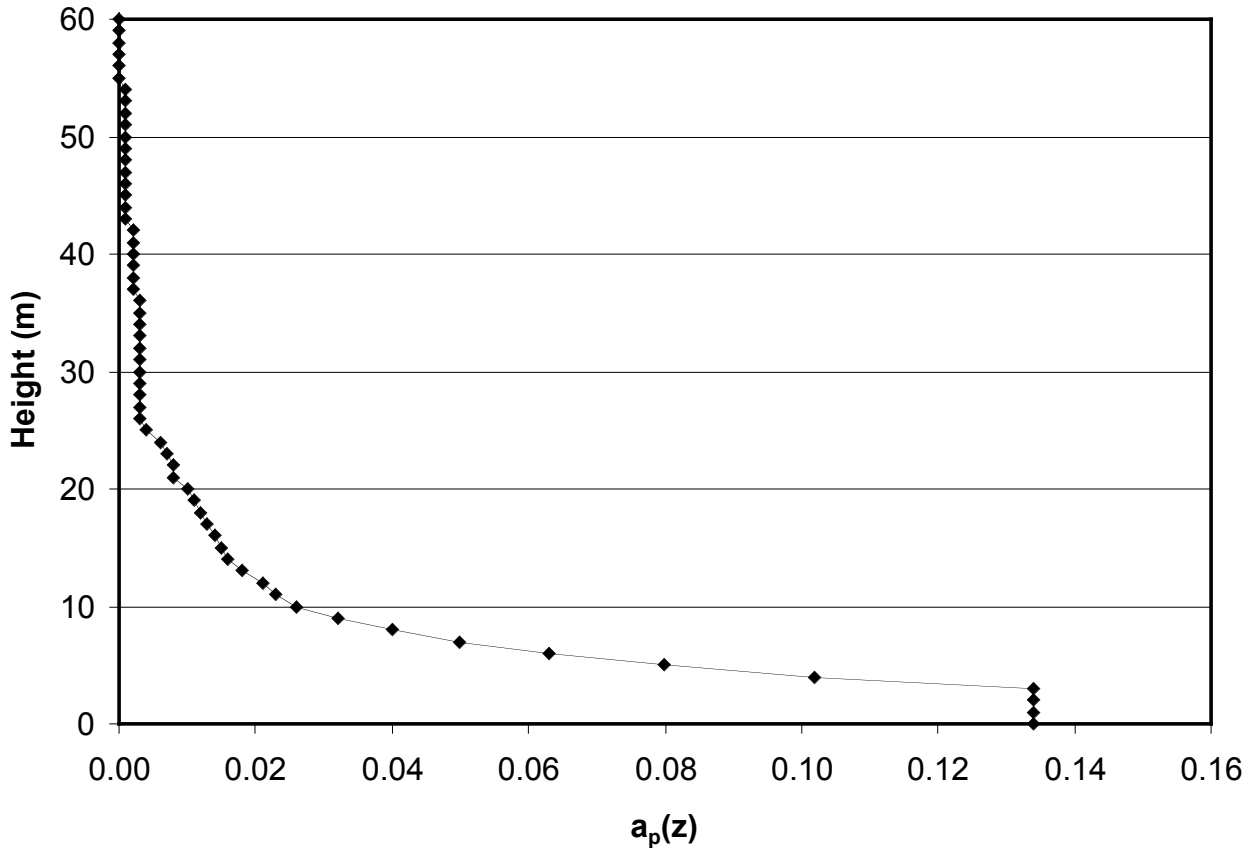


Figure 26. Building plan area density function ($a_p(z)$) for the entire 48.5-km² Albuquerque study area.

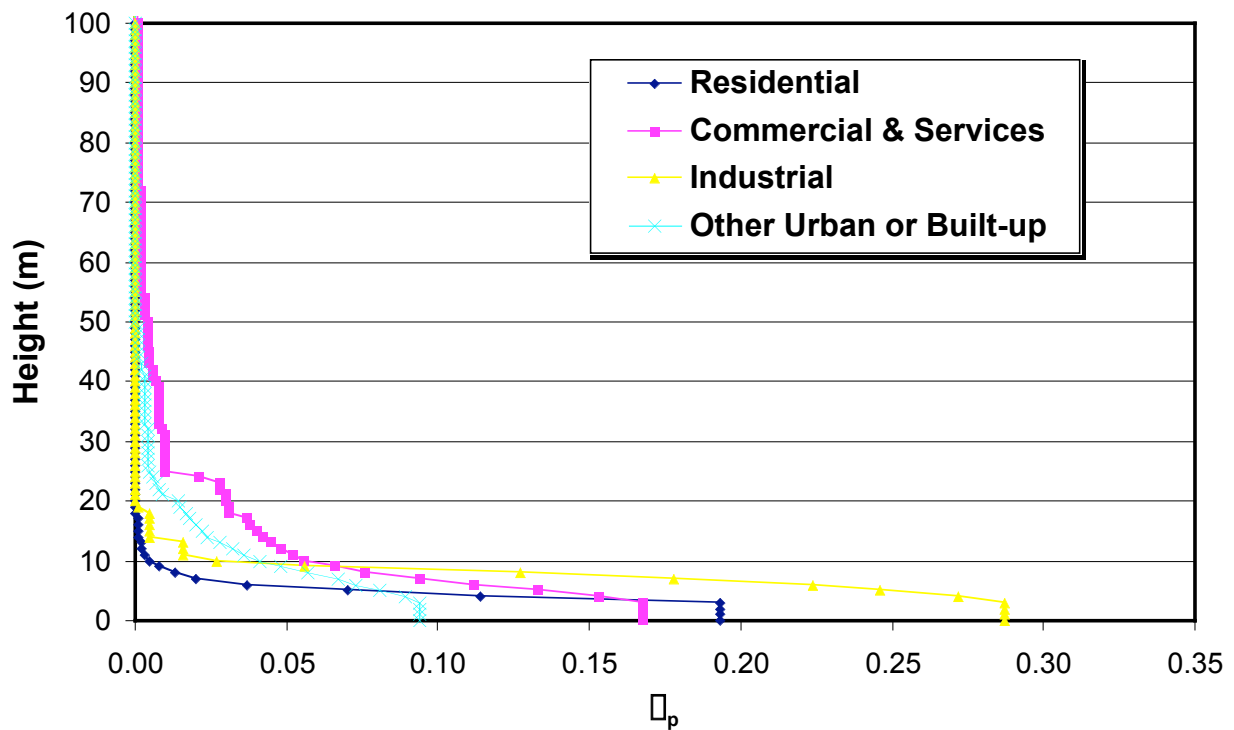


Figure 27. Building plan area density function ($a_P(z)$) for four of the land use classes in the 7-category classification scheme.

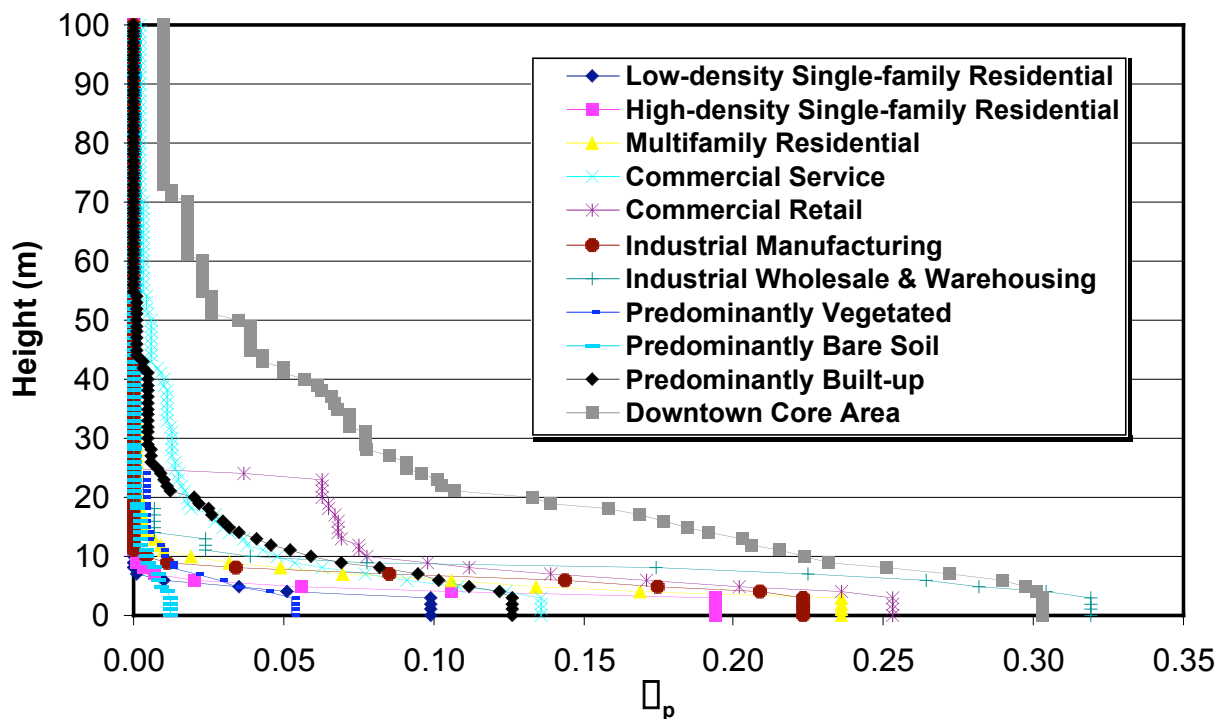


Figure 28. Building plan area density function ($a_P(z)$) for 10 land use types in the 14-category scheme and the Downtown Core Area.

4.4 Roof Area Density ($a_r(z)$)

Background. The rooftop area as a function of a height is important in describing the thermodynamics of the urban canopy. Roofs are interceptors and reflectors of solar radiation, and give off or absorb long-wave radiation. Knowledge of the roof area, therefore, is important in determining the energy balance within the urban canopy. The roof area density is a quantity that can be used to compute roof area as a function of height. The roof area density is analogous to the leaf area density. The leaf area density can be integrated from the top of the vegetative canopy to the ground to yield a leaf area index. The leaf area index gives information on how much long- and short-wave radiation travels through the canopy and how much is intercepted. Roof area density might be used in a similar fashion to help estimate energy fluxes through the urban canopy.

Calculation Methods. The rooftop area within a height increment Δz can be approximated by the difference between the building plan areas at two heights:

$$A_r(z) = A_p\left(\frac{z}{2}\right) - \frac{\Delta z}{2} \frac{dA_p}{dz} + \frac{\Delta z}{2} \frac{dA_p}{dz} \quad (8)$$

where $A_p(z)$ is the plan area of buildings at the specified height and a flat-roofed assumption has been made. The roof area density ($a_r(z)$) can then be defined as the rooftop plan area per height increment Δz divided by the volume of the height increment:

$$a_r(z) = \frac{A_r(z)}{A_T \cdot \Delta z} = \frac{A_p\left(\frac{z}{2}\right) - \frac{\Delta z}{2} \frac{dA_p}{dz} + \frac{\Delta z}{2} \frac{dA_p}{dz}}{A_T \cdot \Delta z} \quad (9)$$

where A_T is the total area within which buildings are contained. Analogous to the leaf area index used in the plant canopy community, the integration of $a_r(z)$ from a specified elevation above ground (z) to the height of the canopy (h_c) is equal to the building area index ($L(z)$):

$$L(z) = \int_z^{h_c} a_r(z) dz \quad (10)$$

The integration of $a_r(z)$ from ground elevation to the canopy height (h_c) is equal to L_p :

$$L(0) = L_p = \int_0^{h_c} a_r(z) dz \quad (11)$$

Results. The roof area density function $a_r(z)$ is shown in Figure 29 for the Albuquerque study area. A significant fraction of the rooftop area is located between 5 and 15 meters of height above ground. The value of $a_r(z)$ is zero below 3 m because no buildings are defined to be below 3 meters (a little less than one story) in height. Figures 30 and 31 show $a_r(z)$ for the 7-category land use scheme and for the 14-category scheme along with the Downtown Core Area, respectively. Figure 30 is limited to the first 60 meters and Figure 31 is limited to the first 80

meters of height to make them more readable because for most of the land use types the first 60-80 meters of height contains all the rooftop area. The Industrial land use has the largest rooftop density fraction within 5-10 meters of the ground, whereas the high-rise land uses have fairly uniform distribution of rooftops up to the 40-50 m level.

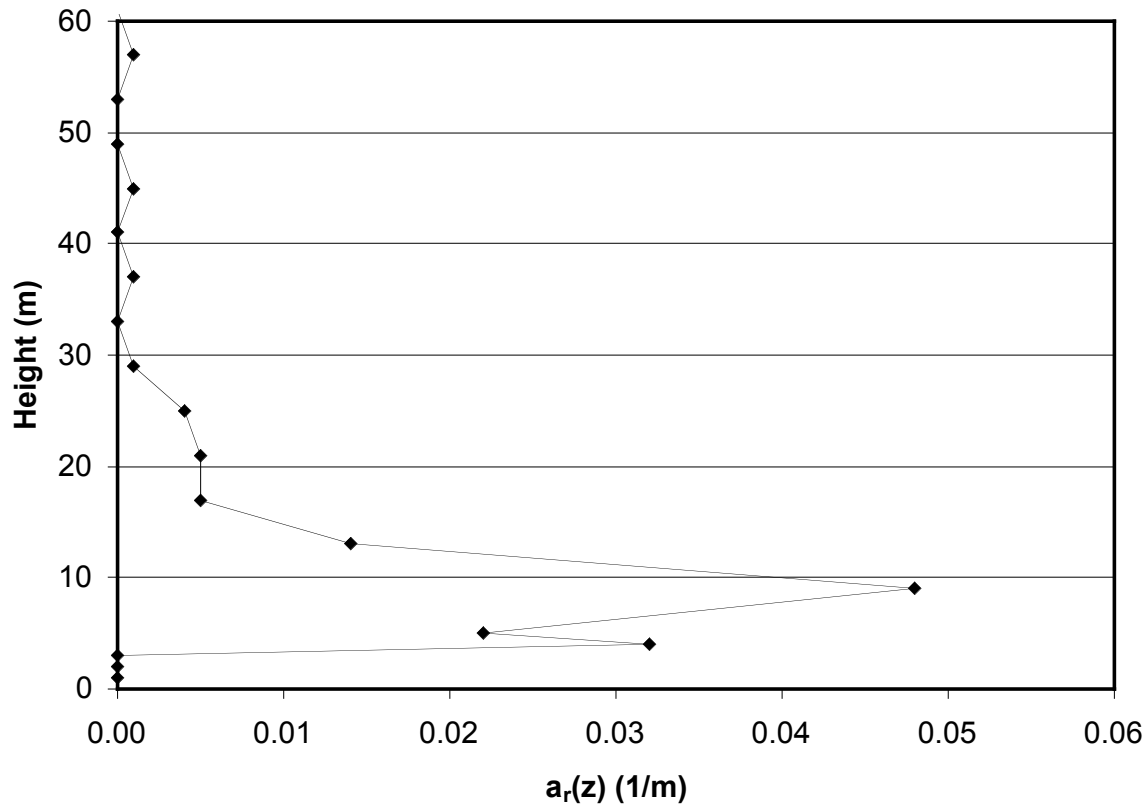


Figure 29. Roof area density function ($a_r(z)$) for the Albuquerque study area. Data are plotted for 1-m height increments up to 4 m and then by 4-m increments (approximately one story) up to 60 m.

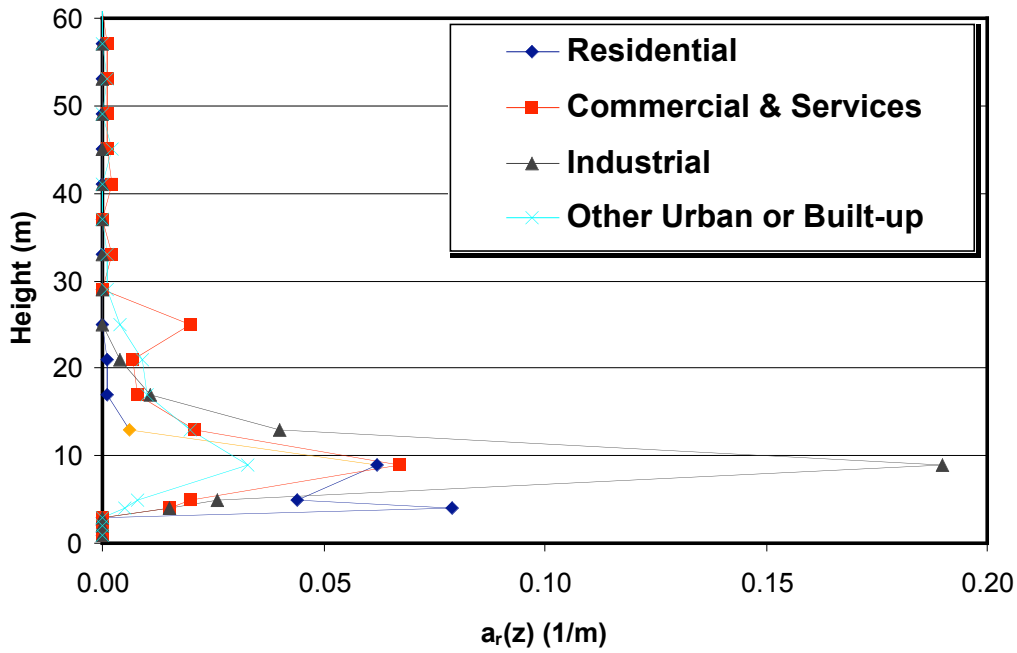


Figure 30. Roof area density function ($a_r(z)$) for the 7-category land use scheme. Data are plotted for 1-m height increments up to 4 m and then by 4-m increments (approximately one story) up to 60 m.

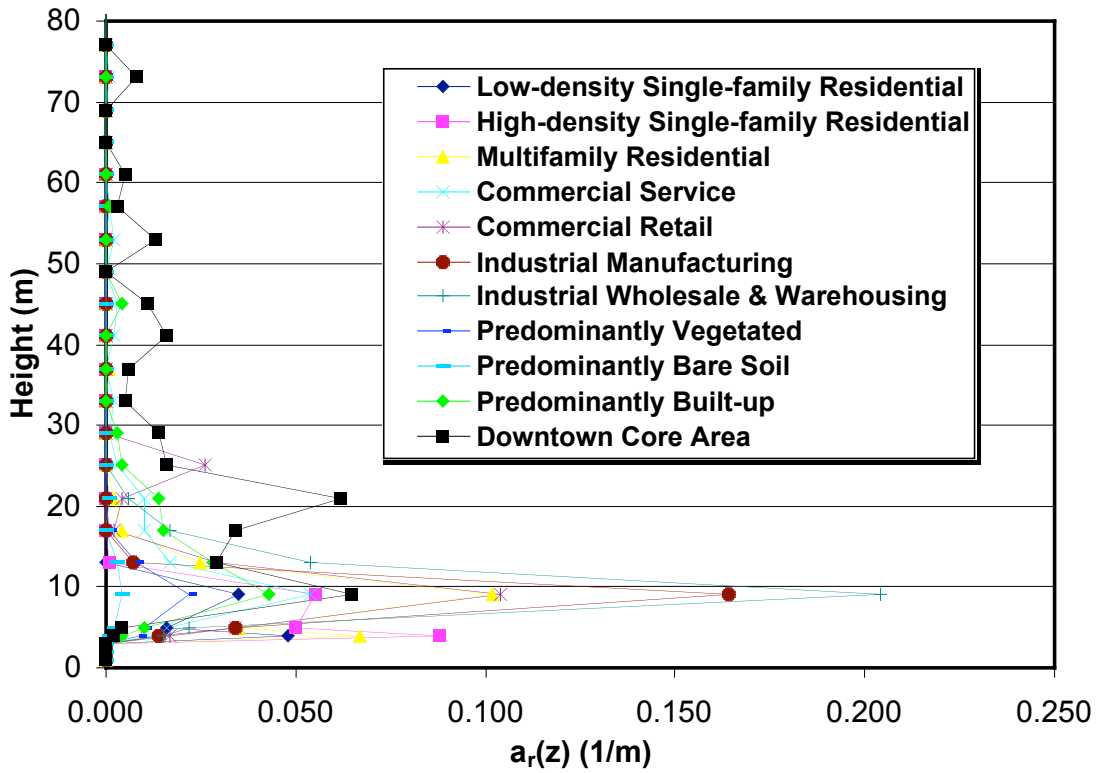


Figure 31. Roof area density function ($a_r(z)$) for the classification scheme 2 land use types and the Downtown Core Area. Data are plotted for 1-m height increments up to 4 m and then by 4-m increments (approximately one story) up to 80 m.

4.5 Building Frontal Area Index (\bar{F})

Background. Building walls facing into the wind impart drag on the air flow. The frontal area index, a measure of the frontal area per unit horizontal area, has been shown to be related to the surface roughness z_o (see Section 4.10). Surface roughness is used in air quality and meteorological models to account for enhanced mixing and the drag effects of the rough surface. The flow regime within urban street canyons is also thought to be a function of the frontal area index and plan area fraction (see Section 4.2).

Calculation Methods. The frontal area index (\bar{F}) is defined as the total area of buildings projected into the plane normal to the approaching wind direction (A_{proj}) divided by the plan area of the study site (A_T):

$$\bar{F}(\theta) = \frac{A_{proj}}{A_T} \quad (12)$$

where θ is the wind direction. Figure 32 illustrates frontal area. A script was written in Avenue (the scripting language for ArcView) during a previous research effort (Burian et al. (2002b) and modified for this analysis to automatically determine the total area of building surfaces in the projected plane normal to a specified wind direction (A_{proj}) and calculate \bar{F} using Eqn. (12).

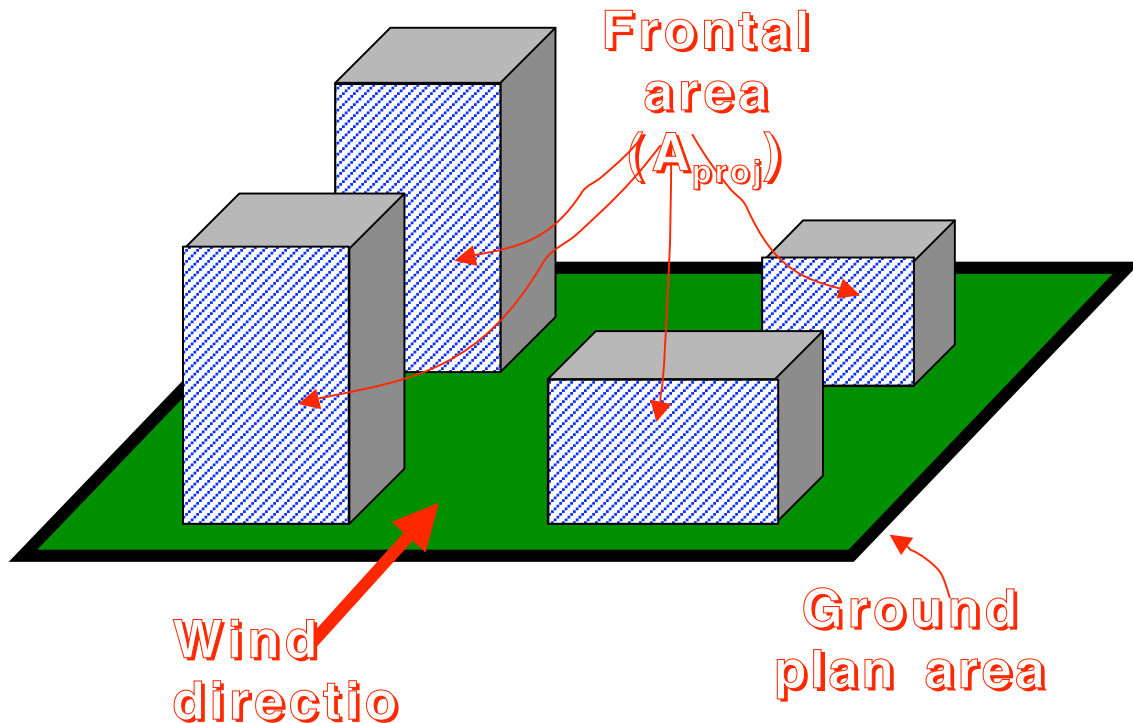


Figure 32. Illustration of projected frontal area. In the schematic of four buildings shown above, the frontal area (A_{proj}) is the total area of the faces exposed to the oncoming wind.

The frontal area index (\square_f) can be approximated from the product of mean height, breadth, and density of roughness elements (Grimmond and Oke 1999):

$$\square_f = \overline{L_y} \overline{H} \square_d \quad (13)$$

where $\overline{L_y}$ is the mean breadth of the roughness elements perpendicular to the wind direction, \overline{H} is the mean roughness element height, and \square_d is the density (number) of roughness elements per unit area ($\square_d = n/A_T$).

Similar to the plan area fraction \square_p , the value of \square_f will be dependent on the location and the size of the area selected for analysis. Therefore, we have calculated \square_f for several different sized areas and as a function of land use. In addition, there is some ambiguity regarding the minimum distance between two adjacent buildings that should be used to distinguish the buildings as two separate buildings. The issue is that as two buildings are placed closer together the upstream building may start to mask the frontal face of the downstream building. For some applications, knowing the exposed frontal area may be more important than knowing the total frontal area. For example, for a cluster of buildings the drag may be better correlated to exposed frontal area as compared to total frontal area. For this study, we consider two separate buildings to be a single building only if the adjacent faces are touching. Using this rule we calculated the \square_f using the Avenue scripts for the entire 48.5-km² study area assuming the wind was approaching the city from the north, northeast, east, southeast, south, southwest, west, and northwest.

Results. Table 6 lists the computed \square_f values for the 48.5-km² study area for eight approach wind directions. For this large study area (i.e., an area with many buildings) \square_f is only slightly sensitive to approach flow wind direction. Because of the symmetrical characteristics of buildings it is expected that opposite wind directions (e.g., North and South) will have nearly identical frontal area indices. For our study area, the majority of streets run in the N-S and E-W directions, but the downtown core area predominantly has streets slightly off the N-S line. Hence, the predominantly along street directions are north, east, south, and west directions and have slightly smaller values.

Table 6. Summary of frontal area index (\square_f) for Albuquerque for several wind approach directions.

	North	Northeast	East	Southeast	South	Southwest	West	Northwest
\square_f	0.05	0.06	0.05	0.06	0.05	0.06	0.05	0.06

The value of \square_f is expected to be a function of land use because of the differences in building characteristics between different land uses. The relationship is also expected to be variable for samples of the same type of land use where building characteristics are highly variable, e.g., Urban High-rise, but not so variable for fairly homogeneous and consistent land uses, e.g., Low-

density Single-family Residential. Table 7 shows the \bar{F}_f values calculated for each land use type. Table 8 compares the computed \bar{F}_f for several land uses in Albuquerque to the computed \bar{F}_f for other cities and land uses. Note that we have not included trees in our calculation of the frontal area index, but several of the other studies cited in Table 8 have included trees.

Figure 33 shows the frontal area index for a north wind azimuth spatially distributed according to the non-uniform grid cell mesh. Calculations were not possible for the uniform 100-m X 100-m mesh because the grid cells are smaller than several buildings and buildings cross grid cell boundaries. This causes problems when trying to calculate the projected wall area in the grid cell. Some cells do not contain any walls because they are completely within the building. Rather than trying to develop a method to calculate \bar{F}_f for these instances we decided to forego the calculation of \bar{F}_f for the uniform grid cell mesh. Similar to the plan area fraction, we see smaller frontal area index values computed for areas including the airport and highways. Also similar to the building plan area fraction distribution, we see the highest computed frontal area index values in the high-rise city center area, and lower values in the industrial regions. In general, the study area has a significant variation in computed frontal area index values. Several grid cells have computed values near zero, while several have computed values greater than 0.75. A direct relationship between land use and frontal area index is not demonstrated in this study area. Although we note the general trend of higher than average frontal area index values in the high-rise areas, this is not universal. For example, several grid cells contain tall buildings with small plan area fractions compared to the grid cell plan area, which results in a smaller than average frontal area index.

Table 7. Frontal area index (\bar{F}_f) as a function of land use type.
Four approach wind directions are included in the table.

Land Use Class	North	Northeast	East	Southeast
Residential	0.08	0.10	0.08	0.10
Low-density Single-family (< 8 units/hectare)	0.04	0.04	0.04	0.04
High-density Single-family (\geq 8 units/hectare)	0.08	0.10	0.08	0.10
Multifamily	0.10	0.12	0.09	0.12
Mixed	---	---	---	---
Commercial & Services	0.06	0.07	0.05	0.07
Service	0.06	0.07	0.06	0.07
Retail	0.05	0.06	0.05	0.06
Industrial	0.08	0.09	0.07	0.09
Manufacturing	0.06	0.08	0.06	0.08
Wholesale & Warehousing	0.08	0.10	0.08	0.10
Transportation/Communications/Utilities	0.00	0.00	0.00	0.00
Mixed Industrial & Commercial	---	---	---	---
Mixed Urban or Built-up	---	---	---	---
Other Urban or Built-up	0.03	0.04	0.03	0.04
Predominantly Vegetated	0.01	0.02	0.01	0.02
Predominantly Bare Soil	0.01	0.01	0.01	0.01
Predominantly Built-up	0.04	0.05	0.04	0.05
Urban High-rise	0.09	0.11	0.09	0.11

Downtown Core Area	0.19	0.22	0.18	0.21
---------------------------	-------------	-------------	-------------	-------------

Table 8. Comparison of frontal area index (\bar{F}_f) for several cities and land uses

Location	Land Use Class	\bar{F}_f	Source
Arcadia, CA	Suburban residential	0.33	Grimmond and Oke (1999)
Chicago, IL	Suburban residential	0.28	Grimmond and Oke (1999)
Los Angeles, CA	Multifamily residential	0.25	Burian et al. (2002b)*
Salt Lake City, UT	Multifamily residential	0.25	Burian et al. (2002e)*
Sacramento, CA	Suburban residential	0.23	Grimmond and Oke (1999)
Chicago, IL	Suburban residential	0.21	Grimmond and Oke (1999)
Tucson, AZ	Suburban residential	0.19	Grimmond and Oke (1999)
Vancouver, BC, Canada	Suburban residential	0.19	Grimmond and Oke (1999)
Portland, OR	Multifamily residential	0.17	Burian et al. (2002d)*
Miami, FL	Suburban residential	0.16	Grimmond and Oke (1999)
San Gabriel, CA	Suburban residential	0.14	Grimmond and Oke (1999)
Los Angeles, CA	High-density single-family residential	0.12	Burian et al. (2002b)*
Albuquerque, NM	High-density single-family residential	0.09	This Report*
Phoenix, AZ	High-density single-family residential	0.05	Burian et al. (2002c)*
Salt Lake City, UT	Industrial	0.15	Burian et al. (2002e)*
Vancouver, BC, Canada	Light industrial	0.13	Grimmond and Oke (1999)
Los Angeles, CA	Industrial	0.10	Burian et al. (2002b)*
Albuquerque, NM	Industrial	0.08	This Report*
Portland, OR	Industrial	0.08	Burian et al. (2002d)*
Phoenix, AZ	Industrial	0.05	Burian et al. (2002c)*
Los Angeles, CA	Urban high-rise	0.45	Burian et al. (2002b)*
Los Angeles, CA	Downtown core area	0.38	Burian et al. (2002b)*
Salt Lake City, UT	Urban high-rise	0.32	Burian et al. (2002e)*
Vancouver, BC, Canada	Central city	0.30	Grimmond and Oke (1999)
Phoenix, AZ	Downtown core area	0.23	Burian et al. (2002c)*
Portland, OR	Downtown core area	0.22	Burian et al. (2002d)*
Albuquerque, NM	Downtown core area	0.20	This Report*
Mexico City, Mexico	Central city	0.19	Grimmond and Oke (1999)
Los Angeles, CA	Non-high-rise commercial & services	0.13	Burian et al. (2002b)*

*The values shown from this study are the average values for four wind directions (north, northeast, east, southeast, south, southwest, west, northwest).

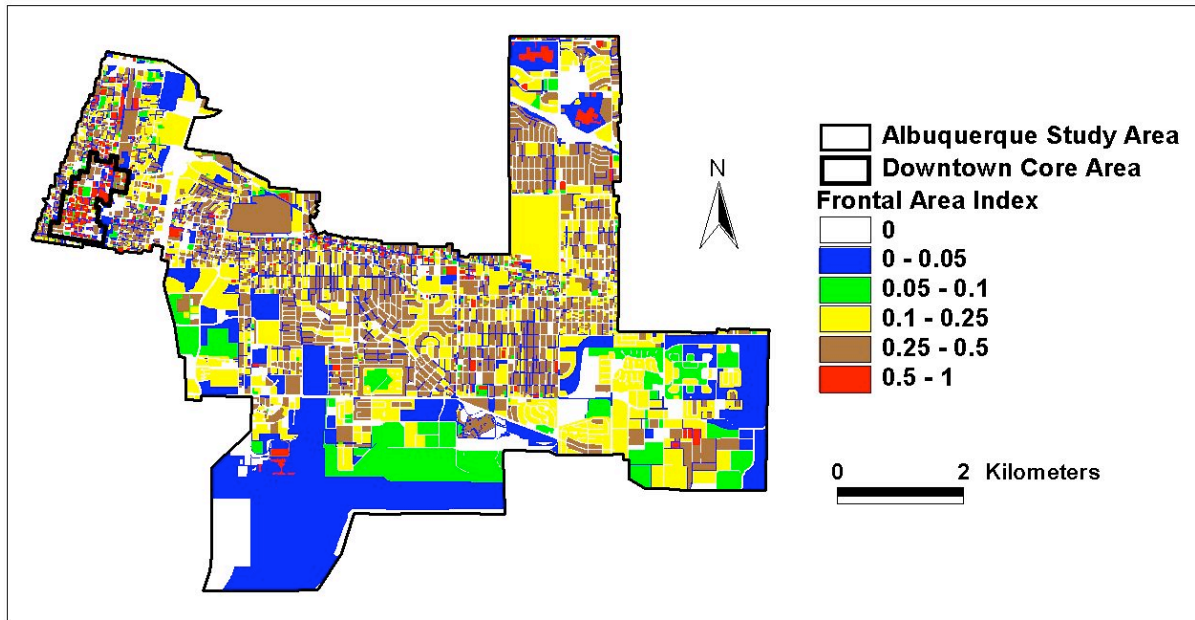


Figure 33. Spatial distribution of building frontal area index (\overline{A}_f) for a north wind azimuth.

4.6 Frontal Area Density ($a_f(z)$)

Background. The frontal area is often used in computing the drag force on solid objects immersed in fluids. The frontal area density, a measure of the frontal area per unit horizontal area per unit height increment, has been used by researchers in the plant canopy and urban canopy communities to help quantify the drag force as a function of height. The drag force approach allows one to compute the area-averaged wind profile within the canopy.

Calculation Methods. The frontal area density ($a_f(z)$) is defined as:

$$a_f(z, \varphi) = \frac{A(\varphi)_{proj(\varphi z)}}{A_T \Delta z} \quad (14)$$

where $A(\varphi)_{proj(\varphi z)}$ is the area of building surfaces projected into the plane normal to the approaching wind direction for a specified height increment (Δz), φ is the wind direction angle, and A_T is the total plan area of the study site. For a specified wind direction, the integral of $a_f(z)$ over the canopy height equates to φ_f .

Results. We performed the frontal area density calculations at one-meter increments. Figure 34 shows $a_f(z)$ for the Albuquerque study area for a wind approaching from the north. Figure 35 shows the $a_f(z)$ functions for the land use types in the 7-category scheme that have a sufficient number of buildings and land area to produce meaningful results. Figure 36 shows the $a_f(z)$ functions for the 14-category land use scheme, the Urban High-rise land use, and the Downtown Core Area.

Interestingly, the frontal area density near the ground is largest for Residential areas. This occurs due to the preponderance of shorter buildings in Residential areas (many short buildings occupying the same volume as a few taller buildings have more frontal area). Industrial has a higher frontal area density near the ground surface than Commercial & Services land use. Presumably Commercial & Services has a relatively low frontal area density near the surface due to large amounts of open space between buildings (e.g., parking lots). The frontal area density decays most rapidly with height for Residential and Industrial areas due to low building heights. The High-density Single-family and Multifamily Residential land uses have the highest frontal area densities near the ground. Note the much smaller frontal area density associated with the Low-Density Single-family Residential compared to the other two Residential land uses. The Urban High-rise and Downtown Core Area land uses decay most slowly with height due to the large number of tall buildings in these land use types.

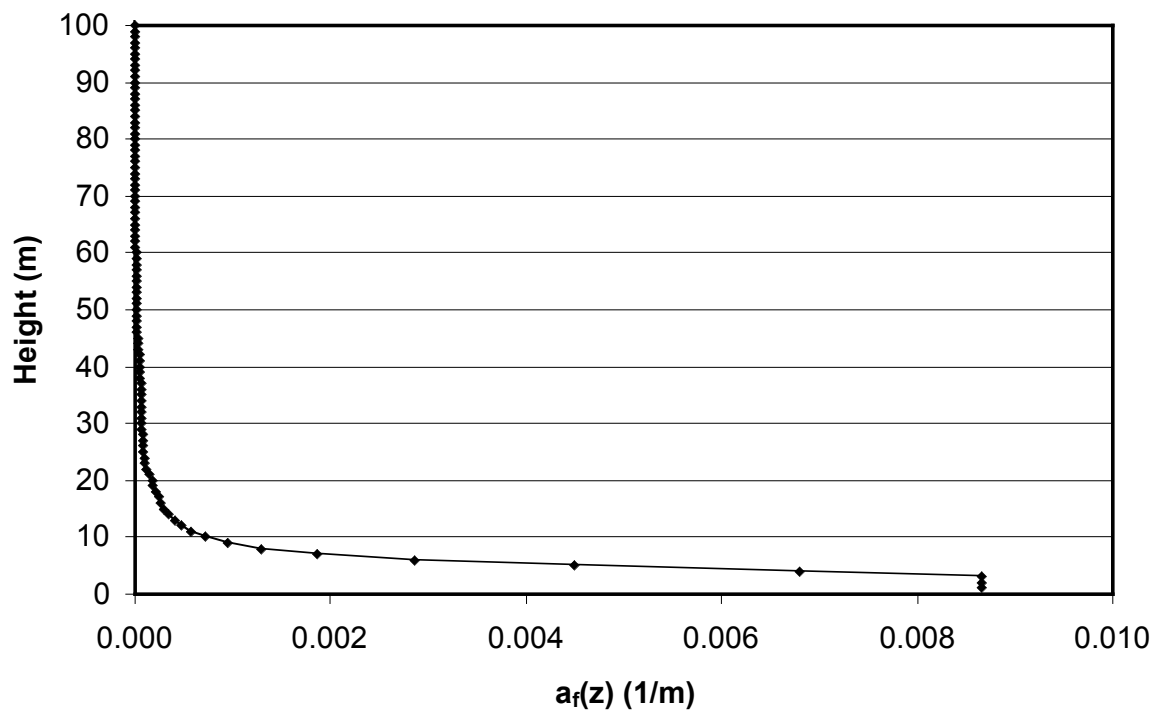


Figure 34. Frontal area density function ($a_f(z)$) for the Albuquerque study area for a wind approaching from the north.

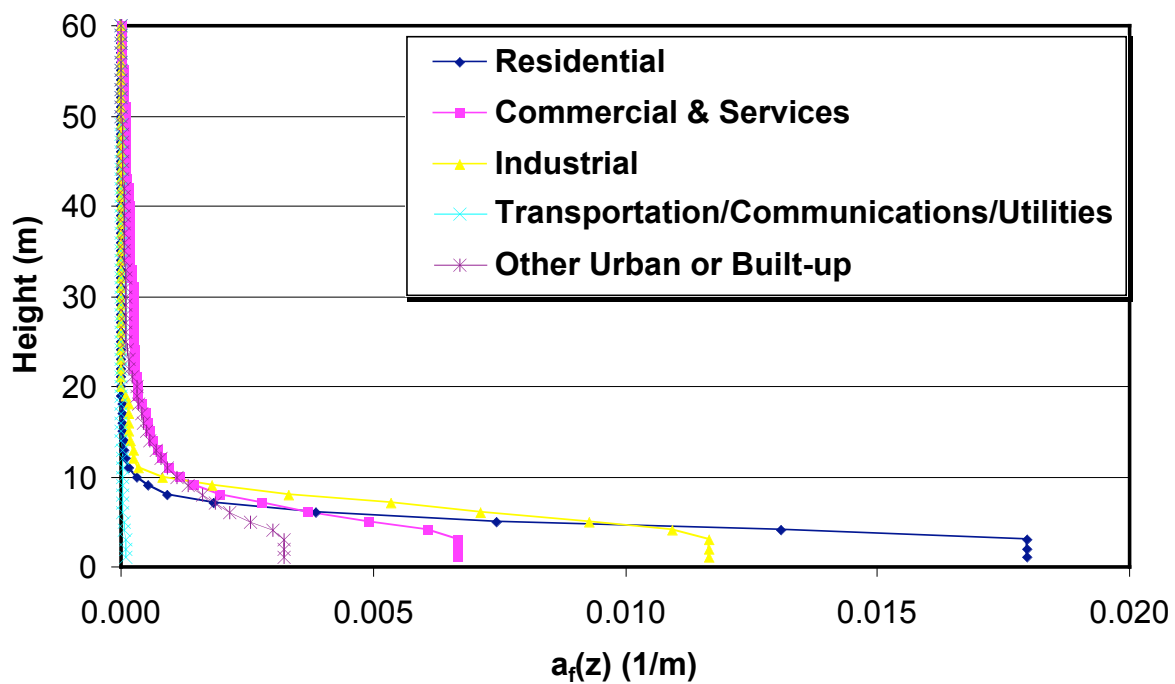


Figure 35. Frontal area density function ($a_f(z)$) for land use types in the 7-category scheme for a wind approaching from the north.

Fi

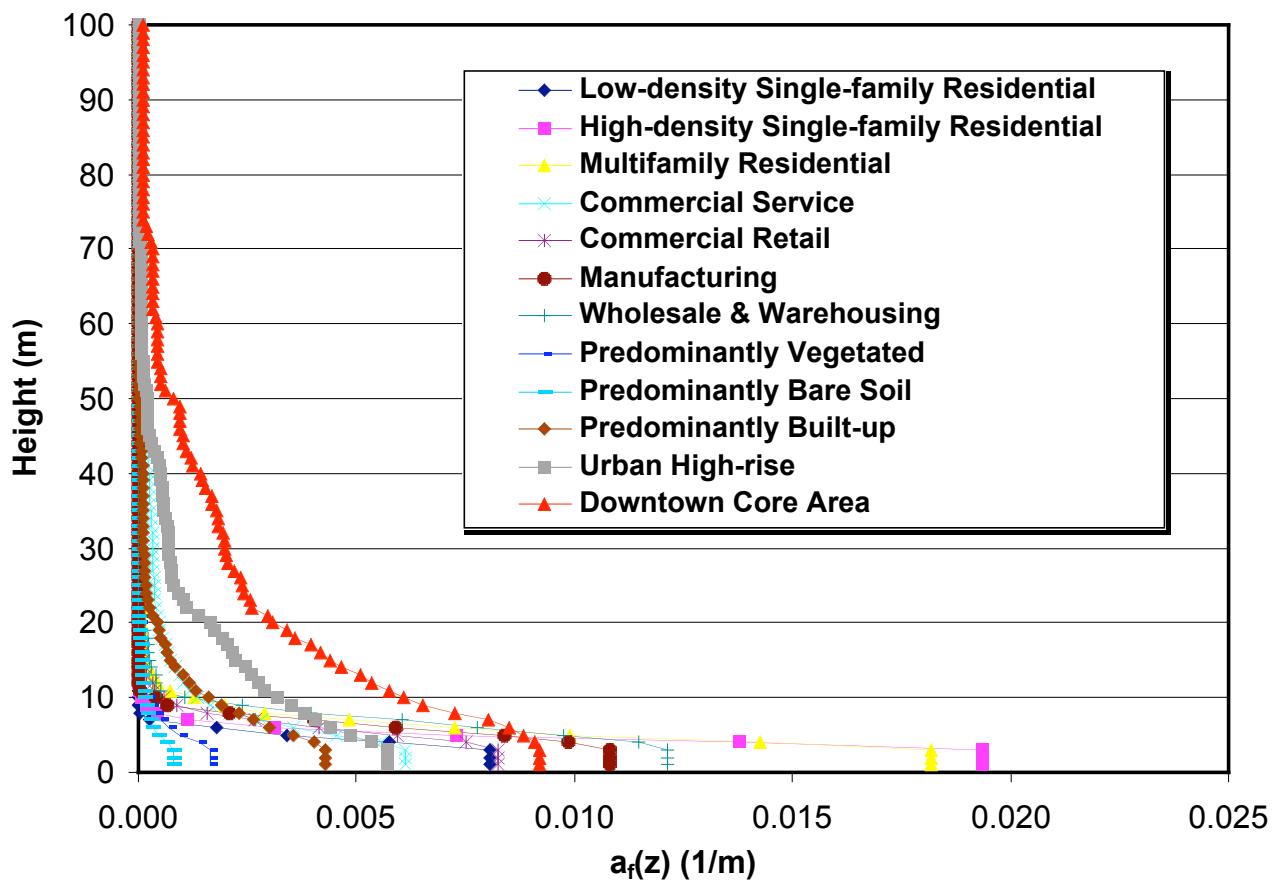


Figure 36. Frontal area density function ($a_f(z)$) for several land use types in the 14-category scheme and the Urban High-rise and Downtown Core Area land uses for a wind approaching from the north.

4.7 Complete Aspect Ratio (\square_C)

Background. The “complete” surface area, including building walls, roofs, and ground surfaces, is important when evaluating the urban canopy energy budget in a city. All of these surfaces act as sources and sinks of heat and need to be accounted for when evaluating the energy balance of an urbanized area. The non-dimensional form of the complete surface area, the complete aspect ratio, is useful in interpreting surface temperatures derived from remote sensing instruments. Used with the plan area \square_p , some notion of the three-dimensionality of the urban fabric can be obtained and better estimates of the “real” skin temperature might be computed.

Calculation Methods. The complete aspect ratio (\square_C) is defined as the summed surface area of roughness elements and exposed ground divided by the total plan area (Voogt and Oke 1997):

$$\square_C = \frac{A_C}{A_T} = \frac{A_W + A_R + A_G}{A_T} \quad (15)$$

where A_C is the combined surface area of the buildings and exposed ground, A_W is the wall surface area, A_R is the roof area, A_G is the area of exposed ground, and A_T is the plan area of the study site. A_C is calculated by summing the surface area of the buildings and the difference between the total plan area of the site and the plan area of buildings at ground level (i.e., the exposed ground surface). For dense urban areas with flat roofed buildings and without much vegetation, A_C can be approximated as the sum of the plan area of the site and the area of building walls (not including rooftops).

Using an Avenue script in the ArcView GIS we automatically calculated \square_C for the entire city for a non-uniform grid cell mesh (shown in Figure 24) and as a function of land use. Calculations were not performed for the uniform 100-m X 100-m mesh for the same reasons described for frontal area index. The rooftop surface area was calculated assuming the rooftops were flat, which a digital orthophoto indicated to be true for most of the land use types, except for some of the Low- and High-density Single-family Residential area. Another source of error in our complete aspect ratio calculation is the neglect of the surface area of trees and bushes. Grimmond and Oke (1999) found the surface area of trees and bushes to be an important component of the complete surface area, especially in residential areas.

Results. For the 48.5-km² study area, the \square_C was calculated to be 1.18. The \square_C for each grid cell was calculated for the non-uniform grid cell mesh (Figure 37). For the non-uniform mesh, the mean \square_C was 1.58, with a standard deviation of 1.87, and a range of 1.0 to 51.3. The high-rise area is located within the conglomeration of red, yellow, and green grid cells in Figure 37 (within the Downtown Core Area boundary). The computed \square_C values for each land use type in our classification schemes are shown in Table 9. The \square_C values for the downtown area are in the range of 1.00 to 51.3 (with a mean of 3.3), which are consistent with the central city values from other studies shown in Table 10.

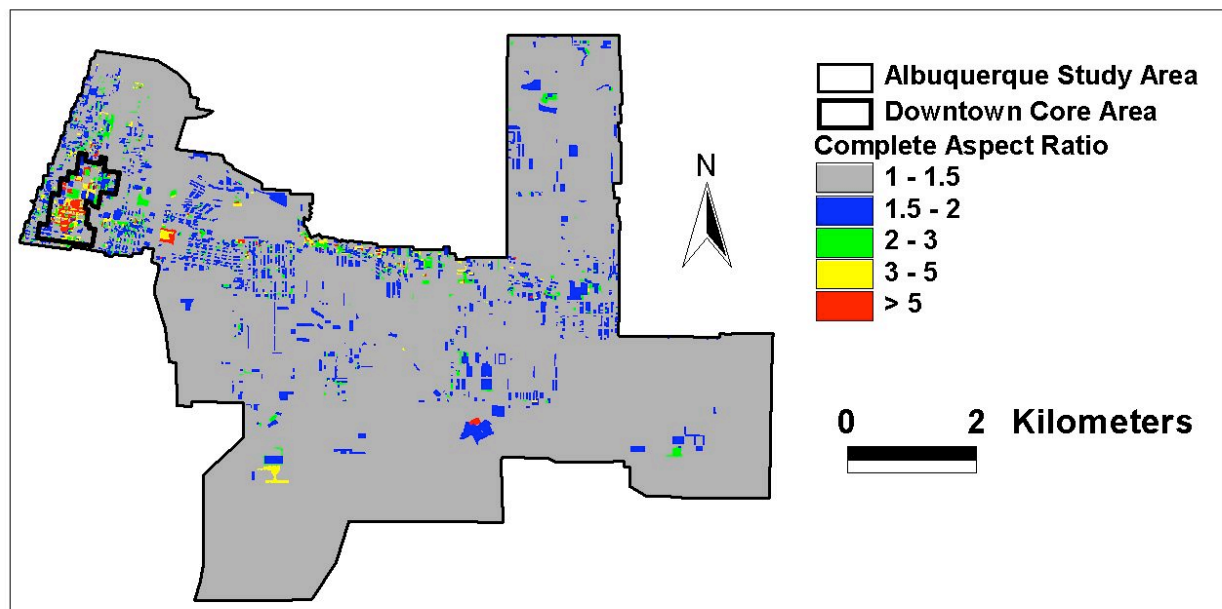


Figure 37. Display of complete aspect ratio ($\bar{\alpha}_c$) calculated for the Albuquerque downtown area per grid cell.

Table 9. Complete aspect ratio ($\bar{\alpha}_c$) for each land use type

Land Use Class	$\bar{\alpha}_c$
Residential	1.30
Low-density Single-family (< 8 units/hectare)	1.13
High-density Single-family (\geq 8 units/hectare)	1.30
Multifamily	1.38
Mixed	---
Commercial & Services	1.21
Service	1.21
Retail	1.23
Industrial	1.26
Manufacturing	1.22
Wholesale & Warehousing	1.28
Transportation/Communications/Utilities	1.00
Mixed Industrial & Commercial	---
Mixed Urban or Built-up	---
Other Urban or Built-up	1.12
Predominantly Vegetated	1.05
Predominantly Bare Soil	1.02
Predominantly Built-up	1.17
Urban High-rise	1.36
Downtown Core Area	1.62

Table 10 compares selected values from Table 9 with \bar{L}_c values computed for other cities. The \bar{L}_c computed for Albuquerque High-density Single-family Residential land use is at the lower end of the range of residential land use values shown. The \bar{L}_c computed for the Industrial land use type is also near the bottom of the range, identical to the value computed for Portland. The Downtown Core Area land use type in Albuquerque has the lowest \bar{L}_c value of the cities listed

Table 10. Complete aspect ratio (\bar{L}_c) for downtown Albuquerque and other cities

Location	Land Use Class	\bar{L}_c	Source
Salt Lake City, UT	Multifamily residential	1.89	Burian et al. (2002e)
Arcadia, CA	Suburban residential	1.78	Grimmond and Oke (1999)
Los Angeles, CA	Multifamily residential	1.77	Burian et al. (2002b)
Chicago, IL	Suburban residential	1.74	Grimmond and Oke (1999)
Vancouver, BC, Canada	Suburban residential	1.65	Voogt and Oke (1997)
Salt Lake City, UT	High-density single-family residential	1.65	Burian et al. (2002e)
Sacramento, CA	Suburban residential	1.63	Grimmond and Oke (1999)
Portland, OR	Multifamily residential	1.53	Burian et al. (2002d)
Chicago, IL	Suburban residential	1.51	Grimmond and Oke (1999)
Tucson, AZ	Suburban residential	1.45	Grimmond and Oke (1999)
Miami, FL	Suburban residential	1.37	Grimmond and Oke (1999)
Los Angeles, CA	High-density single-family residential	1.36	Burian et al. (2002b)
San Gabriel, CA	Suburban residential	1.31	Grimmond and Oke (1999)
Albuquerque, NM	High-density single-family residential	1.30	This Report
Phoenix, AZ	High-density single-family residential	1.14	Burian et al. (2002c)
Salt Lake City, UT	Industrial	1.48	Burian et al. (2002e)
Vancouver, BC, Canada	Light industrial	1.39	Voogt and Oke (1997)
Los Angeles, CA	Industrial	1.30	Burian et al. (2002b)
Albuquerque, NM	Industrial	1.26	This Report
Portland, OR	Industrial	1.26	Burian et al. (2002d)
Phoenix, AZ	Industrial	1.17	Burian et al. (2002c)
Los Angeles, CA	High-rise commercial & services	2.60	Burian et al. (2002b)
Los Angeles, CA	Urban high-rise	2.44	Burian et al. (2002b)
Los Angeles, CA	Downtown core area	2.22	Burian et al. (2002b)
Vancouver, BC, Canada	Central city	2.20	Voogt and Oke (1997)
Salt Lake City, UT	Urban high-rise	2.05	Burian et al. (2002e)
Phoenix, AZ	Downtown core area	1.75	Burian et al. (2002c)
Mexico City, Mexico	Central city	1.73	Grimmond and Oke (1999)
Singapore	Downtown	1.70	Nichol (1996)
Portland, OR	Downtown core area	1.67	Burian et al. (2002d)
Albuquerque, NM	Downtown core area	1.62	This Report

4.8 Building Surface Area to Plan Area Ratio (\square_B)

Background. Another measure of urban terrain character is the ratio of built surface area to the plan surface area. Like the complete aspect ratio (Section 4.7), the building surface area is important when evaluating the urban canopy energy budget in a city. Building walls and roof surfaces act as sources and sinks of heat and need to be accounted for when evaluating the energy balance of an urbanized area. Perhaps some combination of frontal area, plan area, complete surface area, and building surface area parameters will allow for better parameterizations of the urban canopy energy budget.

Calculation Methods. The building surface area to plan area ratio (\square_B) is defined as the sum of building surface area divided by the total plan area:

$$\square_B = \frac{A_R + A_W}{A_T} \quad (16)$$

where A_R is the plan area of rooftops, A_W is the total area of non-horizontal roughness element surfaces (e.g., walls), and A_T is the total plan area of the study location. For the calculations below, we have made a flat-roof assumption.

Results. The \square_B for the 48.5-km² study area in Albuquerque was calculated to be 0.31. Table 11 shows the computed \square_B values for each land use type included in the building analysis. Industrial and the Urban High-rise land use and Downtown Core Area have the largest values due to the presence of tall buildings and fairly high plan area fraction. We did not find values for other cities for this parameter.

Table 11. Building surface area to plan area ratio (\bar{f}_B) for each land use type

Land Use Class	\bar{f}_B
Residential	0.49
Low-density Single-family (< 8 units/hectare)	0.23
High-density Single-family (\geq 8 units/hectare)	0.49
Multifamily	0.62
Mixed	---
Commercial & Services	0.38
Service	0.34
Retail	0.49
Industrial	0.55
Manufacturing	0.44
Wholesale & Warehousing	0.60
Transportation/Communications/Utilities	0.00
Mixed Industrial & Commercial	---
Mixed Urban or Built-up	---
Other Urban or Built-up	0.22
Predominantly Vegetated	0.10
Predominantly Bare Soil	0.03
Predominantly Built-up	0.29
Urban High-rise	0.58
Downtown Core Area	0.93

4.9 Height-to-Width Ratio ($\overline{\lambda}_s$)

Background. The ratio of the height of buildings to the horizontal distance (or street width) between the buildings is called the height-to-width ratio ($\overline{\lambda}_s$). The height-to-width ratio has been found, for idealized arrangements of same-height buildings, to influence the flow regime. Hussain and Lee (1980) performed wind-tunnel experiments and found the three flow regimes develop in idealized urban street canyons: (1) isolated flow, (2) wake interference flow, and (3) skimming flow. The isolated flow regime occurs when elements are spaced relatively far apart ($\overline{\lambda}_s < 0.4$), the wake interference flow occurs when elements are spaced at a medium density level ($0.4 < \overline{\lambda}_s < 0.7$), and the skimming flow regime occurs for high-density building arrangements ($\overline{\lambda}_s > 0.7$) (Oke 1988).

Calculation Methods. The height-to-width ratio ($\overline{\lambda}_s$) (also called the street aspect ratio) is calculated for two buildings by dividing the average height by the distance between the two buildings:

$$\overline{\lambda}_s = \frac{(H_1 + H_2)/2}{S_{12}} \quad (17)$$

where H_1 is the height of the upwind building, H_2 is the height of the downwind building, and S_{12} is the horizontal distance between the two buildings (i.e., the canyon width). Figure 38 illustrates the measures used to compute $\overline{\lambda}_s$. The calculation of $\overline{\lambda}_s$ is performed for each pair of adjacent elements in a building array, which can be very tedious for the complex building shapes and patterns in a city. For idealized arrangements of buildings, the calculation of an average $\overline{\lambda}_s$ can be approximated by taking the average building height divided by the average width between buildings (Grimmond and Oke 1999):

$$\overline{\lambda}_s \approx \frac{\overline{z_H}}{\overline{W}} \quad (18)$$

where $\overline{z_H}$ is the average building height and \overline{W} is the average distance between buildings.

Due to the large number of buildings in the Albuquerque dataset, an automated approach is warranted. Because of the complexity of the Albuquerque downtown area, we did not use the simplified methodology described by Eqn. (18). Instead, we computed $\overline{\lambda}_s$ along linear traverses across the city at different angles using Eqn. (17). Our calculation strategy involved converting the urban building database into a raster digital elevation model (DEM – a matrix of numbers representing building height). Then traversing along each row or column of grid cells the height-to-width ratio was calculated between each pair of buildings. A Fortran code was written to execute this procedure. Since this approach yields $\overline{\lambda}_s$ values in non-preferred directions (e.g., running along a street, not across a street), we then superimposed the matrices of traverses done at different angles, and chose the height-to-width ratio at each grid cell by selecting the largest value.

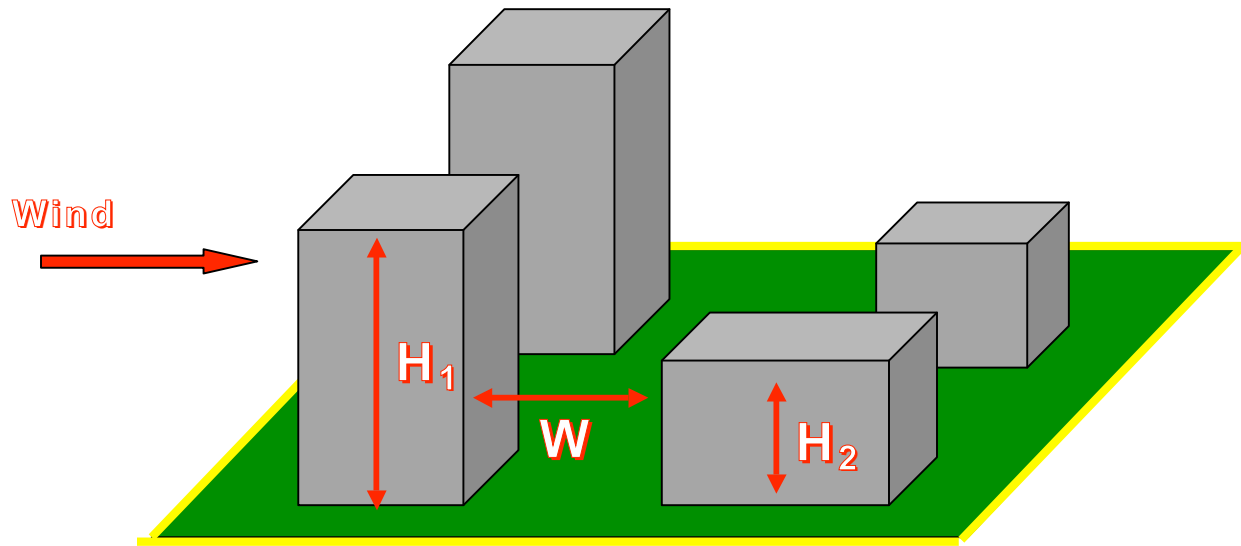


Figure 38. Illustration of height-to-width ratio parameter.

Figures 39 and 40 show the spatial distribution of the computed $\bar{\lambda}_s$ values for the two analysis directions that corresponded with the predominant street directions. Due to the two predominant street orientations in the study area computation of the height-to-width ratio had to be performed using two traverse directions. The first traverses were from north to south and from west to east for 85% of the study area where the streets are oriented in the N-S and W-E directions. For the area oriented approximately 10 degrees off the N-S and W-E orientation (essentially the downtown area at the west end of the study area) the building dataset was first rotated and then the height-to-width ratio was computed for the top-to-bottom and side-to-side directions. Figure 41 shows the composite $\bar{\lambda}_s$ values, which were computed at each grid cell by selecting the largest value from the superimposed matrices from the two traversal directions, i.e., superimposing the values from Figs. 39 and 40. The higher $\bar{\lambda}_s$ values are clearly visible in the downtown area of Albuquerque (the buildings are shaded by height).

Figures 42, 43, and 44 show the composite $\bar{\lambda}_s$ values for areas predominantly composed of Residential, Industrial, and Downtown Core Area land uses, respectively. The figures clearly illustrate the concentration of the highest $\bar{\lambda}_s$ values in the high-rise area. The $\bar{\lambda}_s$ values are fairly similar for the Residential and Industrial land uses.

We also computed the average $\bar{\lambda}_s$ values for the study area and for each land use type in our classification schemes. The average $\bar{\lambda}_s$ was computed by using the area-weighted average of the spatial distribution of the composite height-to-width ratio shown in Figure 41. One could also weight the average $\bar{\lambda}_s$ by number of buildings, streets, or some other quantity. In the approach used here, buildings with larger footprints will exert a greater influence over the area-weighted average. In addition, open areas (e.g., parking lots and parks) and street intersections will be counted in the average.

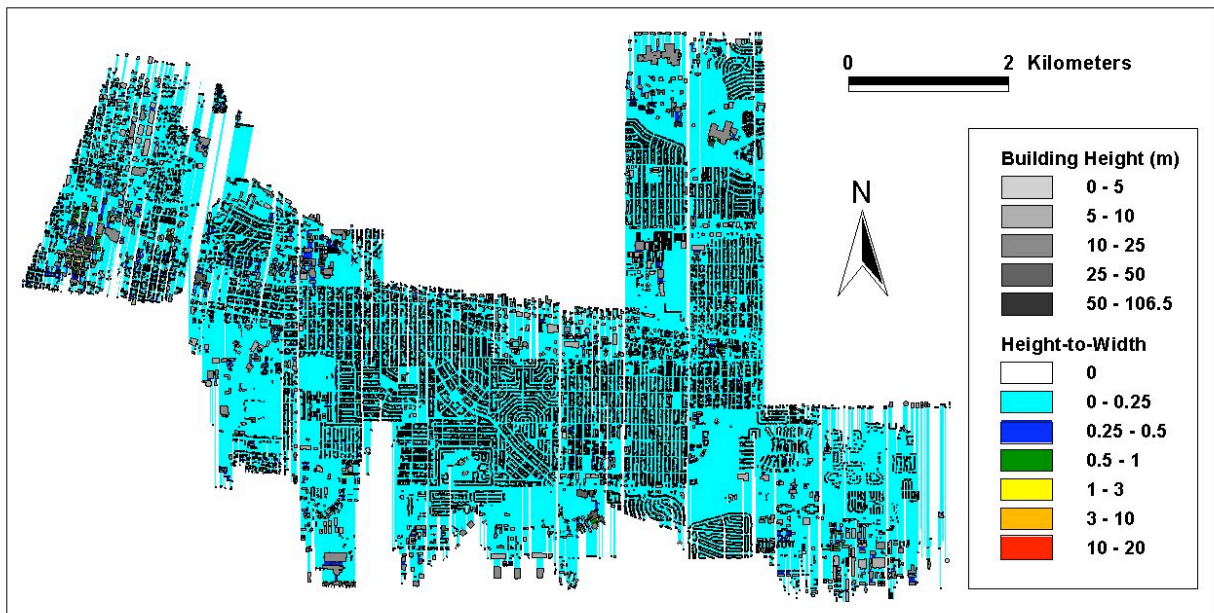


Figure 39. Computed height-to-width ratio (L_s) for the Albuquerque study area (analysis traversal was from the north to south for 85% of the site, and from northeast to southwest for the western edge).

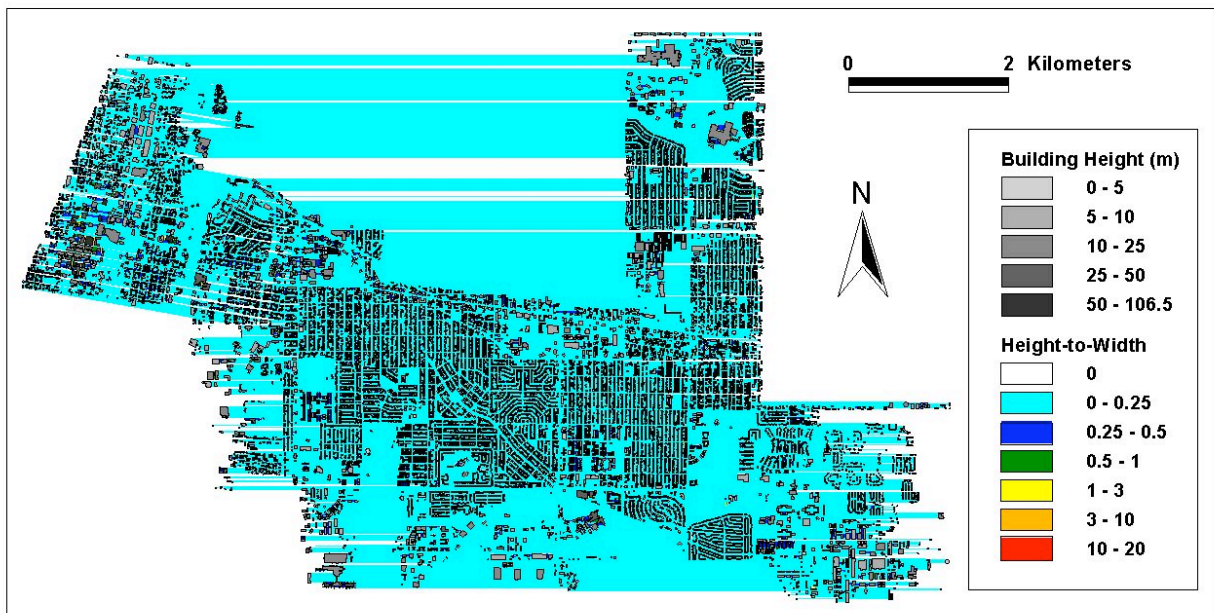


Figure 40. Computed height-to-width ratio (L_s) for the Albuquerque study area (analysis traversal was from the west to east for 85% of the site, and from northwest to southeast for the western edge).

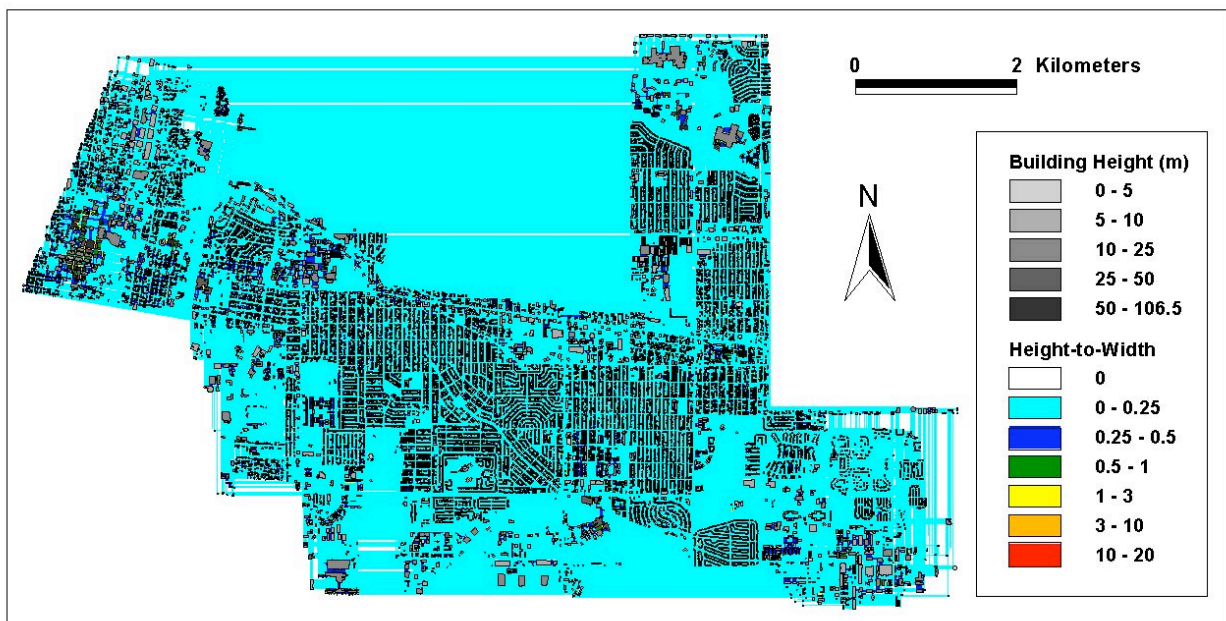


Figure 41. Composite height-to-width ratio (\overline{H}_s) for the Albuquerque study area based on the integration of computed values for the two analysis traversals.

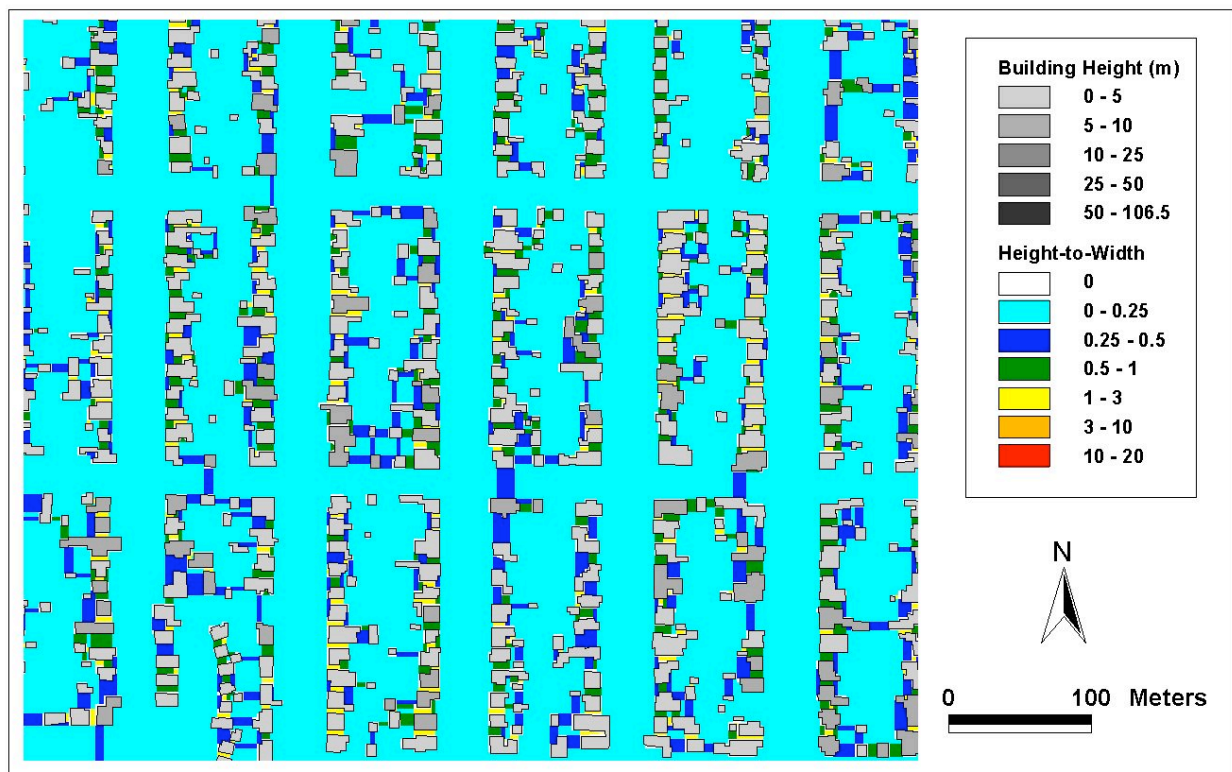


Figure 42. Composite height-to-width ratio (\overline{H}_s) for a residential section of the Albuquerque study area.

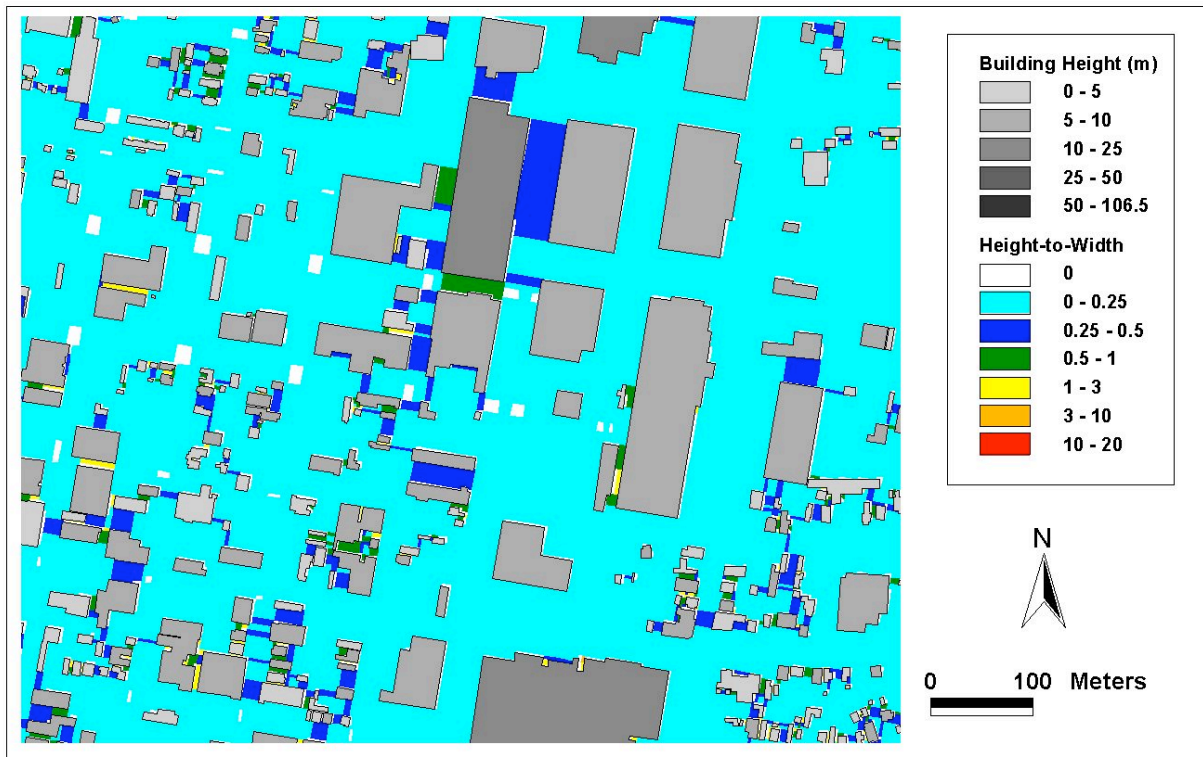


Figure 43. Composite height-to-width ratio (\overline{L}_s) for an industrial section of the Albuquerque study area.

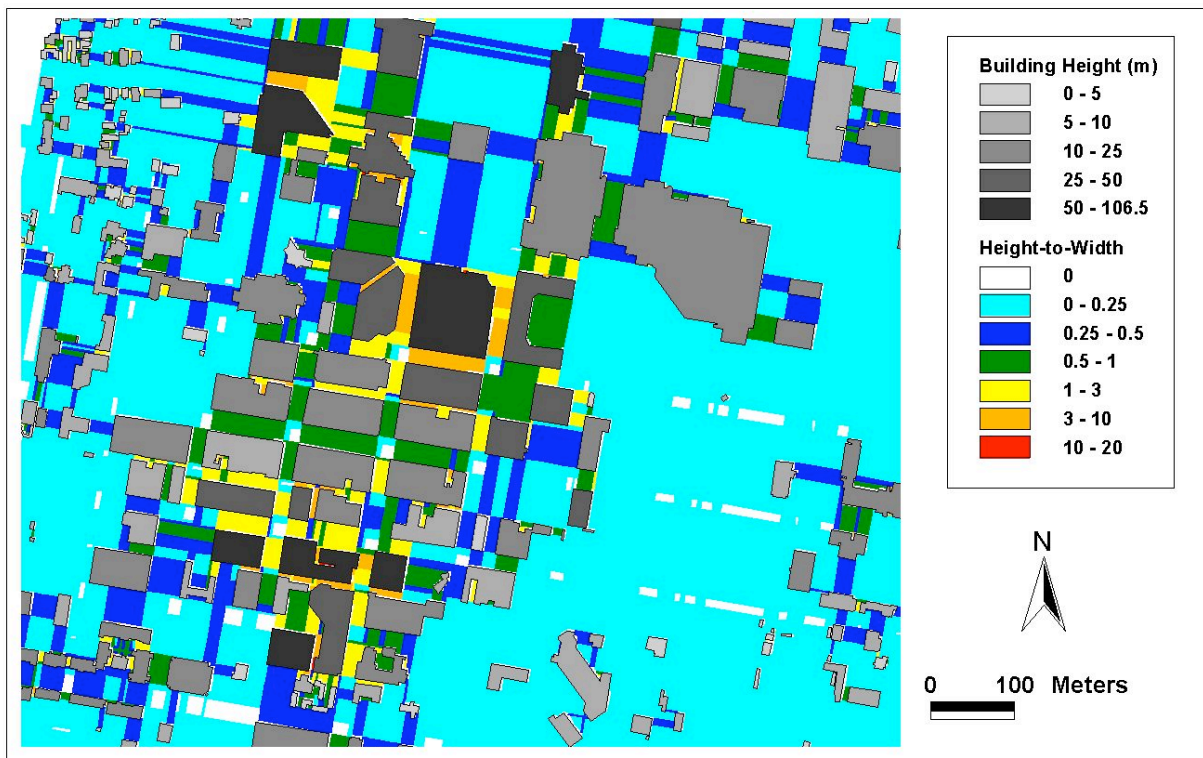


Figure 44. Composite height-to-width ratio (\overline{L}_s) for the downtown section of the Albuquerque study area.

Results. The area-weighted average \overline{L}_s for the study area was calculated to be 0.09. The range of \overline{L}_s for the study area was 0 to 17.5. Zero values occur where buildings are located and in regions where two buildings do not lie on an ‘along-the-street’ or ‘across-the-street’ transect. Table 12 lists the area-weighted average \overline{L}_s values for each land use type.

Table 12. Area-weighted average composite height-to-width ratio (\overline{L}_s)

Land Use Class	\overline{L}_s
Residential	0.15
Low-density Single-family (< 8 units/hectare)	0.06
High-density Single-family (\geq 8 units/hectare)	0.15
Multifamily	0.19
Mixed	---
Commercial & Services	0.10
Service	0.10
Retail	0.10
Industrial	0.13
Manufacturing	0.10
Wholesale and Warehousing	0.15
Transportation/Communications/Utilities	0.01
Mixed Industrial & Commercial	---
Mixed Urban or Built-up	---
Other Urban or Built-up	0.06
Predominantly Vegetated	0.04
Predominantly Built-up	0.07
Predominantly Bare Soil	0.03
Urban High-rise	0.12
Downtown Core Area	0.37

Table 13 compares selected values from our study with values computed for other cities. The values we calculated for Albuquerque are on the lower end of the range of values from other cities. The small values can be partially attributed to the relatively short high-rise buildings (compared to other cities) and the lower density of buildings. Also, the averaging scheme could cause significant differences; sensitivity studies need to be performed.

Table 13. Comparison of height-to-width (\bar{h}_s) for Albuquerque and other cities

Location	Land Use Class	\bar{h}_s	Source
Sacramento, CA	Suburban residential	1.21	Grimmond and Oke (1999)
Arcadia, CA	Suburban residential	1.19	Grimmond and Oke (1999)
Miami, FL	Suburban residential	1.03	Grimmond and Oke (1999)
Chicago, IL	Suburban residential	0.97	Grimmond and Oke (1999)
Vancouver, BC, Canada	Suburban residential	0.90	Grimmond and Oke (1999)
Tucson, AZ	Suburban residential	0.54	Grimmond and Oke (1999)
Salt Lake City, UT	Multifamily residential	0.47	Burian et al. (2002e)
Los Angeles, CA	Multifamily residential	0.45	Burian et al. (2002b)
San Gabriel, CA	Suburban residential	0.43	Grimmond and Oke (1999)
Portland, OR	Multifamily residential	0.31	Burian et al. (2002d)
Los Angeles, CA	High-density single-family residential	0.23	Burian et al. (2002b)
Phoenix, AZ	Multifamily residential	0.22	Burian et al. (2002c)
Albuquerque, NM	High-density single-family residential	0.15	This Report
Vancouver, BC, Canada	Light industrial	0.57	Grimmond and Oke (1999)
Salt Lake City, UT	Industrial	0.23	Burian et al. (2002e)
Los Angeles, CA	Industrial	0.20	Burian et al. (2002b)
Portland, OR	Industrial	0.17	Burian et al. (2002d)
Albuquerque, NM	Industrial	0.13	This Report
Phoenix, AZ	Industrial	0.13	Burian et al. (2002c)
Vancouver, BC, Canada	Central city	1.40	Grimmond and Oke (1999)
Mexico City, Mexico	Central city	1.19	Grimmond and Oke (1999)
Los Angeles, CA	Commercial & services high-rise	0.91	Burian et al. (2002b)
Los Angeles, CA	Downtown core area	0.77	Burian et al. (2002b)
Phoenix, AZ	Downtown core area	0.60	Burian et al. (2002c)
Salt Lake City, UT	Downtown core area	0.54	Burian et al. (2002e)
Portland, OR	Downtown core area	0.46	Burian et al. (2002d)
Albuquerque, NM	Downtown core area	0.37	This Report

4.10 Aerodynamic Roughness Parameters

Background. The representation of surface roughness is a critical first step in many meteorological, wind engineering, and pollutant dispersion modeling activities. It provides an estimate of the drag and turbulent mixing associated with the underlying surface. The displacement height (z_d) and roughness length (z_o) are key parameters in the logarithmic velocity profile based on similarity theory and are commonly used in many models to specify the boundary conditions above built-up areas. The displacement height can be conceptualized as the height of a surface formed by distributing the aggregate volume of roughness elements and their wake re-circulation cavities uniformly over the underlying surface (Macdonald et al. 1998). The roughness length is directly related to the overall drag of the surface. Mathematically, it represents the distance above the displacement height plane at which the velocity goes to zero.

Both z_d and z_o are difficult to estimate with certainty by experiment or theory. Grimmond and Oke (1999) reviewed methods to calculate the z_d and z_o of urban areas based on building and vegetation morphology. They compared the predictions of the morphological methods to those obtained from wind measurements in urban areas. Using the equations rated amongst the most appropriate by Grimmond and Oke (1999), we calculated values of z_d and z_o for the entire Albuquerque study area, spatially over a defined grid and as a function of land use in the study area. Note that the similarity theory is not valid in horizontally inhomogeneous areas and that for many urban areas the roughness parameter concept will not hold or can only be applied well above the roughness elements.

Calculation Methods. A common method used to calculate the displacement height (z_d) and roughness length (z_o) are simple rules-of-thumb (Grimmond and Oke 1999):

$$z_d = f_d \overline{z_H} \quad (19)$$

and

$$z_o = f_o \overline{z_H} \quad (20)$$

where $\overline{z_H}$ is the average building height and f_d and f_o are empirical coefficients. Approximations for urban values are 0.5 for f_d and 0.1 for f_o . Beyond the limitations of applying these equations to horizontally inhomogeneous urban areas, these equations also only hold for medium building density situations, as it is known that z_o and z_d vary with building spacing.

Results. Although Eqns. (19) and (20) may not hold for all areas in our study domain, we have still computed the aerodynamic roughness parameters for the Albuquerque study area for comparison purposes. Using these approximations we found that $z_d \approx 2.35$ m and $z_o \approx 0.47$ m when using the mean building height, and $z_d \approx 4.15$ m and $z_o \approx 0.83$ m when using the plan-area-weighted average building height. Table 14 lists the computed z_d and z_o values for each land use type using the mean building height and Eqns. (19) and (20). Table 15 lists the computed z_d and z_o values for each land use type using the plan-area-weighted average building height and Eqns. (19) and (20), while Figures 45 and 46 show the spatial distribution of the z_d and z_o . The use of the simple equations to compute the spatial distribution of roughness length and displacement

height is inaccurate for grid cells that contains a couple of relatively tall buildings within a large plan area because they neglect the low plan area fraction and frontal area index.

Table 14. Displacement height (z_d) and roughness length (z_o):
simple rules-of-thumb eqns. and average building height

Land Use Class	z_d (m)	z_o (m)
Residential	2.17	0.43
Low-density Single-family (< 8 units/hectare)	2.10	0.42
High-density Single-family (\geq 8 units/hectare)	2.10	0.42
Multifamily	2.52	0.50
Mixed	---	---
Commercial & Services	3.07	0.61
Service	3.29	0.66
Retail	2.62	0.52
Industrial	2.77	0.55
Manufacturing	2.56	0.51
Wholesale & Warehousing	2.91	0.58
Transportation/Communications/Utilities	2.78	0.56
Mixed Industrial & Commercial	---	---
Mixed Urban or Built-up	---	---
Other Urban or Built-up	3.07	11.84
Predominantly Vegetated	2.43	0.49
Predominantly Bare Soil	2.52	0.50
Predominantly Built-up	3.19	0.64
Urban High-rise	4.72	0.94
Downtown Core Area	7.58	1.52

Table 15. Displacement height (z_d) and roughness length (z_o): simple rules-of-thumb eqns. and plan-area-weighted average building height

Land Use Class	z_d (m)	z_o (m)
Residential	2.44	0.49
Low-density Single-family (< 8 units/hectare)	2.20	0.44
High-density Single-family (\geq 8 units/hectare)	2.23	0.45
Multifamily	3.07	0.61
Mixed	---	---
Commercial & Services	6.11	1.22
Service	6.49	1.30
Retail	5.55	1.11
Industrial	3.81	0.76
Manufacturing	3.18	0.64
Wholesale & Warehousing	4.03	0.81
Transportation/Communications/Utilities	4.39	0.88
Mixed Industrial & Commercial	---	---
Mixed Urban or Built-up	---	---
Other Urban or Built-up	5.92	1.18
Predominantly Vegetated	3.77	0.75
Predominantly Bare Soil	4.50	0.90
Predominantly Built-up	6.20	1.24
Urban High-rise	9.58	1.92
Downtown Core Area	12.32	2.46

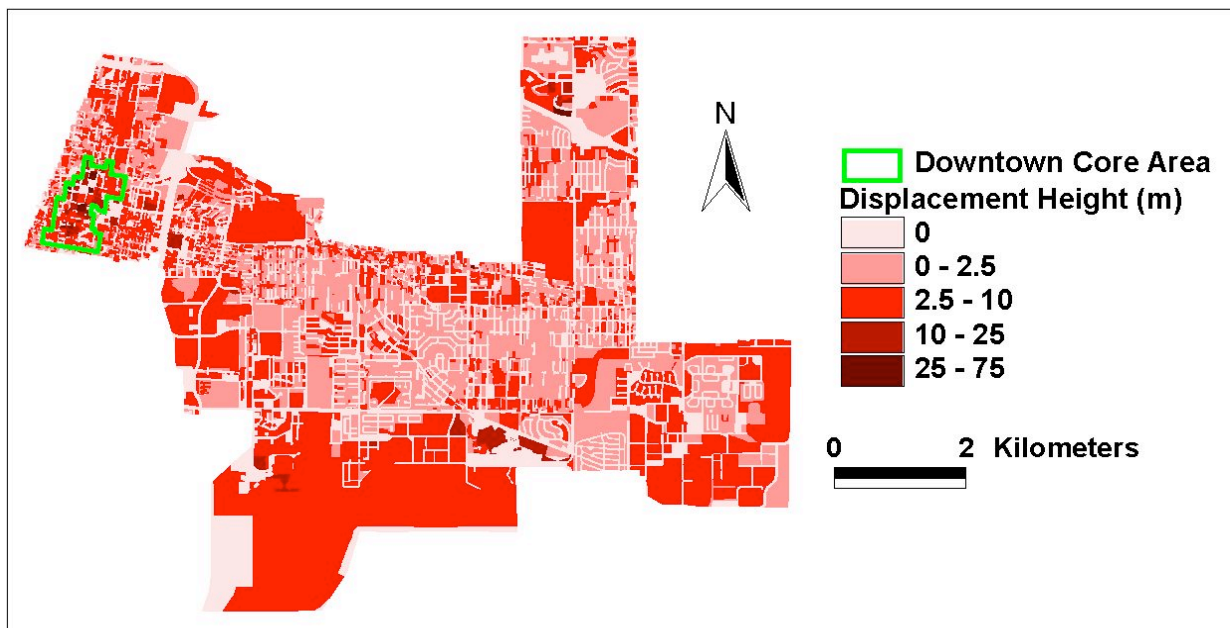


Figure 45. Spatial distribution of displacement height (z_d) in Albuquerque computed using the simple rule-of-thumb (Eqn. (19)) and the plan-area-weighted average building height.

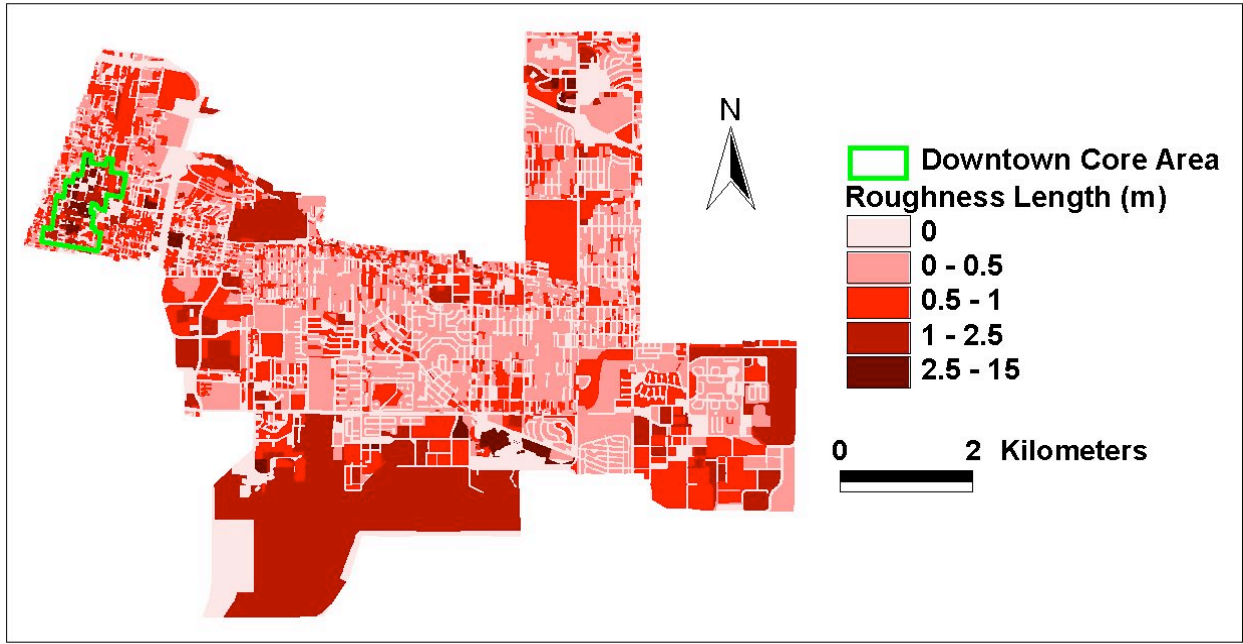


Figure 46. Spatial distribution of the roughness length (z_o) in Albuquerque computed using the simple rule-of-thumb (Eqn. 20) and the plan area-weighted average building height.

Calculation Methods. We also computed the z_d and z_o using two more complex equations described by Grimmond and Oke (1999). Although they compared results produced by different equations and concluded that it is difficult to measure their predictive accuracy, they did suggest an ordering of the morphometric equations. One set of equations ranked highly were those developed by Raupach (1994):

$$\frac{z_d}{z_H} = 1 - \frac{1 - \exp\left[-\left(c_{d1} z_f\right)^{0.5}\right]}{\left(c_{d1} z_f\right)^{0.5}} \quad (21)$$

and

$$\frac{z_o}{z_H} = \frac{z_d}{z_H} \exp\left[k \frac{U}{u_*} + \ln k\right] \quad (22)$$

where

$$\frac{u_*}{U} = \min\left[\left(c_s + c_R z_f\right)^{0.5}, \frac{u_*}{U_{\max}}\right] \quad (23)$$

and \square_k is the roughness sublayer influence function, U and u^* are the large-scale wind speed and the friction velocity, respectively, c_S and c_R are drag coefficients for the substrate surface at height z_H in the absence of roughness elements and of an isolated roughness element mounted on the surface, respectively, and c_{dl} is a free parameter. Raupach (1994) suggested $\square_k = 0.193$, $(u^*/U)_{max} = 0.3$, $c_S = 0.003$, $c_R = 0.3$, and $c_{dl} = 7.5$.

Results. Using these values, a von Kármán constant (k) of 0.4, and the values computed for the average building height and the average frontal area index, we calculated $z_d \square 1.61$ m and $z_o \square 0.21$ m. When using the plan-area-weighted average building height we found $z_d \square 2.85$ m and $z_o \square 0.38$ m. These values are significantly different than the values computed using the simple method (Eqns. (19) and (20)) because of the relatively high level of open space in the Albuquerque study area (which is represented in the frontal area index). The simple computation approach does not account for the high degree of open space and thus computes higher roughness lengths and displacement heights. Tables 16 and 17 list the computed z_d and z_o for each land use type using the average building height and the plan-area-weighted average building height, respectively.

Table 16. Displacement height (z_d) and roughness length (z_o):
Raupach (1994) equations with the average building height

Land Use Class	z_d (m)	z_o (m)
Residential	1.77	0.31
Low-density Single-family (< 8 units/hectare)	1.28	0.14
High-density Single-family (≥ 8 units/hectare)	1.72	0.30
Multifamily	2.20	0.42
Mixed	---	---
Commercial & Services	2.17	0.30
Service	2.40	0.35
Retail	1.80	0.24
Industrial	2.17	0.36
Manufacturing	1.92	0.29
Wholesale & Warehousing	2.37	0.41
Transportation/Communications/Utilities	---	---
Mixed Industrial & Commercial	---	---
Mixed Urban or Built-up	---	---
Other Urban or Built-up	1.77	0.17
Predominantly Vegetated	0.99	0.05
Predominantly Bare Soil	0.86	0.03
Predominantly Built-up	2.03	0.23
Urban High-rise	3.99	0.73
Downtown Core Area	7.95	1.77

Table 17. Displacement height (z_d) and roughness length (z_o): Raupach (1994) equations with the plan-area-weighted building height

Land Use Class	z_d (m)	z_o (m)
Residential	1.99	0.35
Low-density Single-family (< 8 units/hectare)	1.34	0.14
High-density Single-family (\geq 8 units/hectare)	1.83	0.32
Multifamily	2.68	0.51
Mixed	---	---
Commercial & Services	4.33	0.61
Service	4.73	0.70
Retail	3.80	0.50
Industrial	2.99	0.49
Manufacturing	2.38	0.37
Wholesale & Warehousing	3.29	0.57
Transportation/Communications/Utilities	---	---
Mixed Industrial & Commercial	---	---
Mixed Urban or Built-up	---	---
Other Urban or Built-up	3.42	0.33
Predominantly Vegetated	1.53	0.07
Predominantly Bare Soil	1.54	0.05
Predominantly Built-up	3.94	0.46
Urban High-rise	8.10	1.48
Downtown Core Area	12.93	2.89

Calculation Methods. The second set of equations was derived by Macdonald et al. (1998). These equations incorporate the drag coefficient and displacement height into the expression for roughness length (z_o):

$$\frac{z_d}{z_H} = 1 + \alpha_p \left(\frac{z_p}{z_H} - 1 \right) \quad (24)$$

and

$$\frac{z_o}{z_H} = \frac{z_d}{z_H} \exp \left[-0.5 \frac{C_D}{k^2} \left(\frac{z_d}{z_H} \right)^2 f \right]^{0.5} \quad (25)$$

where α is an empirical coefficient, C_D is a drag coefficient, k is the von Kármán constant, and f is a correction factor for the drag coefficient (the net correction for several variables, including velocity profile shape, incident turbulence intensity, turbulence length scale, and incident wind

angle, and for rounded corners). Macdonald et al. (1998) recommended for staggered arrays of cubes that $\beta = 4.43$ and $\beta = 1.0$. These values were used by Grimmond and Oke (1999) and are also used here. We also set $C_D = 1.2$ (the same value used Grimmond and Oke (1999) in their analysis) and the von Kármán constant $k = 0.4$.

Results. We found $z_d = 1.33$ m and $z_o = 0.25$ m for the Albuquerque study area. Using the plan-area-weighted average building height we found $z_d = 2.35$ m and $z_o = 0.44$ m. This method gives slightly smaller values of z_d and slightly larger values of z_o compared to the values computed using the Raupach (1994) equations. Tables 18 and 19 list the computed z_d and z_o for each land use for the average building height and the plan-area-weighted average building height, respectively.

Table 20 compares the computed aerodynamic roughness parameters to those calculated for other cities. The roughness parameters shown in Table 20 for Albuquerque were calculated using the Raupach (1994) equations with the plan-area-weighted average building height. The values for Albuquerque are comparable to values from other locations. The High-density Single-family Residential land use in Albuquerque has a displacement height and a roughness length that are at the lower end of the range for residential land use. The displacement and roughness lengths for Industrial land use in Albuquerque is in the middle of the range, but the downtown core area is in the bottom part of the range. The computed roughness length of 0.32 m for the tract of High-density Single-family Residential using the Raupach (1994) equations is nearly double the range presented by Wieringa (1993) for homogeneous suburban low buildings.

Table 18. Displacement height (z_d) and roughness length (z_o):
Macdonald et al. (1998) equations with the average building height

Land Use Class	z_d (m)	z_o (m)
Residential	1.69	0.29
Low-density Single-family (< 8 units/hectare)	0.94	0.17
High-density Single-family (\geq 8 units/hectare)	1.64	0.28
Multifamily	2.36	0.32
Mixed	---	---
Commercial & Services	2.18	0.29
Service	1.98	0.41
Retail	2.53	0.13
Industrial	2.98	0.20
Manufacturing	2.24	0.21
Wholesale & Warehousing	3.36	0.17
Transportation/Communications/Utilities	0.00	0.00
Mixed Industrial & Commercial	---	---
Mixed Urban or Built-up	---	---
Other Urban or Built-up	1.25	0.22
Predominantly Vegetated	0.57	0.05
Predominantly Bare Soil	0.12	0.03
Predominantly Built-up	1.80	0.26
Urban High-rise	4.13	0.06
Downtown Core Area	8.36	1.21

Table 19. Displacement height (z_d) and roughness length (z_o):
Macdonald et al. (1998) equations with the plan-area-weighted average building height

Land Use Class	z_d (m)	z_o (m)
Residential	1.90	0.33
Low-density Single-family (< 8 units/hectare)	0.99	0.18
High-density Single-family (\geq 8 units/hectare)	1.75	0.03
Multifamily	2.88	0.39
Mixed	---	---
Commercial & Services	4.35	0.57
Service	3.92	0.80
Retail	5.36	0.29
Industrial	4.10	0.28
Manufacturing	2.79	0.27
Wholesale & Warehousing	4.65	0.24
Transportation/Communications/Utilities	0.00	0.00
Mixed Industrial & Commercial	---	---
Mixed Urban or Built-up	---	---
Other Urban or Built-up	2.42	0.43
Predominantly Vegetated	0.89	0.08
Predominantly Bare Soil	0.22	0.05
Predominantly Built-up	3.51	0.50
Urban High-rise	8.38	1.22
Downtown Core Area	13.60	1.97

Table 20. Displacement height (z_d) and roughness length (z_o) for different cities

Location	Land Use Class	z_d (m)	z_o (m)	Source
Salt Lake City, UT	Multifamily residential	9.26	2.12	Burian et al. (2002e)*
Los Angeles, CA	Multifamily residential	9.24	2.12	Burian et al. (2002b)*
Arcadia, CA	Suburban residential	6.75	1.50	Grimmond and Oke (1999), Fig. 4
Portland, OR	Multifamily residential	5.83	1.26	Burian et al. (2002d)
Salt Lake City, UT	High-density single-family residential	5.18	1.15	Burian et al. (2002d)*
Vancouver, BC, Canada	Suburban residential	4.10	0.95	Grimmond and Oke (1999), Fig. 4
Chicago, IL	Suburban residential	4.00	0.75	Grimmond and Oke (1999), Fig. 4
Miami, FL	Suburban residential	3.25	0.80	Grimmond and Oke (1999), Fig. 4
Sacramento, CA	Suburban residential	3.10	0.75	Grimmond and Oke (1999), Fig. 4
San Gabriel, CA	Suburban residential	2.35	0.6	Grimmond and Oke (1999), Fig. 4
Los Angeles, CA	High-density single-family residential	2.24	0.44	Burian et al. (2002b)*
Tucson, AZ	Suburban residential	2.10	0.40	Grimmond and Oke (1999), Fig. 4
Albuquerque, NM	High-density single-family residential	1.83	0.32	This Report
Phoenix, AZ	Multifamily residential	1.76	0.27	Burian et al. (2002c)*
Salt Lake City, UT	Industrial	6.10	1.27	Burian et al. (2002c)*
Portland, OR	Industrial	3.18	0.52	Burian et al. (2002b)*
Los Angeles, CA	Industrial	3.04	0.54	Burian et al. (2002b)*
Albuquerque, NM	Industrial	2.99	0.49	This Report*
Phoenix, AZ	Industrial	2.35	0.29	Burian et al. (2002c)*
Vancouver, BC, Canada	Light industrial	2.25	0.5	Grimmond and Oke (1999), Fig. 4
Los Angeles, CA	Commercial & services high-rise	32.11	5.31	Burian et al. (2002b)*
Los Angeles, CA	Downtown core area	27.38	535	Burian et al. (2002b)*
Salt Lake City, UT	Downtown core area	21.54	4.78	Burian et al. (2002c)*
Vancouver, BC, Canada	Central city	20.00	4.50	Grimmond and Oke (1999), Fig. 4
Albuquerque, NM	Downtown core area	12.93	2.89	This Report*
Phoenix, AZ	Downtown core area	11.55	2.63	Burian et al. (2002c)*
Portland, OR	Downtown core area	9.97	2.26	Burian et al. (2002d)*
Mexico City, Mexico	Central city	8.00	1.60	Grimmond and Oke (1999), Fig. 4

* Albuquerque, Portland, Phoenix, SLC, and LA values computed using the Raupach (1994) equations and the plan-area-weighted building height

5.0 Summary

This report summarizes the results of the derivation of building morphological characteristics for a 48.5 km² area of Albuquerque, New Mexico. A three-dimensional building dataset and detailed land use/land cover information were integrated and analyzed using a geographic information system (GIS). Building height characteristics (e.g., mean height, height variance, height histograms) were determined for the entire study area and broken down by land use type. Parameters describing the urban morphology were also calculated including the building plan area fraction ($\overline{f_p}$), building area density ($a_p(z)$), rooftop area density ($a_r(z)$), frontal area index ($\overline{f_f}$), frontal area density ($a_f(z)$), complete aspect ratio ($\overline{f_c}$), building surface area to plan area ratio ($\overline{f_B}$), and the height-to-width ratio ($\overline{f_s}$). These urban morphological parameters were calculated for the entire study area, for different land use types, and in some cases as a function of height above ground elevation. Using the urban morphological parameters, the aerodynamic roughness length (z_o) and displacement height (z_d) were calculated for the entire study area and for each land use type using standard morphometric equations. Most of the calculated morphometric parameters were found to be similar to values computed for other cities by other researchers. Synthesis of the results indicates that the urban morphological parameters vary significantly between different land uses. Moreover, the urban land uses containing tall buildings were found to have significantly different morphological characteristics than other urban land uses.

References

- Anderson, J. R., Hardy, E. E., Roach, J. T. and Witmer, R. E. (1976). *A land use and land cover classification system for use with remote sensor data*. USGS Professional Paper 964, U.S. Geological Survey.
- Brown, M.J. (1999). *Urban parameterizations for mesoscale meteorological models*. Mesoscale Atmospheric Dispersion, Edited by Z. Boybeyi, WIT Press, pp. 193-255, LA-UR-99-5329.
- Burian, S.J. and Brown, M.J. (2001). *Summary of Los Angeles, California urban building and land use/cover data*. LA-UR-01-4055, Los Alamos National Laboratory, Los Alamos, New Mexico.
- Burian, S.J., Brown, M.J., and Velugubantla, S.P. (2002a). "Building height characteristics in three U.S. cities." *Preprints, Fourth Symposium on the Urban Environment*, 20-24 May 2002, Norfolk, VA.
- Burian, S.J., Brown, M.J., and Linger, S.P. (2002b). *Morphological analyses using 3D building databases: Los Angeles, California*. LA-UR-02-0781, Los Alamos National Laboratory, Los Alamos, NM.
- Burian, S.J., Velugubantla, S.P., and Brown, M.J. (2002c). *Morphological analyses using 3D building databases: Phoenix, Arizona*. LA-UR-02-6726, Los Alamos National Laboratory, Los Alamos, NM.
- Burian, S.J., Velugubantla, S.P., Chittineni, K., S. Maddula, and Brown, M.J. (2002d). *Morphological analyses using 3D building databases: Portland, Oregon*. LA-UR-02-6725, Los Alamos National Laboratory, Los Alamos, NM.
- Burian, S.J., Velugubantla, S.P., and Brown, M.J. (2002e). *Morphological analyses using 3D building databases: Salt Lake City, Utah*. LA-UR-, Los Alamos National Laboratory, Los Alamos, NM.
- Cionco, R.M. and Ellefsen, R. (1998). "High resolution urban morphology data for urban wind flow modeling." *Atmospheric Environment*, 32(1): 7-17.
- Ellefsen, R. (1990) "Mapping and measuring buildings in the canopy boundary layer in ten U.S. cities." *Energy and Buildings*, 15-16: 1025-1049.
- Grimmond, S. and Oke, T. (1999). "Aerodynamic properties of urban areas derived from analysis of surface form." *J. Appl. Met.*, 38: 1262-1292.
- Hanna, S.R. and Britter, R. (2002). "The effect of roughness obstacles on flow and dispersion in urban industrial areas." *Proceedings, 7th International Conference on Harmonization within Atmospheric Dispersion Modeling for Regulatory Purposes*, Belgirate, Italy, 28-30, May 2002.
- Macdonald, R.W., Griffiths, R.F., and Hall, D.J. (1998). "An improved method for estimation of
-

surface roughness of obstacle arrays.” *Atmospheric Environment*, 32: 1857-1864.

Nichol, J.E. (1996). “High-resolution surface temperature patterns related to urban morphology in a tropical city: A satellite-based study.” *J. Appl. Meteor.*, 35: 135-146.

Oke, T.R. (1988). “Street design and urban canopy layer climate.” *Energy and Buildings*, 11: 103-113.

Ratti, C., Di Sabatino, S., Britter, R., Brown, M., Caton., F., and Burian, S. (2001). “Analysis of 3-D urban databases with respect to pollution dispersion for a number of European and American Cities.” *The Third International Conference on Urban Air Quality: Measurement, Modelling, and Management*, March 19-23, 2001, Loutraki, Greece.

Raupach, M.R. (1994). “Simplified expressions for vegetation roughness length and zero-plane displacement as functions of canopy height and area index.” *Boundary-Layer Meteorology*, 71: 211-216.

Voogt, J. and Oke, T. (1997). “Complete urban surface temperatures.” *J. Appl. Met.*, 36: 1117-1132.

Wieringa, J. (1993). “Representative roughness parameters for homogeneous terrain.” *Boundary Layer Meteorology*, 63: 323-363.

Appendix 1

Description of Land Use Types

The land use/ land cover classification we used for the building analysis was divided into two levels as shown in Table A1.1. The first level corresponds to the Anderson Level 2 classification used by the USGS for its standard national dataset. The second level includes the subdivision of the level 1 **Residential, Commercial & Services, Industrial, and Other Urban or Built-up** categories. Descriptions of the level 1 and level 2 categories included on our land use classification follow Table A1.1. In addition to the multi-level classification we also categorize all the land use parcels that contain high-rise buildings as **Urban High-rise**. Finally, using aerial photographs and other information we defined the downtown city center area and termed this land use as **Downtown Core Area**. Note that **Urban High-rise** and **Downtown Core Area** contain the level 1 and level 2 land use categories, i.e., Table A1.1 will have overlap.

Table A1.1. Land use classification. Level 1 categories are shown in boldface, level 2 categories are indented.

Land Use Class
Residential
Low-density Single-family (\leq 8 units/hectare)
High-density Single-family ($>$ 8 units/hectare)
Multifamily
Mixed
Commercial & Services
Commercial Service
Commercial Retail
Industrial
Manufacturing
Wholesale & Warehousing
Transportation/Communications/Utilities
Mixed Industrial & Commercial
Mixed Urban or Built-up
Other Urban or Built-up
Predominantly Vegetated
Predominantly Bare Soil
Other Predominantly Built-Up
Urban High-rise
Downtown Core Area

Residential

Includes areas of single-family residences, multi-unit dwellings, mobile homes, and mixtures of residential land use types. Level 2 categories of Residential land use are:

Low-density Single-family: Detached residential housing units with an average density less than or equal to 8 units per hectare (\leq 3 units/acre).

High-density Single-family: Detached residential housing units with an average density greater than 8 units per hectare ($>$ 3 units/acre).

Multifamily: Residential housing units designed to contain multiple families in a single structure. Includes apartments and condominiums.

Mixed: A mixture of low-density single-family, high-density single-family, and multifamily residential land uses.

Commercial & Services

Commercial & services land use includes areas which are used predominantly for business or the sale of products and their associated services. Includes shopping malls, business districts, office buildings, strip malls, educational and institutional, and other commercial areas. Level 2 categories of Commercial & Services land use are:

Commercial Retail: Includes retail centers, large shopping malls, and strip malls.

Commercial Service: Includes office complexes and high-rise office buildings.

Industrial

Industrial land use includes areas where manufacturing, assembly, processing, packaging, or storage of products takes place. Level 2 categories of Industrial land use are:

Manufacturing: Includes manufacturing related industrial land use.

Wholesale & Warehousing: Includes storage buildings and wholesale centers.

Transportation/Communication/Utilities

Areas devoted to major transportation, such as airports, freeways, roads, railways and harbor facilities. Also included are areas devoted to communications and utilities.

Mixed Industrial & Commercial

Areas included are a mixture of industrial and commercial land uses.

Mixed Urban or Built-Up

Areas included are a mixture of the other urban land uses with none being the dominant.

Other Urban or Built-Up

Other land use areas that cannot be categorized in the above categories. Urban vegetation and bare soil classes are categorized in this class for this scheme.

Predominantly Vegetated: Areas included are urban land uses that are predominantly vegetation, such as golf courses, parks, recreation fields, cemeteries, and so on. Some buildings may be contained on the site.

Predominantly Bare Soil: Areas included are urban land uses that are predominantly bare soil. Includes open spaces not vegetated.

Predominantly Built-up: Includes urban land uses not categorized in any of the above land uses and that are not predominantly vegetated. These land uses are generally ambiguous or unknown.

Urban High-rise

Land use that contains high-rise buildings. High-rise buildings are subjectively selected based on their relative size compared to the surrounding buildings. For Albuquerque Urban High-rise a land use polygon was designated as Urban High-rise if it contained at least 1 building with a height greater than 17.5 meters.

Downtown Core Area

Subjective designation of the downtown core area based on aerial photograph, street maps, building datasets, and other information.

Appendix 2

AGIS Land Use Aggregation

The aggregation of the AGIS land use to more general levels is relatively simple because there are only a few land use types to aggregate. Table A2.1, shown below, lists the mapping from AGIS land use to the 7-category and 14-category schemes. We also note which land uses are mapped to Urban High-rise. Note that in some cases land use can be classified as Urban High-rise based on other information than the mapping shown in Table A2.1.

Table A2.1. AGIS LULC aggregation.

AGIS Land Use Type	Classification Level 1	Classification Level 2	High-rise or Non-high-rise
Agriculture	Other Urban or Built-up	Predominantly Vegetated	Variable**
Commercial Retail	Commercial & Services	Commercial Retail	Variable**
Commercial Service	Commercial & Services	Commercial Service	Variable**
Drainage and Flood Control	Transportation/Communication/Utilities	Transportation/Communication/Utilities	Variable**
Industrial and Manufacturing	Industrial	Manufacturing	Variable**
Multifamily Residential	Residential	Multifamily Residential	Variable**
Parking Lots and Structures	Commercial & Services	Commercial Services	Variable**
Parks and Recreation	Other Urban or Built-up	Predominantly Vegetated	Variable**
Public and Institutional	Other Urban or Built-up	Predominantly Built-up	Variable**
Single Family Residential	Residential	Single-family Residential*	Variable**
Transportation and Utilities	Transportation/Communication/Utilities	Transportation/Communication/Utilities	Variable**
Vacant/Other	Other Urban or Built-up	Predominantly Bare Soil	Variable**
Wholesale and Warehousing	Industrial	Wholesale and Warehousing	Variable**

* low-density or high-density depends on the building density, as described in Section 3 of the report.

** high-rise or non-high rise classification depends on building height analysis in individual land use polygon, as described in Section 3 of the report.